THE INFLUENCE OF ELEVATION AND ASPECT ON PERMAFROST DISTRIBUTION IN CENTRAL YUKON TERRITORY

by

Michelle M. Côté, B.Sc. (Hons)

A thesis submitted to

the Faculty of Graduate Studies

in partial fulfilment of

the requirements for the degree of

Master of Arts

Carleton University

Ottawa, Ontario

The undersigned recommend to

the Faculty of Graduate Studies

acceptance of the thesis:

"THE INFLUENCE OF ELEVATION AND ASPECT

ON PERMAFROST DISTRIBUTION

IN CENTRAL YUKON TERRITORY"

submitted by **Michelle M. Côté, B.Sc. (Hons)**

in partial fulfillment of the requirements for

the degree of Master of Arts

Thesis Supervisor

C.R. Burn

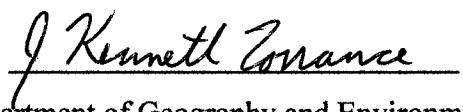

Chair, Department of Geography and Environmental Studies

CARLETON UNIVERSITY

May 2002

ABSTRACT

Air and ground temperature at eleven sites within various biogeoclimatic zones along a N-S cross-section of Lightning Creek valley, near Keno, demonstrate the significance of atmospheric inversions on mean annual temperature. The mean annual air temperature increases with elevation by 2.2°C over the lower 160 m of Keno Hill, but declines above this level. Permafrost is present on the N-facing slope of Sourdough Hill but is absent on part of the S-facing aspect of Keno Hill, due to winter inversions and high summer solar radiation. The association of biogeoclimatic zones with permafrost was defined with thermal and physical data from the sites. With vegetation interpreted from aerial photographs and topographic information from a digital elevation model these associations were tested in the wider Keno area. Coniferous and alpine tundra are diagnostic of continuous permafrost, while S-facing slopes with aspen trees are permafrost-free. Permafrost is discontinuous beneath other vegetation classes.

ACKNOWLEDGEMENTS

As with all worthwhile endeavors, this thesis is the product of a lot of hard work by numerous people, to each of whom I must express my sincere gratitude.

Dr C.R. Burn provided excellent guidance and support throughout the entire project. His independent approach to teaching has allowed me to become a better researcher and scientist. Discussions with Dr M.W. Smith (Carleton University) and Dr A.G. Lewkowicz (University of Ottawa) have greatly contributed to the development of field methods and interpretation of results.

This project would not have been completed without generous financial support from the Natural Sciences and Engineering Research Council of Canada in the form of a PGSA to the author and an Operational Grant to C.R. Burn; the Northern Scientific Training Program assisted with the costs of conducting field work in Yukon; the Village of Mayo and Yukon College supplied funds to hire local field assistants; the Polar Continental Shelf Project, NRCan, provided two ATVs.

Field assistance was provided by Chad Peck, Ross Cooper, and Robin Kuhn, as well as by family and friends Peter Martin, Tony Côté, Camille Tyo, Marcy Jordan, Valerie Horsfall, and Jennifer Sled, who in exchange for Keno hospitality, performed various field tasks. Additional expert advice and assistance in the field was provided by vegetation specialist Catherine Kennedy, Department of Renewable Resources, YTG and by soil scientist Scott Smith, Pacific Agri-Food Research Centre. William Cody, an emeritus scientist with Agriculture Canada identified numerous plant specimens.

Special thank-yous go to Larry Boyle for his assistance with preparing the field

equipment, to Caroline Duchesne for help her with the DEM and the vegetation mapping, to Marilyn Dobbin-White and Mary White at the Mooseberry Bakery in Keno for their great breads and treats, and to Lisa Huisman for her motivation, fun lunch breaks and, of course, her cooking and baking.

To my fellow "Permafrost Panel" members, Lisa Huisman, Kumari Karunaratne, Marcia Phillips, and Vickie McCoy, thank-you for your friendship and your support. You have made this experience memorable and enjoyable. I wish you all much happiness as you venture down new paths.

Finally, to my husband Peter, who spent many weeks at home alone in the summers, week-ends alone at the cottage and evenings alone in front of the T.V., "When Michelle is done her thesis..." has arrived at last.

TABLE OF CONTENTS

LIST OF TABLES

LIST OF FIGURES

CHAPTER 1
OVERVIEW AND OBJECTIVES

1.1 Introduction

The objective of this thesis is to investigate the influence of elevation and aspect on the distribution of permafrost in a mountainous area of central Yukon Territory. The study examines air and shallow ground temperatures collected along two elevational transects within various biogeoclimatic zones on the adjacent north- and south-facing slopes of Sourdough and Keno hills. Observations of terrain and soil variables at each site were used to develop an empirical model associating these variables with the presence or absence of frozen ground at the sites near the end of the thaw season. The empirical model was tested against a second data set of terrain and soil conditions from the same region collected independently.

1.2 Context of this Project

Permafrost underlies approximately 25% of the world's land surface and nearly half of Canada (French 1996, 56). The most important factor determining the occurrence of permafrost is climate (French 1996, 58). In general, the colder the climate, whether due to increases in latitude or elevation, the greater the proportion of the ground that is underlain by permafrost. So-called alpine permafrost occurs in various high mountains of the world at both low and high-latitudes (Harris 1988), but has been studied relatively infrequently in Canada, particularly at high-latitudes (Harris 1982; 1987; Taylor *et al.* 1998).

A major difference in the climate of low- and high-latitude alpine environments is

the seasonal variation of incoming solar radiation. In winter, the low amount of incoming solar radiation in polar areas can result in prolonged temperature inversions, where it is warmer at high elevation than in the valleys (Taylor *et al.* 1998). When solar radiation is abundant, a normal environmental lapse rate is observed (Barry 1992, 45). An objective of this thesis is to determine how this particular climatic effect influences the distribution of permafrost at a high-latitude site (63°55'N, 135°15'W).

Most current climatological studies suggest that the global climate is warming at an unprecedented rate and that, with continued warming, northern areas will experience the greatest increases in temperature (e.g. Roots 1989; Overpeck *et al.* 1997; Serreze *et al.* 2000). Winter temperatures in Yukon are projected to increase by 2-5°C in southern regions, and by as much as 8°C along the north coast in the next century (Adaptation and Impacts Research Group 1999, 2-1). Summer warming is estimated at 3-6°C for southern Yukon, and 2-4°C in the north (Adaptation and Impacts Research Group 1999, 2-1). It is important to develop an understanding of the permafrost conditions in mountainous regions as a baseline for future work so that changes in the permafrost regime, due to climatic warming or other short- or long-term events, may be identified.

Permafrost degradation from warmer temperatures and increased snowfall may lead to a decrease in terrain stability resulting in landslides and gelifluction in mountainous regions that could put wildlife habitat, villages, roads and other anthropogenic structures at risk of damage or destruction. Knowledge in this area may contribute to land-use planning, particularly in the routing of planned gas pipelines in Yukon and the Mackenzie Valley. In valley bottoms, thermokarst may develop if ground ice melts, leading to ground subsidence altering the current landscape.

In areas of discontinuous permafrost, frozen ground can rarely be directly observed. To avoid the costs and restricted access for site-by-site testing of ground thermal conditions in mountainous terrain, it would be useful to infer ground conditions from surficial terrain characteristics.

1.3 Summary of Research Questions

Several specific questions, which address two broad themes, will be answered in this thesis. The first part of the research documents the strength and duration of temperature inversions and the occurrence permafrost along adjacent north- and south-facing elevational transects. Using site-specific data, relations between permafrost occurrence and terrain and soil variables are identified. The second part of the research determines whether these relations can be used to predict the occurrence of permafrost in the local area using variables derived from secondary data sources, namely aerial photographs and terrain characteristics generated from a digital elevation model.

The following specific questions will be addressed in this thesis:

1) What temperature inversions occur in central Yukon and how does their mean strength and duration vary seasonally?
2) How do the mean annual air temperature, the ratio of thawing degree-days (DDT) to freezing degree-days (DDF), and the distribution of permafrost, change with elevation and aspect?
3) Can associations between terrain and soil variables be developed with respect to the presence or absence of frozen ground near the end of the thaw season and used to construct an empirical model of permafrost occurrence in the study area?

4) Can this empirical model be extrapolated from the specific sites studied to predict the presence or absence of frozen ground in a broader region of central Yukon?

1.4 Organization of the Thesis

This thesis is presented in seven chapters. The next chapter reviews the distribution of permafrost at global, national and territorial scales as well as the macro and microscale factors that influence its spatial distribution. Chapter 3 describes the study area and discusses the frequency and seasonality of mesoscale inversions in central Yukon. Chapter 4 presents the methodology used in collecting the field data and other techniques used. The results of fieldwork and the development of the empirical model are discussed in chapter 5, and chapter 6 presents the testing of the empirical model. Chapter 7 summarizes and concludes the thesis, and identifies limitations in the application of this permafrost mapping technique.

CHAPTER 2
FACTORS THAT INFLUENCE THE DISTRIBUTION OF PERMAFROST

2.1. Introduction

In this chapter, the relation between climate and permafrost distribution will be discussed at three spatial scales. Broad patterns of temperature and precipitation influence the distribution of permafrost at global and Canada-wide scales. While climatic patterns are important for permafrost distribution in Yukon Territory and the Mayo-Keno area, local factors also influence the ground thermal regime and may help explain why ground underlain by permafrost may occur adjacent to permafrost-free areas. The influence of vegetation, snow cover, soil properties, and topography on the ground thermal regime and the distribution of permafrost will be discussed in this chapter.

2.2. Permafrost Distribution at Different Spatial Scales

Permafrost is defined as ground that remains cryotic, at or below 0°C, for at least two consecutive years (ACGR 1988). Globally, 25% of the landmass is underlain by permafrost and in Canada, approximately half the land area is affected by perennially frozen ground (French 1996, 56) (Fig. 2.1). Above the permafrost, a layer of ground that is seasonally cryotic exists called the active layer. The active layer thaws in summer to depths ranging from 0.3 m to several metres, depending on location, and refreezes in winter (Briggs *et al.* 1993, 420).

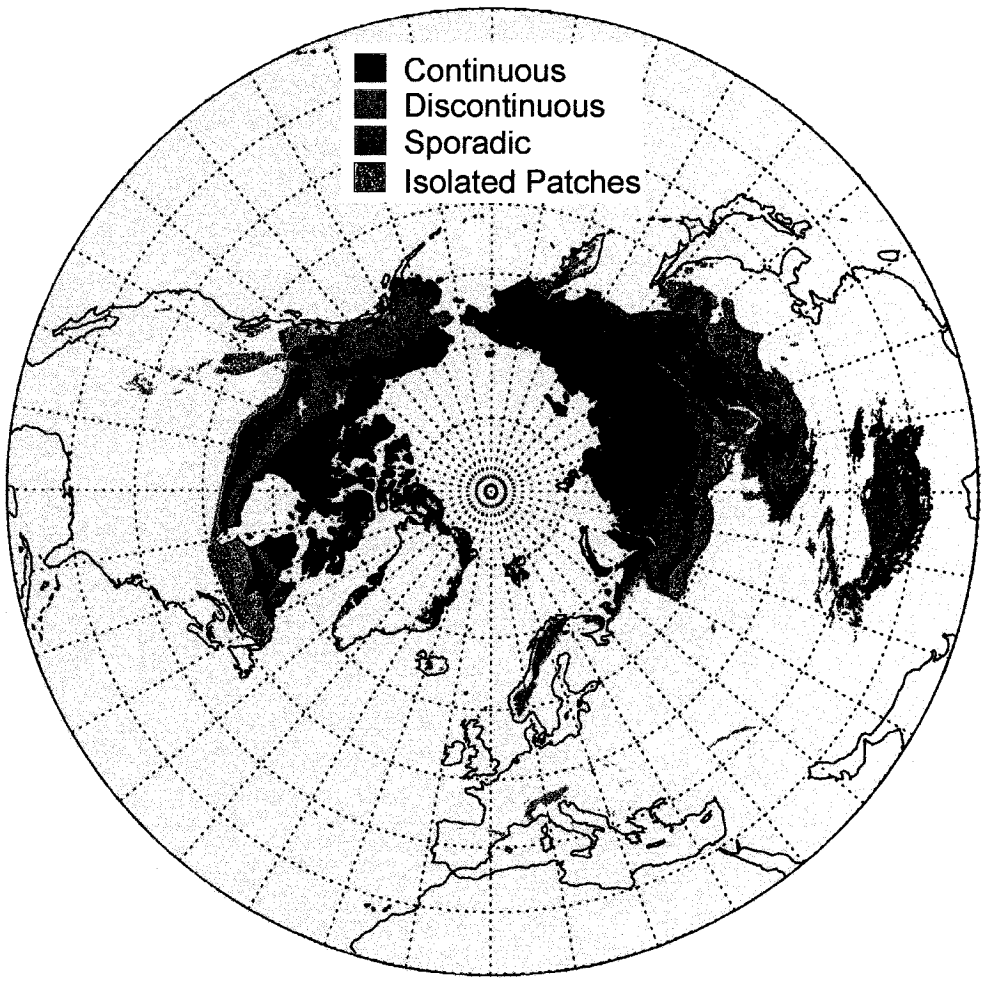

Figure 2.1 - Distribution of permafrost in the Northern Hemisphere (from Zhang *et al.* 1999, Fig. 2)

The energy exchanges at the earth's surface and the geothermal heat flow determine the temperature regime of the ground and, thus, if permafrost is present or absent. Since the geothermal heat at a location is generally constant, the ground thermal regime is influenced primarily by seasonal differences in conditions at the ground surface, most notably by climate (French 1996, 65). Globally, permafrost increases in spatial extent and thickness as air temperature decreases, due to increases in latitude and/or altitude. The ground temperature at the depth of zero annual amplitude is usually 3 to 4°C warmer than the mean annual air temperature (MAAT), largely due to the effect of snow (Brown 1966). With this in mind, the MAAT is frequently used to predict the broad geographical or zonal distribution of permafrost.

The zones of permafrost distribution are usually defined in terms of the percentage by area of the ground that is frozen. These zones range from continuous, where 90 to 100% of the ground is underlain by permafrost, equatorwards through to sporadic distributions where permafrost is patchy and exists only under specific local microclimatic conditions (Williams and Smith 1989, 60). Permafrost is also present in some offshore areas below seabed as a result of past colder climates and fluctuations in sea level (Sellman and Hopkins 1984). The lack of permafrost in western Europe at northern latitudes compared to Russia and North America is attributed to the moderation of the climate in this region by the North Atlantic Current (Barry and Chorley 1998; Zhang *et al.* 1999) (Fig. 2.1).

The spatial distribution of permafrost in Canada also reflects the spatial variation in climate with a general zonal gradation northwards from areas of no permafrost through to the continuous permafrost zone (Fig. 2.2). The climate of central Canada is

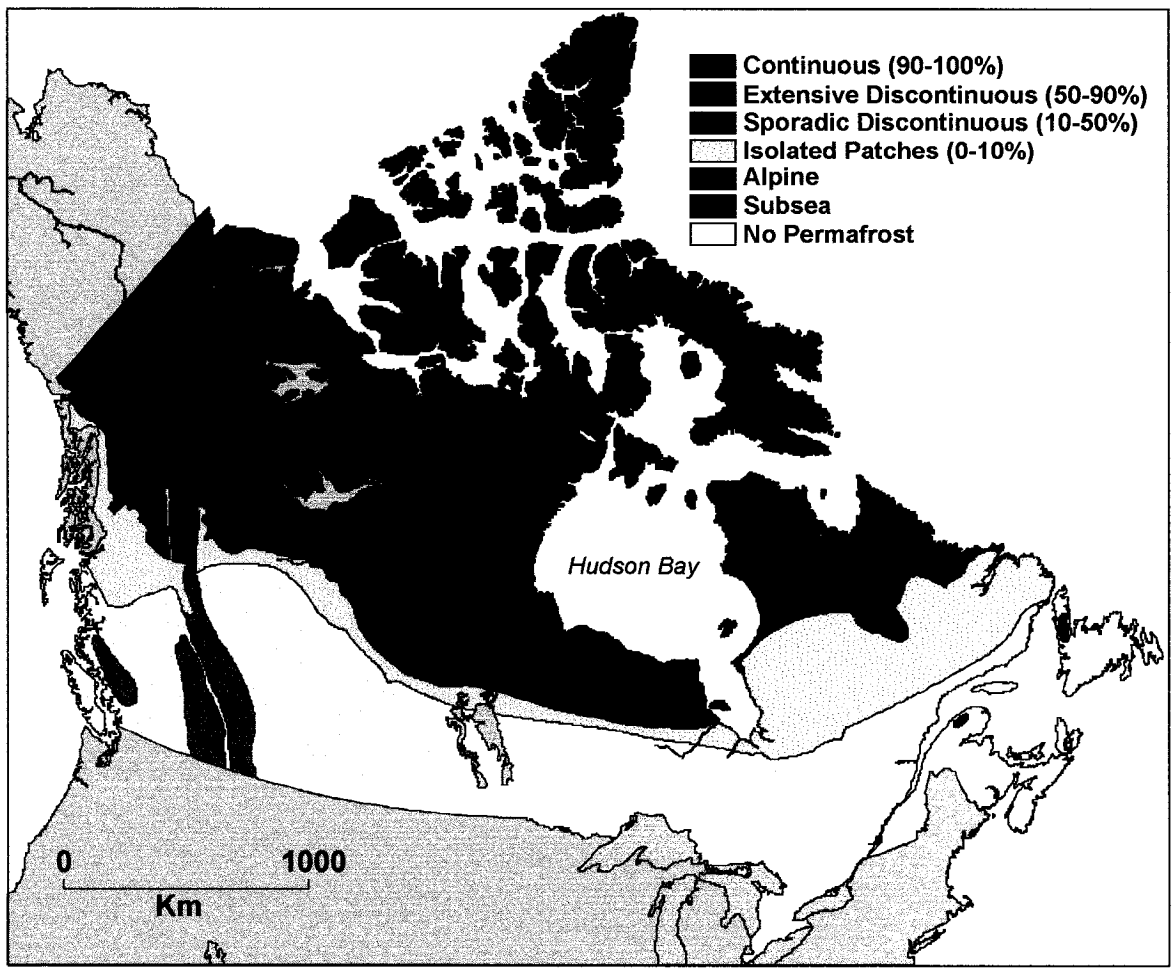

Figure 2.2 - Distribution of permafrost in Canada (after Heginbottom *et al.* 1995)

continental, despite the presence of Hudson Bay: MAAT and precipitation both decrease with distance from the east and west coasts. The two to three month ice-free season on Hudson Bay begins in mid-July, and much of the summer heat energy is used to melt the ice, creating a cooler than expected summer climate in this region (Rouse 1993, 77). These climatic patterns result in the boundaries of the continuous and extensive discontinuous zones occurring at a more southerly latitude in central Canada than near the east and west coasts. Climatic patterns are also manifest in the treeline, with the northern limit of tree growth coinciding with the modal position of the frontal zone between Arctic and Pacific air masses in July (Bryson 1966), as well as with the southern limit of continuous permafrost. The difference in the distribution of permafrost on the east and west sides of Hudson Bay is believed due to the greater snow accumulation in autumn to the east of Hudson Bay, resulting in warmer ground temperatures and less extensive permafrost (French 1996, 58).

In Yukon Territory, the Wrangell-St Elias and Coast mountains block Pacific maritime air masses from entering the region, leading to a sub-arctic continental climate. The climate of Yukon is characterised by large annual ranges in temperature, and moderate to light, seasonally irregular precipitation, conditions that are conducive to permafrost (Wahl *et al.* 1987, 33). Permafrost occurrence in Yukon Territory ranges from scattered patches in the south, through to continuous permafrost near Old Crow and the Beaufort Sea coast (Fig. 2.3). The corresponding MAATs for the boundary of these two permafrost zones is just below 0°C and –8°C, respectively (Wahl *et al.* 1987, 33; Burn 1998a). Alpine permafrost is found at higher elevations in mountainous areas such as the St Elias Mountains in southwest Yukon (Slaymaker 1993, 191).

Figure 2.3 - Permafrost map of Yukon (after Heginbottom *et al.* 1995)

A wide range of permafrost thicknesses have been observed or estimated in the Territory. In northern coastland areas that were unglaciated during the Late Wisconsinan, permafrost is estimated to be at least 300 m thick (Rampton 1982). In central Yukon, permafrost thicknesses of up to 40 m have been measured near Mayo (Burn 1991; 2000), and up to 60 m near Dawson (McConnell 1905; Brown 1970, 169). Permafrost is less than 20 m thick in the scattered zone in the southern portion of the Territory (Burn 1998a; 1998b).

2.3. Distribution of Alpine Permafrost

Alpine permafrost occurs at both high- and low-latitudes in many parts of the world. Three types of alpine permafrost are recognized: 1) permafrost at higher elevations but not in the valleys below, 2) permafrost both at higher elevations and in the valley bottoms, but not at mid-elevations, and 3) permafrost throughout the elevational gradient. Within these different types of alpine permafrost, zones of continuous, discontinuous and sporadic permafrost, based on the percentage of frozen ground may also be defined, similar to latitudinal permafrost (Gorbunov 1978; Harris and Brown 1982; King 1986). The spatial distribution of these different types of alpine permafrost is also broadly governed by climate. The first type is found most frequently in low- and mid-latitude mountains such as the European Alps (e.g. Haeberli 1978; Hoelzle 1992; Keller *et al.* 1998; Lieb 1998), the Rocky Mountains (e.g. Ives 1973; Harris and Brown 1982; Harris 2001), and regions in Middle and Central Asia (Zhou *et al.* 1991; Wang and French 1995). Types 2 and 3 are more common in circumpolar mountainous areas,

although descriptions of these occurrences are limited (King 1986; Etzelmüller *et al.* 1998).

In eastern Canada, alpine permafrost has been documented in the Chic-Choc Mountains of Québec (Gray and Brown 1979) and in the Long Range and Mealy Mountains of Newfoundland and Labrador (Brown 1975; Ives 1979). Most of the alpine permafrost research in Canada has occurred in the western Cordillera, particularly in the eastern ranges (e.g. Mathews 1955; Harris 2001). However, the spatial distribution of permafrost in the Rocky Mountains is still poorly understood because of limited field observations in the area, much of which is remote. In general, alpine permafrost tends to occur only at very high altitudes in the southern part of the Cordillera, with a decrease in altitude of permafrost occurrences in the northern mountains. Harris and Brown (1982) identified the lower limit of the continuous permafrost zone using twenty-eight borehole records through 50 to 53°N in southwest Alberta. They determined that the lower boundary lies between 2180 and 2575 m ASL, but that it does not simply decline in elevation northwards. Instead, the lower limit of continuous permafrost drifts higher from 50.5 to 51.5°N due to increased snowfall around ice caps and glaciers, and then decreases in elevation through to 53°N.

2.4. Factors that Influence the Ground Thermal Regime

The thermal regime of the ground is governed by the exchange of heat and moisture between the atmosphere and the ground surface. At the ground surface, temperatures fluctuate in response to changes in the energy balance. The depth to which

these changes propagate into the ground depends upon the thermal properties of ground materials.

The energy balance equation is generally used to describe the energy exchanges between the atmosphere and the ground surface, and can therefore be useful in analysing ground surface temperature and the occurrence of permafrost. The energy balance (eq. 1) equates the net exchange of radiation (Q^*) between the surface and the atmosphere, the convective exchange of sensible heat (Q_H) and latent heat (Q_{LE}) with the atmosphere, and the transfer of heat into the ground by conduction (Q_G).

$$Q^* = Q_H + Q_{LE} + Q_G \qquad \text{(eq. 1)}$$

The energy balance equation is very practical in specific applications where data characterizing each component are available. For more spatially broad analyses, a functional model describing the climate-permafrost relation is necessary (Lachenburch *et al.* 1988; Smith and Riseborough 2002) (Fig. 2.4). Smith and Riseborough (1996) developed the TTOP model (eq. 2) that associates temperature at the top of permafrost with seasonal climate properties (*nt*, scaling factor between summer air and ground surface temperature; *nf*, scaling factor between winter air and ground surface temperature; *It*, air thawing index; *If*, air freezing index) and soil properties (*rk*, thermal conductivity ratio of thawed and frozen soil) through time (P).

$$TTOP = \frac{(rk * nt * It) - (nf * If)}{P} \qquad \text{(eq. 2)}$$

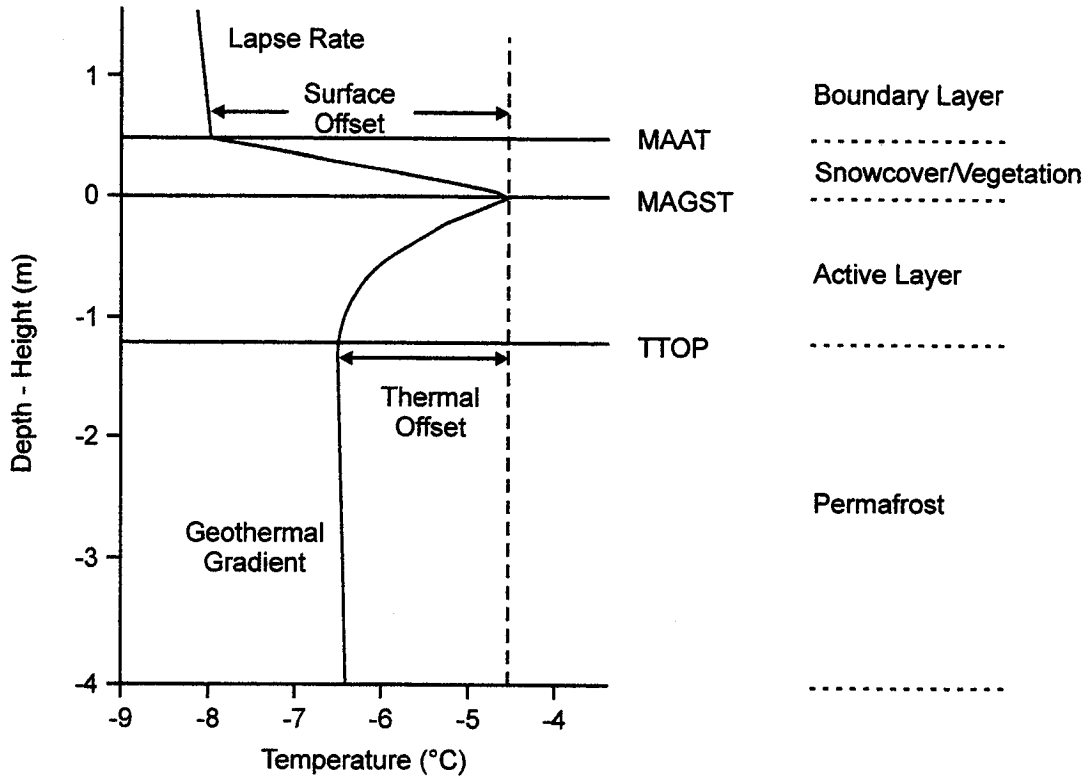

Figure 2.4 - Schematic mean annual temperature profile through the surface boundary layer, showing the relation between air temperature and permafrost temperature (from Smith and Riseborough 2002, Fig.3).

TTOP helps illustrate the varying microclimatological conditions that can influence energy exchanges between the atmosphere and the ground and can account for permafrost occurrence at one location but not at another. These local conditions can be divided into factors that affect the surface offset and those that affect the thermal offset (*rk*) (Fig. 2.4). The surface offset is the difference between the MAAT and the mean annual ground surface temperature due to surface cover. The surface cover has a summer component of vegetation and the ground surface organic material, and a winter component of snow cover. The vegetation and snow cover effects are frequently represented by n-factors (e.g. Lunardini 1978; Jorgenson and Kreig 1988; Klene *et al.* 2001).

The thermal offset describes the difference in mean annual temperature between the top of permafrost and the ground surface. Due to changes in ground thermal properties associated with freezing and thawing, the ground surface is often warmer than the top of permafrost (Burn and Smith 1988). In combination, these two offset conditions may cause large variations in mean annual ground temperatures in areas with relatively uniform climate (Nelson *et al.* 1998) (Fig. 2.4).

There are five major factors that influence the surface offset and the thermal offset and hence the ground thermal regime. The effects of vegetation, organic layer, and snow cover in modifying the air-ground temperature relation will be discussed, followed by an examination of the influence of soil properties and topography on the microclimate and hence the ground thermal regime. Many of these factors that influence the spatial distribution of permafrost are interrelated. Both positive and negative feedback loops may complicate seemingly simple relations.

2.4.1. Vegetation and Organic Layer

Local variation in vegetation composition, the species of plants, and configuration, the three-dimensional pattern of vegetation, can modify the temperature of the soil throughout the year. The primary effect of tree and shrub vegetation is to shield the ground surface from incoming solar radiation during the summer (Brown and Péwé 1973) and to affect the distribution and persistence of snow in winter (Luthin and Guymon 1974; Rouse 1984). Veireck (1965) has shown that individual white spruce trees may alter the energy exchange at the ground surface sufficiently for a small area of permafrost to exist around the base of trees in an area where permafrost is otherwise absent. The soil beneath a tree may be cooler than the area between trees because of lower snow accumulation and a thicker moss layer beneath the boughs (Veireck 1965). Although shrubs shade the ground surface, some of this cooling may be offset by the accumulation of snow that is blown from areas of low vegetation cover and becomes trapped in adjacent shrubs (Smith 1975; Rouse 1984; Sturm and Holmgren 1994).

Although the broad effect of vegetation is cooling of the ground surface due to shading, the density, shape and height of trees may also modify the ground surface wind regime leading to a slight warming in some terrain types. Near surface wind speeds, and hence convective heat transfer away from the surface, are lower in areas with dense vegetation growth compared to locations where trees are sparse or absent (Brown and Péwé 1973). This may lead to lower air and ground temperatures in areas of sparse tree growth (Brown and Péwé 1973).

At the ground surface, the presence of organic material, particularly peat, protects the soil from atmospheric heat and is thus usually associated with the existence of

permafrost in marginal areas (e.g. Brown 1963; French 1996, 66). Peat layers have a year-round influence on the ground thermal regime because their thermal conductivity may vary seasonally as the moisture content changes. During the summer, evaporation dries the surface layers of peat resulting in a low thermal conductivity, so that the warming of the ground is impeded. In the fall, thermal conductivity of the peat increases and rapid ground cooling may occur as the peat becomes saturated from increased precipitation and decreased evaporation. When the peat freezes in winter, many of the interstices become filled with ice, of relatively high thermal conductivity, which further promotes soil cooling (Luthin and Guymon 1974). The importance of the peat/moss/organic soil layer has been documented by a number of researchers. For example, Williams and Burn (1996) found a threshold thickness of 11 cm for this horizon was diagnostic for predicting the presence of permafrost in central Yukon. In a study along an altitudinal transect on the north-slope of a mountain near Kluane Lake, Yukon Territory, Harris (1987) found that active-layer thicknesses decreased as the organic-layer thickness increased.

The broad result of increased vegetation, independent of other physical factors, is a cooling of the soil and a decrease in active-layer thickness. This relation was demonstrated by Price (1971) for mountainous terrain in SW Yukon where the active layer was thinnest and most variable on southeast-facing slopes in association with dense vegetation in contrast with nearby north-facing slopes, which received less solar radiation and had less vegetation.

2.4.2. Snow Cover

Snow cover affects the regional and local distribution of permafrost and active layer thickness, as well as the ground thermal regime, by seasonally interposing a layer of low conductivity between the ground surface and the air (e.g. Smith 1975; Nicholson 1976; Goodrich 1982; Desrochers and Granberg 1988; Mackay 1993). With low thermal conductivity values ranging from 0.086 W m^{-1} K for loose new snow to 0.340 W m^{-1} K for dense snow (Table 2.1), snow limits the heat loss from the ground during the coldest part of the year and also serves to retain the heat introduced in summer.

The thickness of the snow cover is also important in limiting ground heat loss in winter. The snow cover thickness increases the effective depth below the surface of a point in the ground. Therefore, cold air is less effective at cooling the ground at depth as snow cover increases because the cold winter temperatures are dampened within the snow (Fig. 2.5).

In addition to snow density and thickness, the timing of snowfall is of importance to ground temperature (e.g. Mackay and MacKay 1974; Smith 1975; Goodrich 1982). A heavy snowfall in early autumn will inhibit frost penetration, whereas a late snowfall or low accumulation will allow frost to penetrate further into the ground. On the other hand, although a thick snowcover will minimise frost penetration, it will also delay ground thawing in the spring because the snow will take longer to melt. The ground surface beneath the snow is at or below 0°C for as long as the snow cover is present. Therefore, the longer the ground is covered by snow, the shorter the length of the thaw season in the ground (Vonder Mühll *et al.* 1998).

Table 2.1. Comparison of thermal conductivity of materials found in a natural soil environment and of fresh and compacted snow.

Material	Thermal conductivity ($W\ m^{-1}\ K^{-1}$)
Air	0.024
Water (at 0°C)	0.602
Ice (at 0°C)	2.22
Quartz	8.8
Clay minerals	2.92
Peat – dry	0.05
Peat – saturated unfrozen	0.5
Peat – saturated frozen	2.00
Snow – fresh	0.086
Snow – compacted	0.340

Sources: Williams and Smith 1989, Table 4.1 and French 1996, Table 5.3

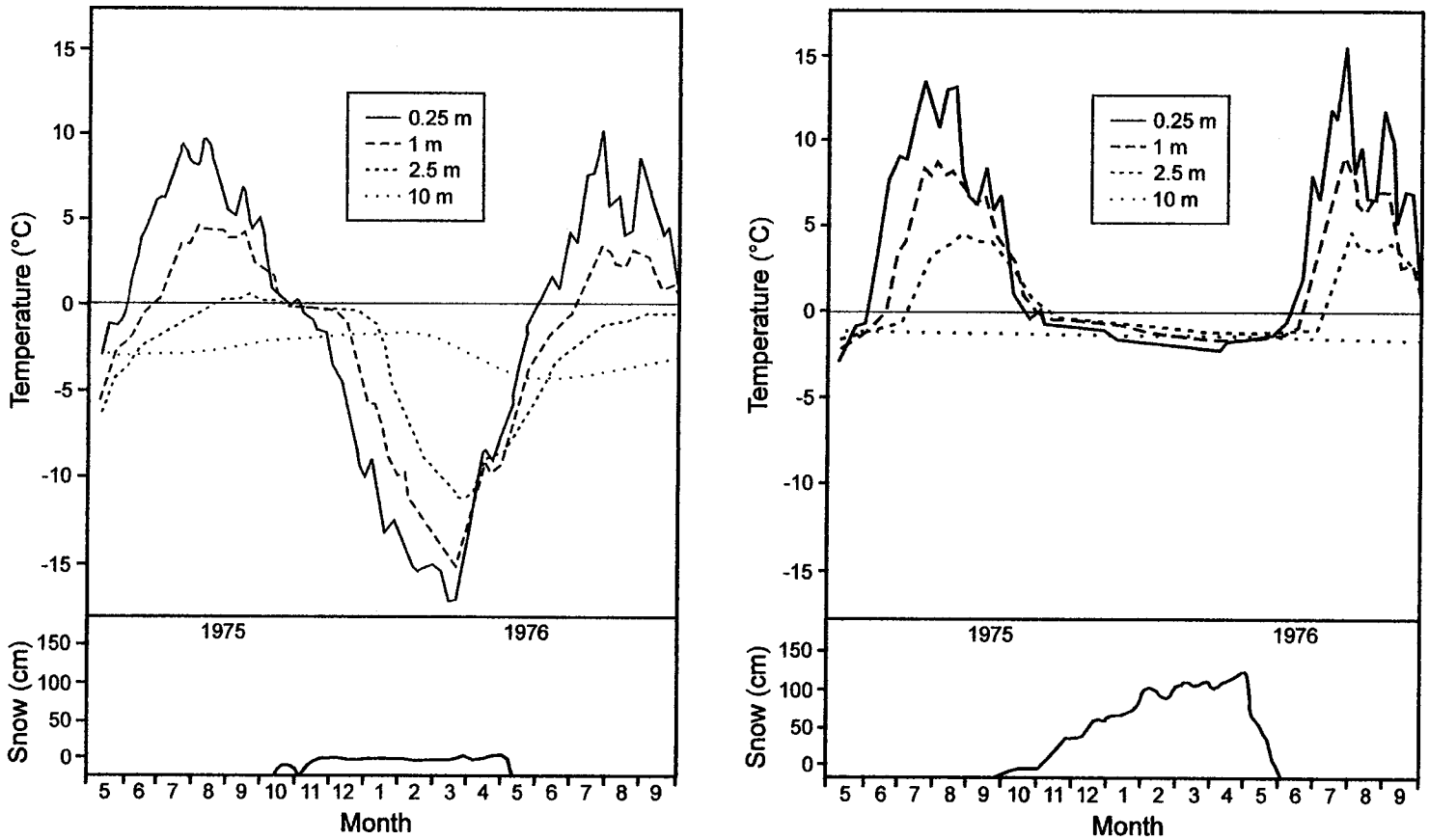

Figure 2.5 - Annual temperature variations at two sites of contrasting snow cover, Schefferville, Québec (modified from Nicholson 1978, Fig. 1).

Field observations have shown that the presence of snow cover leads not only to higher ground temperatures in winter, but also on a mean annual basis (Smith 1975). For example, in the Fort Simpson region, NWT, the mean annual ground surface temperatures range between 0.7 and 1.3°C while the MAAT is approximately –4°C (Burgess and Smith 2000). These warm ground surface temperatures relative to air temperature are attributed to the snow cover properties in this region.

Recent numerical modelling (Riseborough 2001; Smith and Riseborough 2002), as well as field observations (Burn 2000), have shown that snow cover of a given depth has a greater influence on mean annual ground surface temperature as the MAAT increases. In general, the active layer is thicker in areas with warmer air temperatures. The ground cannot become extremely cold until freeze-back is complete, which generally takes longer in ground with a thick active layer than a thin one, given the same air temperature.

In most permafrost regions, the period in which the ground is covered with snow is longer than the snow-free period. This has led Smith and Riseborough (2002) to suggest that in permafrost areas, the nival offset has a greater influence on the ground thermal regime than the vegetation offset. It is difficult to fully evaluate this hypothesis because the majority of field data originate from the summer season, since field work in northern Canada is more difficult in winter.

2.4.3. Soil Thermal Properties and Drainage

Differences in the thermal properties and moisture content of soils can also lead to variations in the occurrence and thickness of permafrost and the thickness of the active

layer. The rate of heat transfer into and out of the soil depends on the thermal conductivity, the ability of a material to transmit heat by conduction. The thermal conductivity of ice is four times that of water (Gold and Lachenbruch 1973); therefore frozen soils have higher thermal conductivities than unfrozen soils. No single value for thermal conductivity of a frozen soil can be given because the proportion of ice versus water in a volume of soil is temperature dependent and the unfrozen water content is also influenced by soil texture (Williams and Smith 1989, 89).

This change in thermal conductivity between the frozen and thawed state can lead to a thermal offset (Goodrich 1978; 1982). Burn and Smith (1988) documented an offset from 0.4 to 1.7°C between 10 cm and the base of the active layer, where the coldest mean annual ground temperature occurs, at seven sites near Mayo, YT. The observed thermal offset range represented dry and wet soil conditions, where the seasonal variation in thermal conductivity is relatively small and large respectively. The thermal offset explains why equilibrium permafrost can be present at locations where the mean annual ground surface temperature is above 0°C (Smith and Riseborough 1996).

The volumetric heat capacity of a soil is the amount of heat required to raise the temperature of a unit volume by 1°C. Heat capacity can be closely approximated by the sum of the heat capacities of the proportion of soil particles, water, ice and air. Therefore it is also affected by soil texture, mineral composition, bulk density and water content. Most dry soils have similar heat capacities because quartz, feldspar and clay minerals, the common soil mineral components, have heat capacities of 800-900 J kg^{-1} K^{-1} (Williams and Smith 1989, 91). The heat capacity of a soil increases linearly with an increase in

soil moisture due to the high heat capacity of water compared to other materials (Williams and Smith 1989, Table 4.1). Therefore, a wet soil requires more heat to raise its temperature than a dry one.

When a phase change takes place, the soil's *apparent heat capacity* includes the effects of latent heat that is consequently released or absorbed (Williams and Smith 1989, 92). During freeze-back of the active layer, latent heat is released as the freezing front advances and water turns to ice. The release of latent heat produces a "zero-curtain effect" in which soil temperatures remain near 0°C for an extended period of time despite cold temperatures at the ground surface (Outcalt *et al.* 1990). Once the zero-curtain has closed and the water is converted to ice, conductive processes dominate the heat transfer and the soil cools more rapidly.

The rate at which a temperature wave penetrates into the ground is defined by the soil's thermal diffusivity. Thermal diffusivity is the ratio of thermal conductivity to heat capacity. Water content greatly affects the diffusivity of a soil. At low soil moisture contents, the thermal conductivity increases more rapidly than the heat capacity, resulting in an increase in diffusivity with an increase in water. When the soil moisture content is high, the conductivity varies little with addition of water while the heat capacity continues to increase at a constant rate, which may cause the diffusivity to decrease. Figure 2.6 illustrates the relation between soil moisture and diffusivity for three soil types. It is interesting to note the consistently low diffusivity of peat below 80% volumetric moisture content, which accounts for its insulating properties.

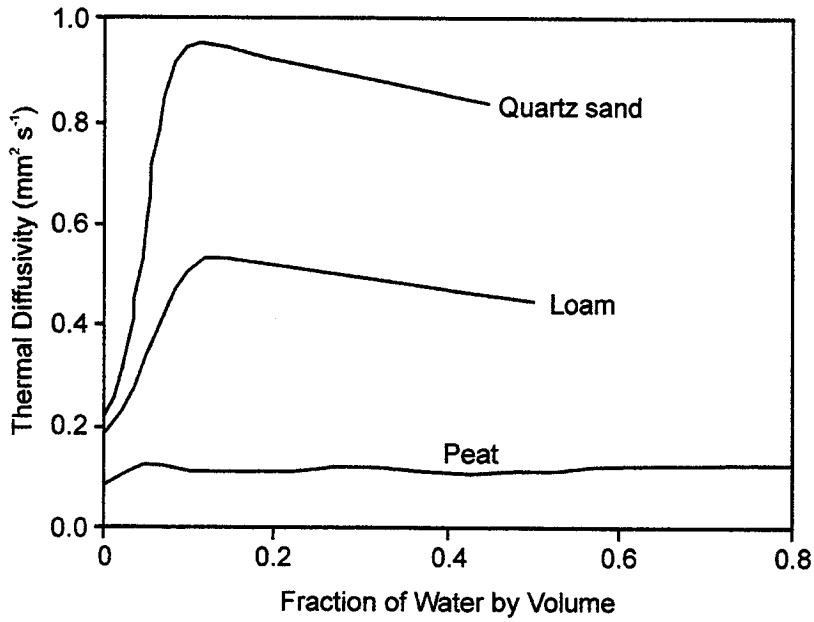

Figure 2.6 - Thermal diffusivity versus water content for three soil types (Farouki 1981, Fig. 77).

Many of the thermal properties of soil are related to soil moisture content, soil texture and drainage. In general, fine-textured silt and clay soils tend to be poorly drained compared to coarse textured sand and gravel soils. The low moisture content of sands and gravels results in low heat capacity and low latent heat effects, and therefore are more likely to be either permafrost free or associated with permafrost beneath relatively thick active layers.

2.4.4. Topographic Influences

In areas with varying topography, nearly every climate element is influenced by elevation (Wahl *et al.* 1987, 34). Patterns of solar radiation received at the ground surface, air temperature, and the spatial and temporal distribution of precipitation are the primary climate parameters that are of particular concern when investigating permafrost in mountainous terrain. These variables are all interrelated through variations in slope angle, aspect and elevation.

Slope aspect and angle create local variations in the amount of solar radiation received in areas with varying relief (Ives 1973). In the northern hemisphere, steep, north-facing slopes receive the least amount of direct solar radiation throughout the year. For example, at 65°N a 30° north-facing slope will receive approximately 40% less solar radiation on an annual basis and a 30° south-facing slope will receive about 45% more solar radiation annually than a horizontal surface at the same latitude (Kondratyev and Federova 1977). In areas of discontinuous permafrost, this may result in permafrost occurring on north-facing slopes, but not on adjacent slopes facing south (e.g. Brown and Péwé 1973; Funk and Hoelzle 1992). In the continuous permafrost zone, permafrost may

be thicker and the active layer thinner on north-facing slopes (French 1970). However, variations in vegetation and snow conditions may alter this general trend (Price 1971; Dingman and Koutz 1974). Adjacent topography also creates shading effects in dissected mountainous terrain (Wahl *et al.* 1987, 24). These shadow effects are most pronounced in the valley bottoms and can result in lower than expected amounts of solar radiation in these areas. In high-latitude regions, differences in topographic shading are most apparent in winter when incoming solar radiation is low.

In general, the amount of precipitation that reaches the ground surface increases with elevation, often with substantial difference between the windward and leeward side of a mountain or even a small hill (Barry 1992, 232). In winter this pattern may be difficult to observe because topography and microtopography, particularly above tree-line, may control the redistribution of snow by wind causing accumulation in depressions and lower snow cover on mounds. This can influence the distribution of permafrost, active-layer thickness and ground temperatures (Mackay and MacKay 1974; King 1990). Changes in microtopography can also influence moisture content and vegetation cover, which in turn affect permafrost occurrence.

The proportion of annual precipitation falling as snow also increases with elevation as autumn begins earlier and spring arrives later than at lower elevations, influencing the length of time the ground is exposed directly to the atmosphere (Barry 1992, 239). This reduces the period when the ground is exposed to temperatures above freezing which may affect the distribution of permafrost and the thickness of the active layer.

Two major climatic phenomena that influence air temperature occur in mountainous regions, particularly in winter (Barry 1992, 331-36). First, mountain ranges can act as physical barriers to the incursion of air masses. The most prominent example of this in Yukon is the immense St Elias Mountains in the southwest corner of the Territory. These mountains are an effective block to warm, moist Pacific air entering Yukon and result in a marked difference in air temperature, as well as precipitation, between the coastal maritime conditions and the interior continental regime (Wahl *et al.* 1987, 35). A second climatic occurrence in mountainous areas is cold-air drainage, when a shallow mass of cold, dense air slides downhill under the influence of gravity (e.g. Harris 1982). If the cold air remains in the valley bottoms for a sufficient length of time or if these cold-air drainage events occur frequently enough, MAATs and, therefore, permafrost distribution may be affected (Harris 1988, 384).

Taylor *et al.* (1998) studied the effect of temperature inversions, when air temperature increases with elevation, on ground surface temperatures and permafrost near Norman Wells, NWT (65°17′N, 126°46′W), using both radiosonde data from the Environment Canada weather station at the town site (60-90 m ASL) and paired air and shallow ground temperature instruments at four elevations (469 m, 620 m, 800 m and 969 m ASL) on nearby Mt. Hamar. Early morning radiosonde data for the 1996-1997 year revealed a strong inversion of +8°C km^{-1} below 300 m and a weak inversion of +1.6°C km^{-1} from 300 to 1000 m. The mean annual air temperatures at all four elevations were substantially higher than expected under normal atmospheric lapse conditions (Taylor *et al.* 1998, Fig. 1b). The mean strength of all inversion events recorded from fall 1996 to spring 1997 was 4.7±0.3°C between 75 and 469 m ASL, with a mean duration of 3.0±0.5

days. The mean annual ground temperatures at 3 to 7 cm depth were also influenced by the inversions. At 500 m ASL the mean annual ground temperature was at least 1°C higher than in the valley bottom. Above treeline, at ~575 m, ground temperatures abruptly decreased to below –4°C, compared to –1.6°C in the valley bottom, due to the minimal vegetation and reduced snow cover. The persistent air temperature inversion appears to pinch out or reduce the permafrost thickness in the mid-elevation forested region to less than 50 m from 52-62 m of permafrost in the valley bottom. Springs and icings that were observed around 100 m ASL were cited as evidence for taliks perforating thin permafrost. Taylor *et al.* (1998) also speculated that permafrost thickness may increase above treeline and reach 200-300 m at the summit of Mt. Hamar.

2.5. Chapter Summary

This chapter summarizes the primary factors that influence the distribution of permafrost at various spatial scales. In both mountainous and non-mountainous terrain, climate is the primary influence on the occurrence of permafrost with variations in vegetation cover, organic layer thickness, snow depth, and soil moisture also affecting the ground thermal regime and the occurrence of permafrost.

In areas with varying topography additional factors must be considered that may influence the distribution of permafrost. First, cold-air drainage and winter temperature inversions are unique components of the climatic system in mountainous regions, particularly at high-latitude. In addition to vegetative shading, variations in aspect and topographic shading influence the amount of solar radiation received at the ground surface, which may also alter ground thermal regimes. Finally, slope angles vary in

mountainous terrain, with steep slopes generally resulting in good soil drainage and gentle slopes having poorer drainage. Drainage conditions in turn may influence soil moisture conditions and the occurrence of permafrost.

The following chapters of this thesis will document the methods used and results obtained in determining the occurrence of permafrost in a mountainous area of central Yukon.

CHAPTER 3
THE STUDY AREA

3.1. Introduction

This chapter describes some principal characteristics of the study region and area, including topography, vegetation, soil and permafrost conditions. A climate summary, including an analysis of temperature inversions, which are characteristic of the area, is also presented.

3.2. Physical Characteristics of the Yukon Plateau-North Ecoregion and the Keno Study Area

The study area is located in central Yukon Territory, in the quadrangle defined by approximately 63°58′N, 135°31′W and 63°53′N, 135°04′W (Figs 3.1 and 3.2). The only settlement in the study area is the hamlet of Keno, which is situated about 60 km northeast of the town of Mayo. This area is located within the Yukon Plateau-North Ecoregion at the northern limit of the Boreal Cordillera Ecozone that covers the mid-section of the Canadian Rocky Mountain system from northern British Colombia to central Yukon Territory (Wiken *et al.* 1996; Marshall and Schut 1999).

The terrain in this ecoregion includes rolling uplands, small mountains, and nearly flat tablelands dissected by deeply cut U-shaped valleys (Marshall and Schut 1999). The Gustavus Range, the dominant mountain range in the study area and surroundings, has numerous peaks over 1800 m with the highest being Mount Hinton at 2050 m (Fig.3.3). The mean annual air temperature for the ecoregion is approximately -4°C, with long

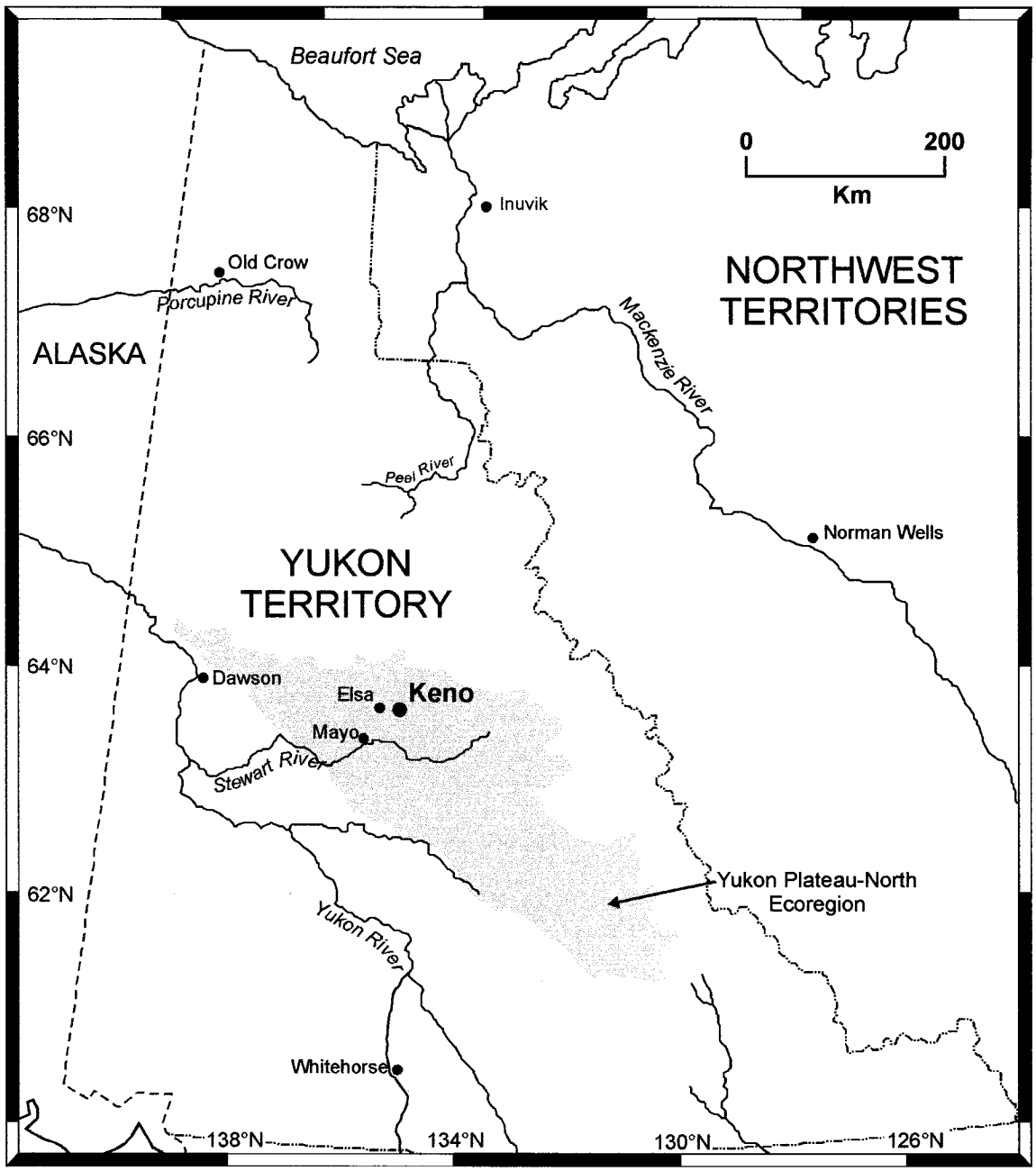

Figure 3.1 - Map of Yukon Territory and adjacent portions of Northwest Territories. The communities of Mayo, Elsa and Keno are identified in relation to other major communities and features in the Territory.

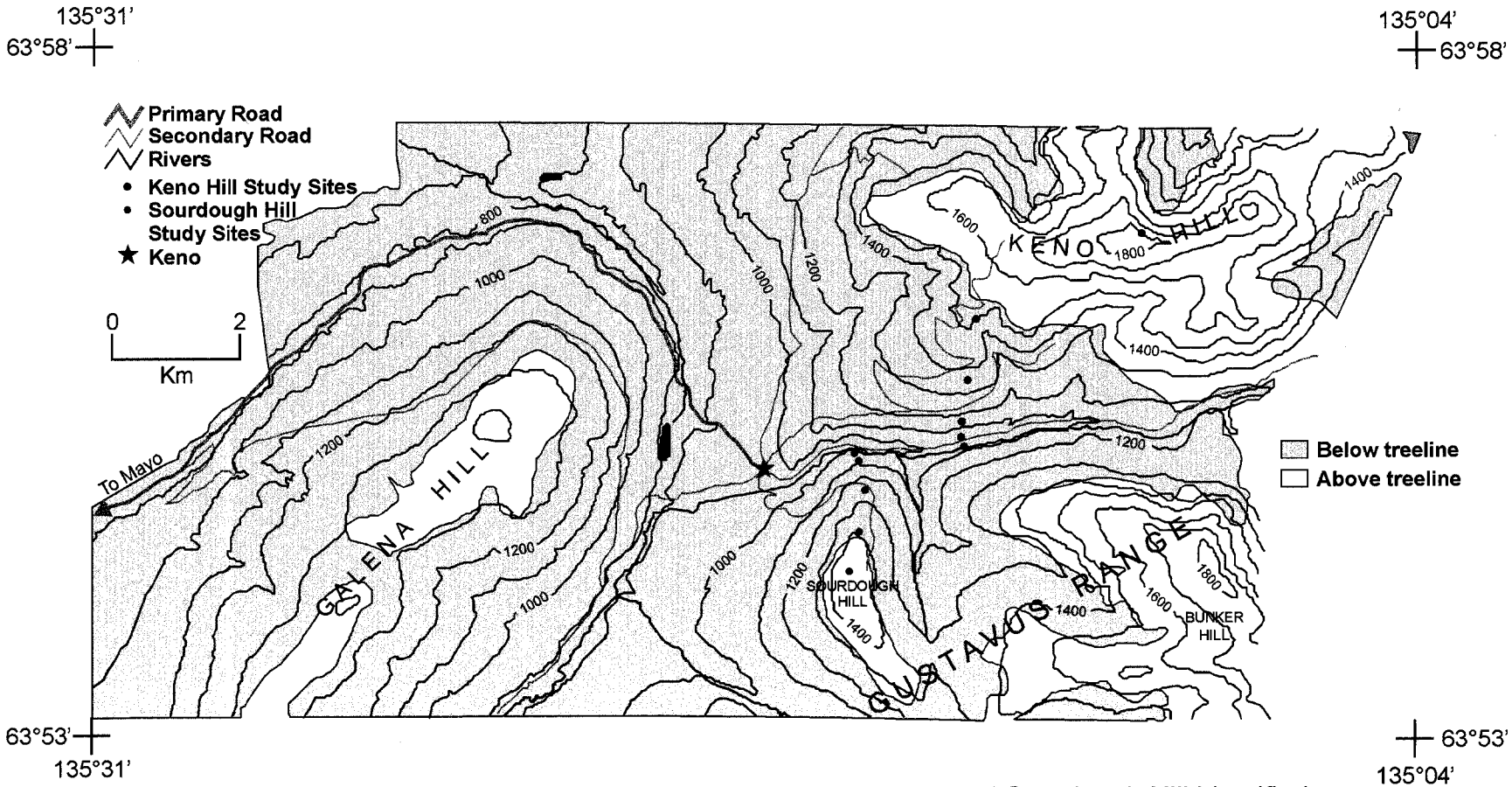

Figure 3.2 - Keno study area with eleven study sites on Keno Hill and Sourdough Hill identified. Contour interval is 100 m (Source: NTS sheet 105M/14).

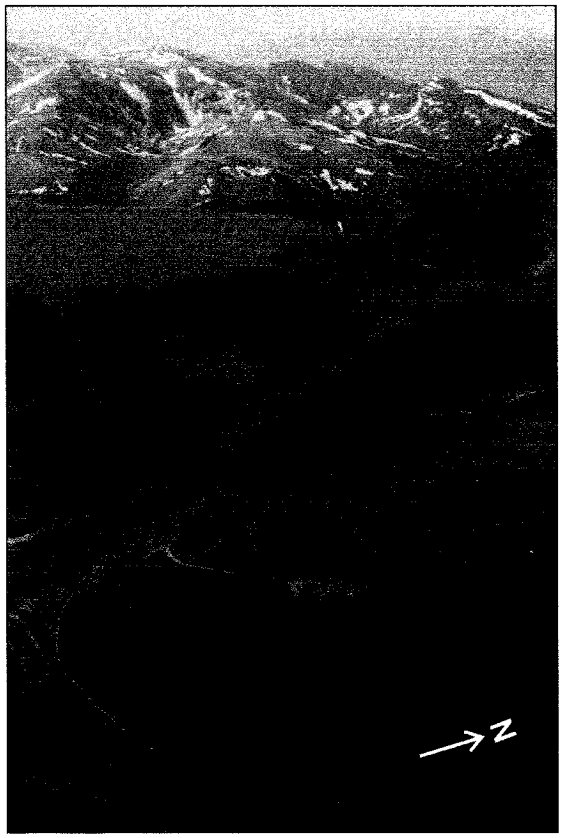

Figure 3.3 - Landscape of the Keno area. Note the rolling hills in the foreground and mountains of the Gustavus Range in the background.

(October to April) winters dominated by cold, dry continental arctic air and short warm summers (Marshall and Schut 1999). Mean annual precipitation ranges from 300 mm in the major valleys to 600 mm in the mountains where the study area is located (Marshall and Schut 1999).

Northern boreal forests, dominated by white spruce (*Picea glauca*), mixed with willow (*Salix* spp.), birch (*Betula* spp.), and ericaceous shrubs, occur at elevations up to 1500 m. Stunted black spruce (*Picea mariana*) and a thick moss ground-cover are found on poorly-drained sites. In subalpine areas, the transition zone from full-grown, dense forest to open alpine tundra (Löve 1970), groups or krummholz of alpine fir (*Abies lasiocarpa*) are interspersed amongst shrub vegetation. Alpine tundra vegetation consists of mountain avens (*Dryas* spp.), dwarf willow, dwarf birch (*Betula glandulosa*), ericaceous shrubs, graminoid species, and mosses.

The ecoregion lies within the zone of extensive discontinuous permafrost where 50 to 90% of the terrain is underlain by permafrost, except along the southwest edge of the region where the sporadic discontinuous permafrost zone occurs (Heginbottom *et al.* 1995; Marshall and Schut 1999). The two principal soil types in this ecoregion are Turbic Cryosols and Eutric Brunisols (White *et al.* 1994), although field investigations for this project encountered Dystric Brunisols in the Keno area (see section 4.3.3).

Cryosolic soils are formed in either mineral or organic material that have permafrost either within 1 m of the soil surface or within 2 m if there is strong cryoturbation (Soil Classification Working Group 1998, 73). Cryosols have a mean annual temperature of $\leq 0°C$ at a depth of 0.5 m. Turbic Cryosols develop primarily in mineral material and have evidence of cryoturbation either at the ground surface in the

form of various types of patterned ground, or mixing of both mineral and organic material from different horizons within the soil profile.

Soils of the Brunisolic order have a weak degree of soil development that excludes them from the Regosolic soil order of undeveloped soils (Soil Classification Working Group 1998, 53), yet have insufficient horizon development to be classed in other orders. Brunisols form in well to imperfectly drained soils under a variety of vegetative and climatic conditions including boreal forest, shrubs and grass, and heath and tundra. Eutric and Dystric Brunisols are distinguished by their pH. Eutric Brunisols have a relatively high level of base saturation as indicated by the requirement for a pH of 5.5 or greater whereas Dystric Brunisols have low base saturation and a pH of less than 5.5.

As on most slopes in the study area, Keno Hill and Sourdough Hill are covered with Pleistocene and Holocene colluvial deposits of diamicton, gravel, shattered bedrock and lenses of sand and silt derived from the physical and chemical weathering of bedrock and surficial materials (Bond 1998). The valley bottoms are covered with a mix of late Pleistocene glacial till veneer and glaciofluvial deposits with Holocene alluvial plains, terraces and complexes of coarse sand and gravel along the modern valley drainage routes. Rock outcrops occur at the top of Keno Hill and on other mountains in the Gustavus Range.

3.3. Climate

The main factor that determines the climate of central Yukon is its geographical location. The area is situated between 63 and 64°N latitude. This results in large

seasonal variability in the amount of solar radiation received, from nearly continuous incoming energy at the summer solstice to very low amounts at the winter solstice (Wahl *et al.* 1987, 23).

Topography not only plays an important role at a broad scale in creating the climate of central Yukon, but it also influences climate at a local scale. Slope angle, the steepness of the slope, and aspect, the direction of the slope, have fundamental effects on the amount of direct and diffuse radiation received at the ground surface, and thus on local temperature conditions. Aspect controls what time of day the ground receives solar radiation, whereas the slope controls the intensity of the incident radiation (Wahl *et al.* 1987, 86). South-facing slopes receive more solar radiation than other slopes, especially those facing north. East-facing slopes are exposed to warming as the sun rises, but may be shaded from noon onwards, whereas steep west-facing slopes are shaded most of the morning and are exposed to maximum solar radiation in the late afternoon. In mountainous or hilly terrain, shading of one hillslope by another can also influence the amount of solar radiation received at a location.

Mayo Airport is the only long-term weather station in the area for which 30-year climatic normals can be calculated. The mean annual air temperature at Mayo is -3.6°C and mean annual precipitation is 318 mm, most of which falls in summer (Fig. 3.4) (Environment Canada 1993). The nearby communities of Elsa and Keno have short climate records, which coincide with the Mayo record for 1974-1982 (Environment Canada 1994). Temperature data for these three stations show no difference in mean annual temperature between Mayo and Elsa, and a slightly lower temperature for Keno (Table 3.1). Examination of mean monthly temperatures for the three stations reveals

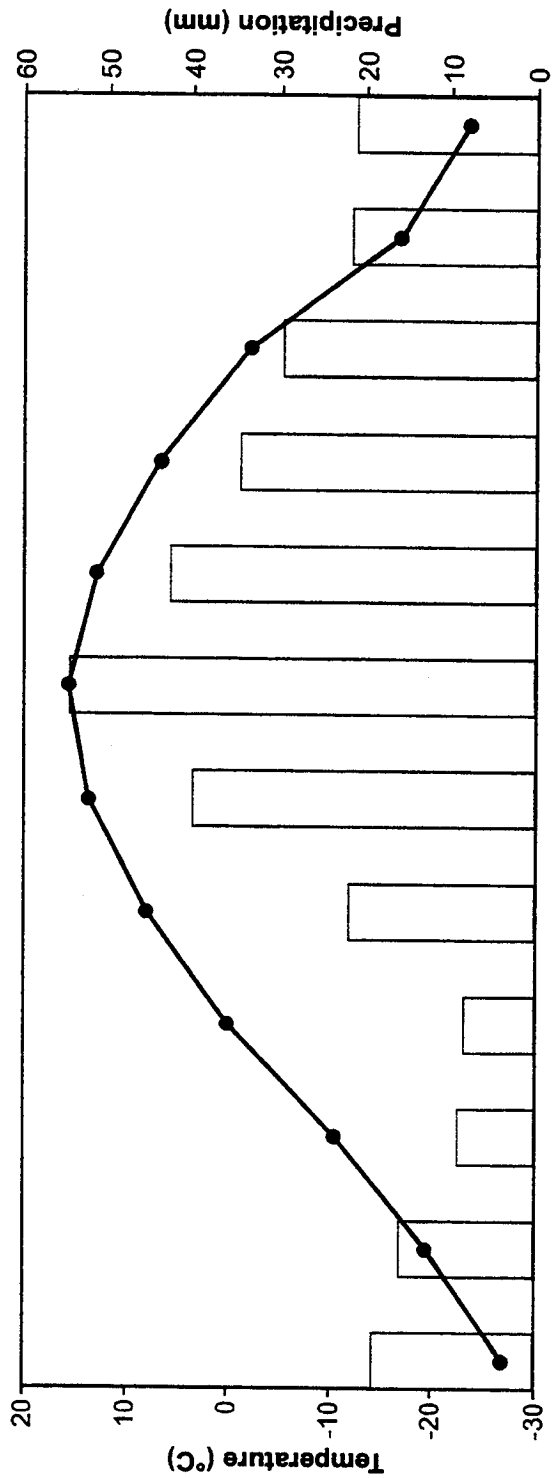

Figure 3.4 - 1961-90 climatic normals for mean monthly temperature (line) and precipitation (bars) from Mayo Airport, central Yukon (Environment Canada 1993).

Table 3.1. Climate comparison of Mayo, Elsa and Keno, central Yukon from 1974 -1982 data. Expected mean annual temperature calculated using normal lapse rate and Mayo mean annual temperature.

	Mayo (504 m)	Elsa (914 m)	Keno (1472 m)
Mean Annual Temperature (°C)	-2.9	-2.9	-3.9
Expected Mean Annual Temperature (°C)	-2.9	-5.4	-8.7
Total Rainfall (mm)	211.4±14.7	212.4±10.5	266.4±19.9
Total Snowfall (cm)	112.7±10.5	180.4±8.8	285.9±16.3
Total Precipitation (mm)	324.1±15.8	392.7±6.4	552.3±31.4

that lower elevations are colder from October to February, but warmer the rest of the year (Table 3.1). Figure 3.5 shows that there is more inter-annual variation in mean monthly temperature in the winter months than the other months. An increase in total precipitation, particularly snowfall, occurs with an increase in elevation (Table 3.1).

The snow cover at higher elevations, particularly above treeline, is redistributed by wind resulting in local snow accumulation in depressions and deflation on hilltops. This contrasts to the apparent relatively uniform spatial distribution of snowcover at lower elevations where there is a continuous forest cover.

Winds in the area are generally light (Environment Canada 1993), although they tend to increase in velocity with elevation due to a decrease in the frictional effect of the terrain on the motion of the air (Barry 1992, 60).

3.4. Winter Temperature Inversions

Under normal conditions, average temperature decreases with height at the mean environmental lapse rate of approximately -6°C km^{-1} (Oke 1987, 45). A temperature inversion occurs when there is an increase in air temperature with height (Billelo 1966). Temperature inversions occur in the atmospheric boundary layer, the lowest part of the troposphere, where the wind, temperature and humidity are influenced by the ground surface (Hartmann 1994, 92). The depth of the layer is commonly about 1 km, but can range from approximately 20 m to several kilometres. Turbulent motion, generated by mechanical forces such as wind or by thermal convection from solar heating, transports mass, momentum and energy through the boundary layer. When the boundary layer is unstable, i.e., there is a lot of turbulence, the layer becomes well-mixed, and momentum,

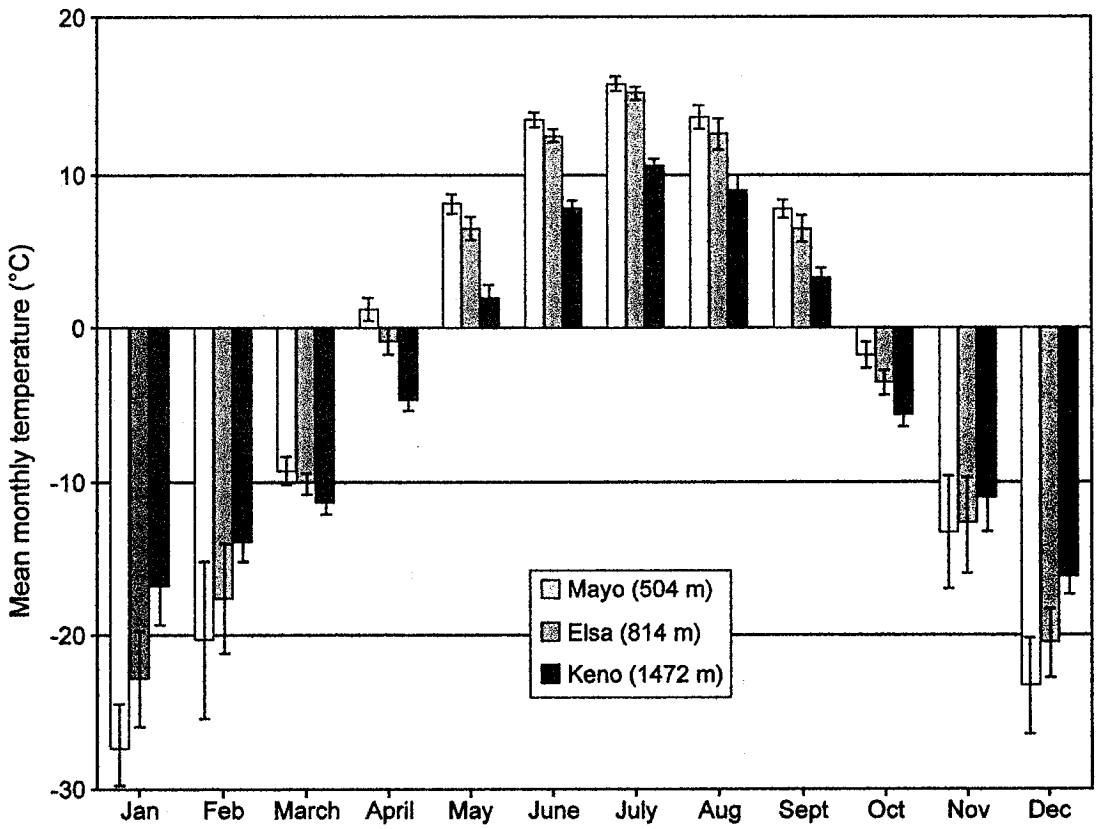

Figure 3.5 - Mean monthly temperature and standard deviation comparison of Mayo, Elsa and Keno, central Yukon for common and complete months.

heat and moisture are independent of height. When the boundary layer becomes stable, temperature inversions can develop.

Three types of temperature inversions can occur over limited vertical distances and usually last only a few hours. The most common temperature inversions occur at night when long-wave emission cools the ground surface more rapidly than the air above it (Barry 1992, 45; Bradley *et al.* 1992). On nights when there is little or no cloud cover and it is calm, the boundary layer may become stable as cold, dense air is trapped near the ground surface. Large-scale subsidence in an anticyclonic weather system, and advection of a warm air mass over a colder ground surface can also create temperature inversions, although these are less frequently observed (Barry 1992, 45).

In Arctic and sub-Arctic environments, winter temperature inversions occur frequently and commonly persist for several days or longer in the no- or low-sun period due to the seasonal radiative imbalance (Bradley *et al.* 1992). Katabatic winds, the gravity-induced downslope flow of cold, dense air due to radiative cooling near the ground surface, result in the pooling of cold air in valley bottoms (Barry 1992). With little incoming solar radiation in winter, the cold-air drainage is not reversed by daytime anabatic flow, leaving the cold air to remain in the valleys for extended periods, producing a temperature inversion.

Although few data have been published on winter temperature inversions in central Yukon, there are some observations from the High Arctic (>70°N), where surface-based inversions were found to occur for >70% of winter (December to March) days (e.g. Kahl 1990; Bradley *et al.* 1992; Kahl *et al.* 1992). The temperatures at the top

of the inversion layer were found to be 8-10°C warmer on average than at the ground surface, but the difference reached >30°C on individual days.

The winter inversion can develop over the Yukon anytime from late October to early March. In central Yukon, high-pressure systems dominate the winter months, producing long periods of calm wind and clear skies that favour the development and maintenance of temperature inversions (Wahl *et al.* 1987, Fig. 7.1). The temperature inversion is most extreme in December, January and early February when limited amounts of solar radiation are received due to low sun angles. For example, Burn (1993) compared the mean daily minimum temperatures from January 28 to February 6, 1975 at Mayo, Elsa and Keno, which are separated by a horizontal distance of approximately 60 km and a vertical interval of 968 m, to illustrate winter temperature inversion conditions in central Yukon (Fig. 3.6). The mean daily temperature is affected by the inversion, with a much colder mean daily January temperature at Mayo of -29.0°C (30-year normal) compared to -19.6°C (adjusted normal based on six-year record) at Keno (Environment Canada 1982). Persistent inversions can also affect the mean annual air temperature for stations at different elevations (Fig. 3.7): in the Mayo-Elsa-Keno temperature transect, the observed mean annual temperature is warmer than what would be expected under normal lapse conditions of –6.0°C km^{-1} (Table 3.1).

To investigate the frequency and the strength of inversions in central Yukon, the mean daily temperature records were analyzed from Mayo Airport (504 m ASL, no aspect), the hamlet of Elsa (814 m ASL, NW slope) and the Keno 700 mine (1472 m ASL, S slope) for the recording period 1974-1982, assuming that any increase in

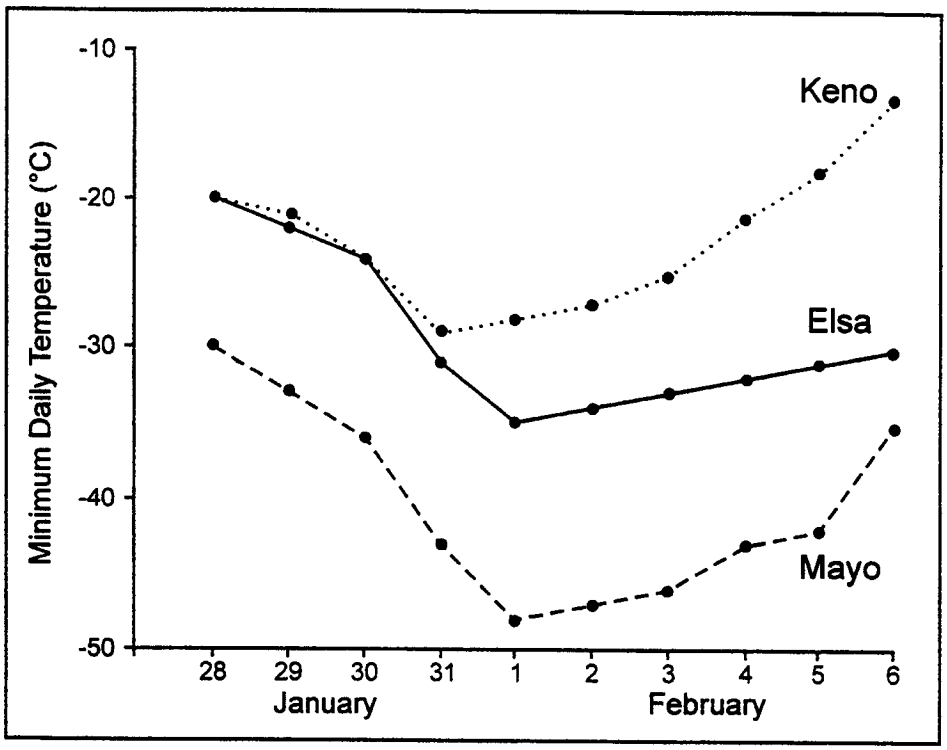

Figure 3.6 - Daily minimum air temperature at Mayo (504 m ASL), Elsa (814 m ASL), and Keno (1472 m ASL), 28 January - 6 February, 1975 (Burn 1993, Fig. 1).

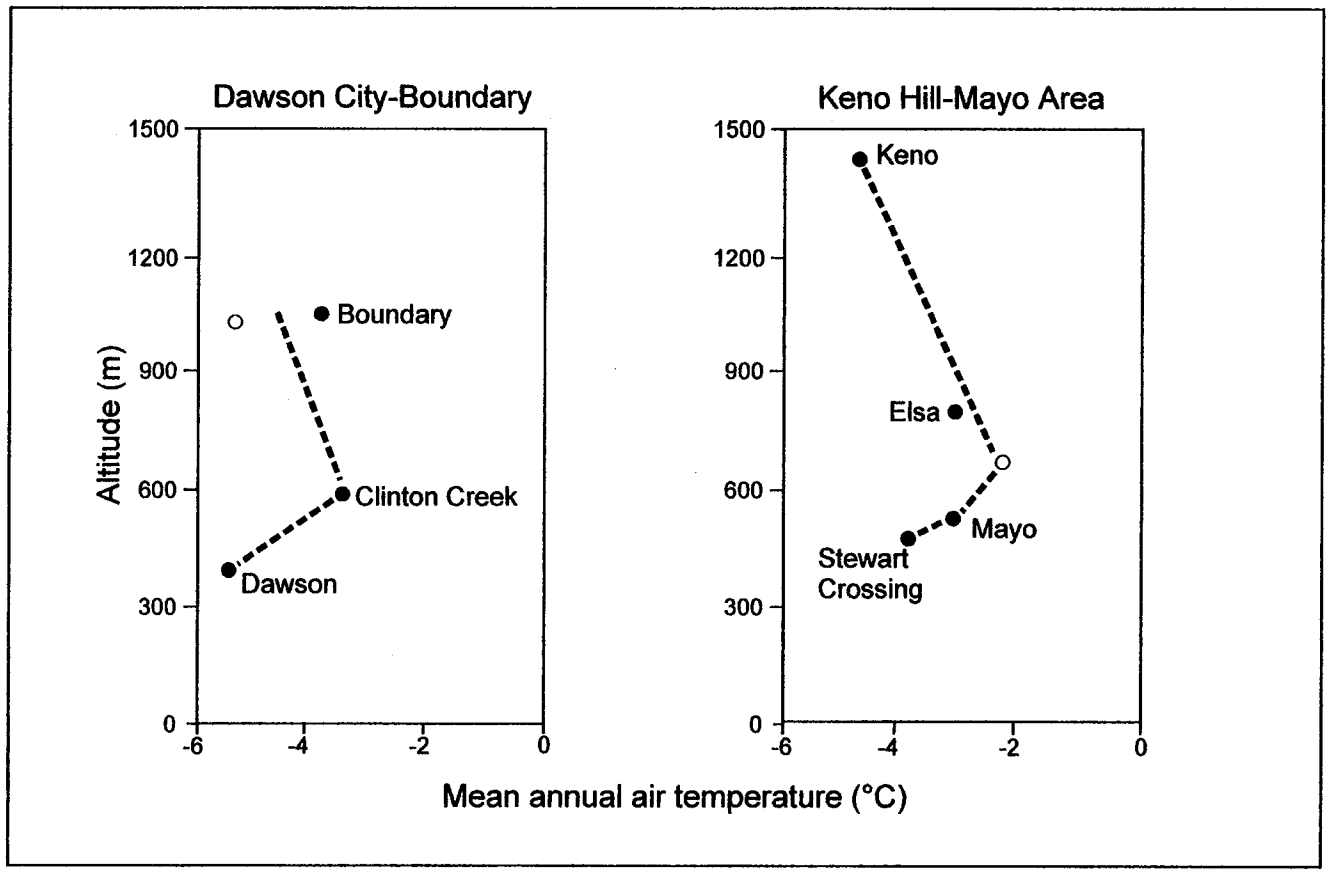

Figure 3.7 - Changes in 1975 and 1976 mean annual air temperature with altitude near Dawson City and Keno, Yukon. Data (filled circles) are from Class A weather stations operated by Environment Canada; open circles are additional unidentified sites (Harris 1983, Fig. 8).

temperature with an increase in elevation represented an inversion (Kahl 1990; Serreze *et al.* 1992). The data were not corrected for the differences in aspect of the recording stations.

Table 3.2 shows the percentage of days with temperature inversions in the Mayo-Elsa-Keno area. As expected, the frequency of temperature inversions is high in winter months (December through February) when there is little solar radiation compared to other months of the year. Weak inversions may occur in the summer months between Elsa and Mayo, possibly due to nocturnal inversions, or differential heating due to differences in slope and aspect. Unfortunately, hourly data required to confirm either of these hypotheses are unavailable (Tables 3.2 and 3.3).

The average strength of inversions was highest during the deep winter months of December, January and February and was more moderate during the winter shoulder months of November and March in all three cases (Table 3.3). The mean frozen season, October to April, inversion was $6.1 \pm 1.3°C\ km^{-1}$ between Keno and Mayo, $6.3 \pm 1.0°C\ km^{-1}$ between Elsa and Keno, and $11.4 \pm 0.9°C\ km^{-1}$ between Elsa and Mayo. The frozen season inversion strength between Elsa and Mayo, a mid-elevational and a valley site, is comparable to the mean frozen season inversion near Norman Wells, NWT, of $12.6 \pm 0.8°C\ km^{-1}$ reported by Taylor *et al.* (1998). The mean duration of the frozen season inversion varied from 3.1 to 4.7 days between the three sites, slightly longer than the average inversion at Norman Wells (3.0 ± 0.5 days) (Table 3.4).

Table 3.2. Frequency (% of days per month) of temperature inversions by month between Mayo, Elsa and Keno, central Yukon, for 1974-1982.

Stations	Jan	Feb	March	April	May	June	July	Aug	Sept	Oct	Nov	Dec
Keno and Mayo	91	75	28	0	0	0	0	0	2	5	60	84
Elsa and Mayo	80	70	26	7	18	28	34	25	24	8	50	70
Elsa and Keno	86	76	29	5	0	0	0	0	7	17	58	77

Table 3.3. Average strength and standard error of inversions (°C km^{-1}) on a monthly basis between different weather stations in central Yukon, 1974-1982. Vertical distance between the stations is also reported.

	Inversion strength and standard error (°C km^{-1})		
Month	Keno and Mayo (968 m)	Elsa and Mayo (310 m)	Elsa and Keno (658 m)
January	12.1±1.8	20.7±1.0	11.1±1.1
February	9.5±1.5	15.8±0.8	8.0±0.9
March	3.2±1.4	8.1±1.0	4.6±1.4
April	-	3.0±0.5	2.2±1.2
May	-	2.6±0.3	-
June	-	4.3±0.5	-
July	-	3.9±0.4	-
August	-	3.2±0.4	-
September	-	3.1±0.4	2.3±1.4
October	1.9±1.7	4.0±0.7	2.2±0.6
November	6.0±1.5	12.0±1.0	6.5±1.1
December	9.1±1.5	16.9±0.9	9.3±1.0
Summer Mean (June to Aug)	0.0±0.0	3.8±0.4	0.0±0.0
Winter Mean (Dec to Feb)	10.2±1.6	17.8±1.0	9.5±1.0
Frozen Season Mean* (Oct to April)	6.1±1.3	11.4±0.9	6.3±1.0

* For comparison with data from Taylor *et al.* 1998.

Table 3.4. Average duration and standard error of the inversion (days) on a monthly basis between different weather stations in central Yukon, 1974-1982. Vertical distance between the stations is also reported.

	Inversion duration (days)		
Month	Keno and Mayo (968 m)	Elsa and Mayo (310 m)	Elsa and Keno (658 m)
January	10.7±2.2	6.4±1.4	9.0±1.6
February	6.5±1.6	3.9±0.9	6.9±1.6
March	2.1±0.3	1.8±0.2	2.1±0.4
April	-	1.2±0.1	-
May	-	1.4±0.2	-
June	-	1.7±0.2	-
July	-	2.6±0.6	-
August	-	1.6±0.2	-
September	-	1.4±0.1	-
October	1.6±0.6	1.3±0.2	1.7±0.3
November	4.4±0.8	3.0±0.4	4.4±1.2
December	7.5±1.4	4.2±0.7	6.4±1.2
Summer Mean (June to Aug)	0.0±0.0	2.0±0.3	0.0±0.0
Winter Mean (Dec to Feb)	8.2±1.7	4.8±1.0	7.4±1.5
Frozen Season Mean* (Oct to April)	4.7±1.0	3.1±0.6	4.4±0.9

* For comparison with data from Taylor *et al.* 1998.

3.5. Permafrost Conditions in Keno Area

Although no formal studies of the permafrost conditions in the Keno area have been undertaken, records from the numerous silver mines provide an indication of the occurrence of permafrost. On Keno Hill, permafrost depths of 135 m were reported at Keno 900 mine near the top of Keno Hill (Pike 1966), and of 120 m on the north-facing slope of Keno Hill (Brown 1970, 153). At the head of Faro Gulch, at an elevation of 1700 m on the northwest slope of Keno Hill, a mineshaft penetrated over 120 m deep without reaching the bottom of the frozen zone (Wernecke 1932). On the northwest slope of Keno Hill, near the Wernecke mine camp at 1200 m, permafrost was penetrated at a depth of 80 m in the Ladue mine, but at the nearby Sadie shaft no permafrost was encountered due to groundwater near the ground surface (Wernecke 1932). Permafrost is at least 110 m thick on the north slope of Keno Hill as documented at the main shaft of the Lucky Queen mine at 1550 m, where ground temperatures of -2.25°C at 30 m, -1.5°C at 60 m and -0.75°C at 90 m were recorded (Wernecke 1932). On Sourdough Hill, ice lenses were encountered in Bellekeno mine (N, 1150 m) at a depth of 75 m (Brown 1970, 153).

No permafrost was encountered at Mount Keno mine on the south-facing slope of Keno Hill at an elevation of 1150 m, which supports Brown's (1970, 153) hypothesis that the south-facing slopes in this area are relatively free of permafrost because of greater receipt of solar radiation. On nearby Galena Hill, permafrost was penetrated at a depth of 90 m at the Elsa mine (NW, 1070 m), and 60 m at the Silver King mine (N, 820 m) (Wernecke 1932).

The observations from these mines, summarized in Table 3.5, support the theory that permafrost occurs in the valley bottoms and at the mountain tops, but that a band of no permafrost occurs at a mid to lower elevation, at least on the south-facing slopes. One of the objectives of this thesis is to confirm these observations through a study to determine whether the persistent winter temperature inversion experienced in central Yukon influences the local occurrence of permafrost.

3.6. Chapter Summary

This chapter summarizes the physical and climatic conditions found in the Yukon Plateau-North ecoregion and in the Keno area where the study takes place. The most notable climatic characteristic exhibited throughout Yukon Territory is the development of winter inversions under long periods of calm wind, clear skies and low solar radiation due to low sun angles. The observations of permafrost occurrence in mine shafts in central Yukon at different aspects and elevations support the hypothesis that winter temperature inversions can influence the local occurrence of permafrost.

Table 3.5. Summary of the observations of the occurrence of permafrost from mines in the Keno area

Location	Aspect	Elevation (m)	Permafrost Observed	Permafrost Thickness (m)
Keno Hill top	None	1800	Yes	120
Keno Hill	N	1700	Yes	120
Faro Gulch, Keno Hill	NW	1700	Yes	>120
Lucky Queen, Keno Hill	N	1550	Yes	110
Belle Keno, Sourdough Hill	N	1150	Yes	75
Mount Keno, Keno Hill	S	1150	No	-
Elsa, Galena Hill	NW	1070	Yes	90
Silver King, Galena Hill	N	820	Yes	60
Ladue, Keno Hill	NW	1200	Yes	80
Sadie, Keno Hill	NW	1200	No	-

CHAPTER 4
DESCRIPTION OF STUDY SITES AND METHODS

4.1. Introduction

This chapter justifies the selection of central Yukon as the location for this project. It outlines the methods used to select and instrument the eleven study sites on two hills. The techniques used to characterize each site with respect to slope, aspect, vegetation, soils, skyview factor, solar radiation and snow cover are also described. Site selection took place in summer 2000 and site characterization was carried out in summer 2000 and 2001.

4.2. Site Selection

The location for this field study is in the Keno area of central Yukon (Fig. 3.1). This area is suitable because the terrain is mountainous and the winter temperature inversion has previously been documented (Burn 1993).

Keno Hill, with an elevation of 1849 m (6065 ft), and Sourdough Hill, with an elevation of 1444 m (4739 ft), provide ideal research sites (Fig. 3.2). The community of Keno, where accommodation is available, is nestled at the base of these two hills. The village of Mayo is only 60 km away, where supplies and reliable field assistants are available.

Extensive gold and silver mining took place in the area from the 1910s until the 1980s, and there are numerous roads zigzagging along the hillsides. These roads provide easy access by truck or all-terrain-vehicle to a large portion of the area at various

elevations and aspects. This degree of accessibility is rare in most northern mountainous terrain.

Prior to commencing the field portion of this research project, aerial photographs were examined to define the broad vegetation classes that are present in the study area. The most recent and spatially complete set of aerial photographs for the study area were taken in August 1984 at a scale of 1:20,000 (National Airphoto Library 1984). Eleven biogeoclimatic zones, areas in which similar soil and climatic conditions may be inferred from vegetation characteristics, were identified from the photos. Five zones were identified on the north-facing slope of Sourdough Hill and five on the south-facing slope of Keno Hill. An additional area in the valley bottom where the two slopes meet was also identified.

The zones were confirmed by completing several transects from the top of the hills to the bottom with the assistance of a Garmin© XL Global Positioning System (GPS). Accessible locations with site characteristics representative of the over-all conditions within each vegetation unit were selected and instrumented as the study sites for this project. These sites were named KH-1 through KH-6, where KH is an abbreviation for Keno Hill, and SD-1 through SD-5, where SD is an abbreviation for Sourdough Hill (Fig. 4.1).

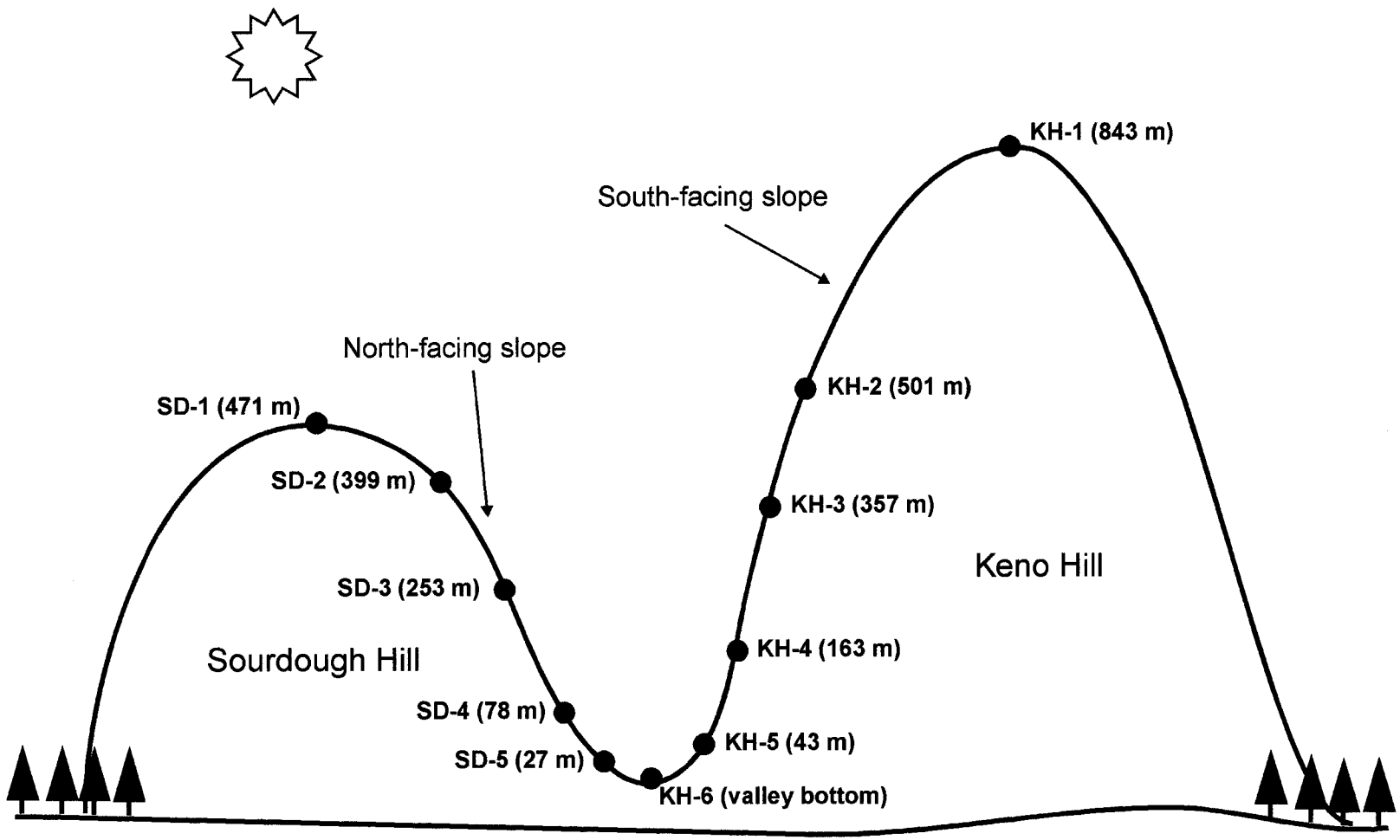

Figure 4.1 - Diagram of eleven study sites on the north-facing slope of Sourdough Hill and the south-facing slope of Keno Hill, central Yukon. Elevation above the valley floor is noted for each site.

4.3. Methods for Determining General Site Characteristics

4.3.1. Location and Elevation

The GPS was used to determine the geographic co-ordinates of each site. Although the GPS provides an estimate for the accuracy of the elevation, it is common for the error to be larger than stated unless a differential GPS technique is used. A second elevation estimate was obtained by plotting the positional co-ordinates obtained from the GPS on the 1:50,000 National Topographic System basemap for the area (105M/14). A final elevation value was obtained by plotting the site co-ordinates on the digital elevation model (DEM) at 10 m resolution for the area. The DEM was created from the digital NTDB contour lines and hydrographic orientation in ARCINFO, a proprietary geographic information system software. All elevation estimates, with a calculated best estimate are presented in Table 4.1, along with the elevation above the valley bottom for each site.

4.3.2. Slope and Aspect

The aspect of each site was determined using a compass. The slope was estimated using an Abney level. The surveyor stood at a spot that was representative of the slope conditions at the site. Twelve slope estimates, six upslope and six downslope from the surveyor at 5 m intervals, were obtained by sighting. An average of these estimates was taken and the average slope (°) was converted to a slope class following the classes outlined in The Canadian System of Soil Classification (Soil Classification Working Group 1998) (Table 4.2).

Table 4.1. Three estimates of the elevation (m) of each study site using three techniques: GPS, plotting co-ordinates on paper 1:50,000 NTDB map and interpolating the elevation using the contour lines, plotting co-ordinates on the DEM generated from the contours on the digital NTDB 1:50,000 map. Estimate of the elevation above the valley bottom is also provided.

	Measured Elevation (m)				
Site	GPS	NTDB Map	DEM	Average	Elevation above valley bottom (m)
KH-1	1853	1848	1833	1845	831
KH-2	1526	1501	1518	1515	501
KH-3	1395	1334	1385	1371	357
KH-4	1208	1146	1176	1177	163
KH-5	1076	1036	1058	1057	43
KH-6	999	1021	1023	1014	0
SD-1	1458	1444	1437	1446	471
SD-2	1395	1341	1385	1374	399
SD-3	1211	1247	1225	1228	253
SD-4	1058	1060	1040	1053	78
SD-5	999	1006	1001	1002	27

Table 4.2. Summary of the slope and aspect characteristics of the eleven study sites on Keno Hill and Sourdough Hill, central Yukon.

Site	Aspect	Slope
KH-1	None (mountain top)	Nearly level (0°30')
KH-2	182°	Moderate slope (6°00')
KH-3	175°	Strong slope (11°10')
KH-4	122°	Very strong slope (20°20')
KH-5	172°	Very strong slope (19°50')
KH-6	None (valley bottom)	Gentle slope (3°40')
SD-1	None (mountain top)	Very gentle slope (1°50')
SD-2	350°	Moderate slope (5°40')
SD-3	340°	Very strong slope (17°50')
SD-4	330°	Very strong slope (19°20')
SD-5	350°	Strong slope (12°40')

4.3.3. Soil Properties

Soil pits were dug near each site to a depth of 1 m where possible, to classify the major mineral and organic soil horizons following the Canadian System of Soil Classification (Soil Classification Working Group 1998). C.A.S. Smith, a Yukon soil scientist with the Pacific Agri-Food Research Centre, spent three days in the field during the study and contributed significantly to the soil classifications. Soil descriptions presented in Table 4.3 were compiled from both field and laboratory data.

Soil pH was determined using the standard method for determining soil pH in 0.01M $CaCl_2$ (Soil and Plant Analysis Council 2000, 31). Particle size analysis, the determination of the grain size distribution of the whole soil including the coarse fraction (>2 mm), was conducted using sieving techniques for the coarse fractions and the standard pipette method for the fine-grained materials (Canadian Society of Soil Science 1993, 499-511). All of the sites except KH-6, SD-4 and SD-5, contained numerous stones (>250 mm) and cobbles (75-250 mm), therefore field observations supplemented the particle size analyses to determine the family particle size class in Table 4.3 as defined by the Soil Classification Working Group (1998, 136).

The gravimetric water content of soil samples taken at a depth of approximately 30 cm from the top of the mineral soil in early summer and late summer was determined by drying in a soil oven (Table 4.4). It was not possible to take a volumetric sample for moisture or bulk density determination because the soil was too stony at the sites.

Table 4.3. Summary of soil description at the eleven study sites based on field and laboratory work.

Site	Parent Materials	Slope Position	Drainage	Subgroup[1]	Family Particle Size Class	MAST[2] (°C)	Depth to PF[3] (cm)	Organic layer thickness (cm)	Comments
KH-1	Loess/bedrock fragments	Summit	Imperfectly	Orthic Dystric Turbic Cryosol	Fragmental	-2.4	200	Trace	Active sorted circles
KH-2	Loess/colluvium	Upper slope	Moderately well	Orthic Dystric Cryosol	Loamy skeletal /fragmental	-1.0	ND	10	Solifluction lobes, bedrock at 150 cm
KH-3	Colluvium	Upper slope	Moderately well	Orthic Dystric Brunisol	Loamy skeletal /fragmental	+1.1	ND	10	Bedrock at 150 cm
KH-4	Colluvium	Mid slope	Well	Eluviated Dystric Brunisol	Loamy skeletal /fragmental	+1.9	—	5	Warm, dry site, mid slope
KH-5	Colluvium	Lower slope	Moderately well	Orthic Dystric Brunisol	Sandy skeletal /fragmental	+0.5	—	15	Cumulic LF horizon, mixture of mineral and organic matter
KH-6	Alluvium	Valley bottom	Imperfectly	Gleyed Dystric Cryosol	Sandy skeletal	-0.3	—	20	Seepage at 40 cm, floodplain location

[1] Both Brunisols and Cryosols are considered as Dystric subgroups because of pH <5.5 with the exception of site SD-4.
[2] Annual mean soil temperature at 50 cm. All soils fall into the soil temperature regime of Very Cold (-7 to +2°C).
[3] Depth to permafrost not determined (ND) when bedrock was encountered within control section. Sites without permafrost within the control section are labelled '—'.

Table 4.3 (continued). Summary of soil description at the eleven study sites based on field and laboratory work.

Site	Parent Materials	Slope Position	Drainage	Subgroup[1]	Family Particle Size Class	MAST[2] (°C)	Depth to PF[3] (cm)	Organic layer thickness (cm)	Comments
SD-1	Loess/bedrock fragments	Summit	Imperfectly	Orthic Dystric Turbic Cryosol	Loamy skeletal	Insufficient data	75	20	Non-sorted circles
SD-2	Colluvium	Upper slope	Moderately well	Orthic Dystric Brunisol	Loamy skeletal	Insufficient data	—	10	No evidence of patterned ground
SD-3	Colluvium	Mid slope	Imperfectly	Histic Dystric Turbic Cryosol	Loamy skeletal	Insufficient data	50	30	Very thick surface organic matter accumulation, seepage present over pf table.
SD-4	Colluvium	Lower slope	Poorly	Histic Eutric Turbic Cryosol	Loamy skeletal	-1.7	50	25	Strongly cryoturbated active layer, seepage present
SD-5	Alluvium	Valley bottom	Poorly	Histic Dystric Turbic Cryosol	Sandy	-1.3	60	30	Floodplain soil, evidence of cumulic formation

[1] Both Brunisols and Cryosols are considered as Dystric subgroups because of pH <5.5 with the exception of site SD-4.
[2] Annual mean soil temperature at 50 cm. All soils fall into the soil temperature regime of Very Cold (-7 to +2°C).
[3] Sites without permafrost within the control section are labelled '—'.

Table 4.4. Early and late season gravimetric moisture content (%) for all study sites.

	Gravimetric Moisture Content (%)		
	Early Season (July 5, 2001)	Late Season (Aug 13, 2001)	Sample Depth (cm)
KH-1	20	15	~25
KH-2	26	21	~30
KH-3	19	21	~25
KH-4	24	23	~30
KH-5	22	16	~30
KH-6	12	41	~30
SD-1	22	22	~25
SD-2	25	24	~25
SD-3	114	18	~30
SD-4	Frozen	101	~30
SD-5	39	28	~30

4.3.4. Vegetation Description

During summer 2000, a sampling of the vegetation was conducted at each site using the nested plot technique (Mueller-Dombois and Ellenberg 1974). Once the species lists were established, the community structure was described by noting the vegetation layering.

During summer 2001, Catherine Kennedy, a Vegetation Specialist with the Department of Renewable Resources, Yukon Territorial Government, spent three days at the field sites and provided invaluable guidance in plant identification and strata classification. A comparison of the percent cover of major strata layers, which are defined by height, is presented in Table 4.5. Trees are defined as the uppermost vegetation layer with a height greater than 1.5 m, shrubs are a mid-height canopy layer ranging from 0.5 to 1.5 m, the herbaceous layer includes all vascular plants less than 0.5 m in height and encompasses ground shrubs, forbes and grasses, and the moss/lichen strata class includes all non-vascular plants. The final class, labelled "other", includes rocks, leaf litter and woody debris.

4.3.5. Solar Radiation Estimates

Three methods were used to estimate the amount of solar energy received by the ground surface at each location.

First, hemispherical canopy photography, an indirect optical technique that has been widely used in canopy structure and forest light transmission studies, was used (e.g. Becker *et al.* 1989; Rich 1990; Trichon *et al.* 1998). Photographs at each site were taken in early August using a 180° hemispherical (fisheye) lens placed approximately 50 cm

Table 4.5. Percent cover of vegetation in each summary strata layer and plot size (m^2) required to describe the vegetation community at each site on Keno Hill and Sourdough Hill, central Yukon.

Site	Trees	Shrubs	Herbs	Moss/lichen	Other	Plot size (m^2)
KH-1	0	0	50	70	20	4
KH-2	0	50	25	75	20	2
KH-3	5	60	25	70	10	16
KH-4	40	50	15	35	5	16
KH-5	40	20	20	50	50	32
KH-6	20	30	20	80	Trace	8
SD-1	0	30	30	40	25	8
SD-2	1	60	50	70	10	8
SD-3	10	25	25	80	10	4
SD-4	1	30	50	60	Trace	32
SD-5	10	25	10	75	Trace	4

above the ground surface (Figs 4.2a and b). The photographs were all taken with the lens pointing perpendicular to the sky, and the slope was not taken into consideration due to limitations with the equipment. These photographs are circular images that record the size, shape, and location of gaps in the vegetation overstory. The photographs were scanned and convert into bitmaps, which were analysed using Gap Light Analyser (GLA) (Frazer *et al.* 1999), a specialised image analysis software available on the Internet (http://www.rem.sfu.ca/forestry/gla/, accessed May 16, 2002). GLA was used to compute estimates of site openness and the amount of shading produced by the vegetation canopy (Table 4.6).

Mean annual direct solar radiation was calculated for the study area using the DEM and "*shortwavc.aml*" function in ARCINFO (Kumar *et al.* 1997; Zimmermann 2000) (Table 4.6). This function took into account the shadowing effect of adjacent topography to produce an estimate of annual direct insolation for each pixel in the DEM at a 120-minute time interval for incrementing daily solar path. Sites on the south-facing slope received approximately 11 to 55% more radiation than sites at similar elevations on the north-facing slope on an annual basis when only topographic effects were considered (Table 4.6). When the vegetation canopy information from the fisheye lens photographs was combined with the mean annual direct solar radiation data, an estimate of the annual amount of direct solar radiation that reaches the ground surface was obtained (Table 4.6).

As expected, sites that were the most shaded occurred at the lower elevations primarily due to topographic obstructions of incoming radiation. A comparison of the rankings of the sites based on the annual shortwave radiation and the shortwave radiation reaching the ground surface demonstrates the importance of the vegetation canopy. For

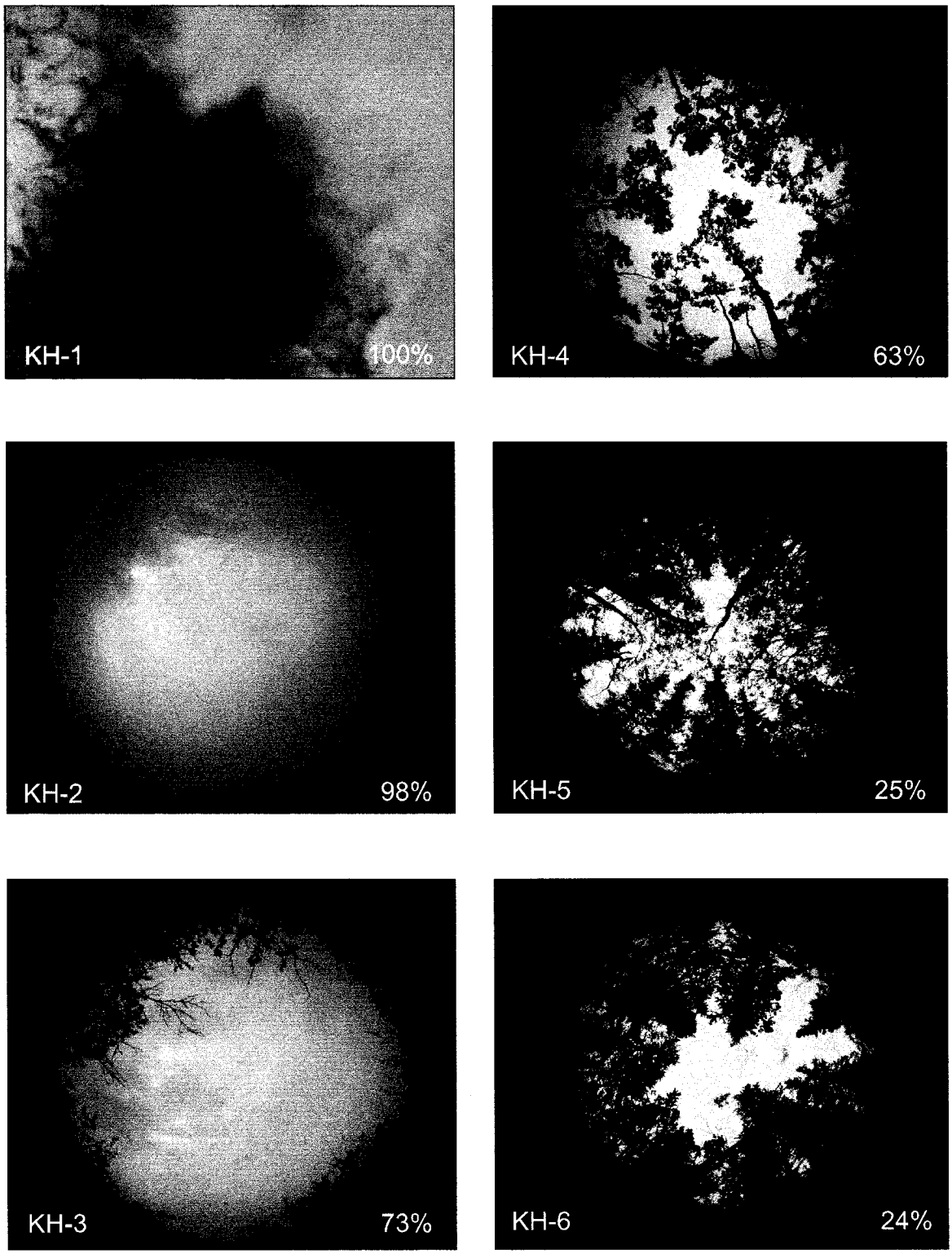

Figure 4.2a - Series of fisheye lens photos for the Keno Hill sites. Site number is identified in the bottom left-hand corner. Percent canopy openness as computed by GLA is indicated in the bottom right-hand corner.

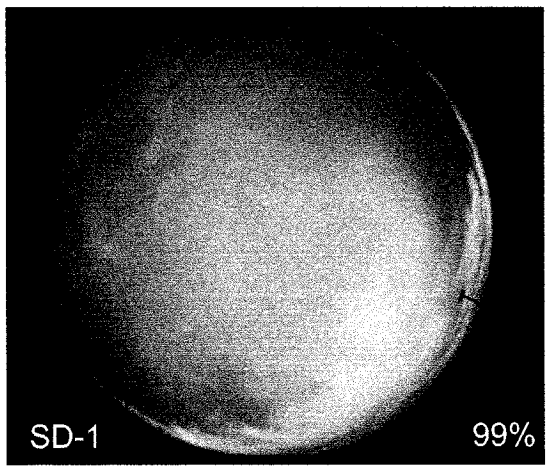

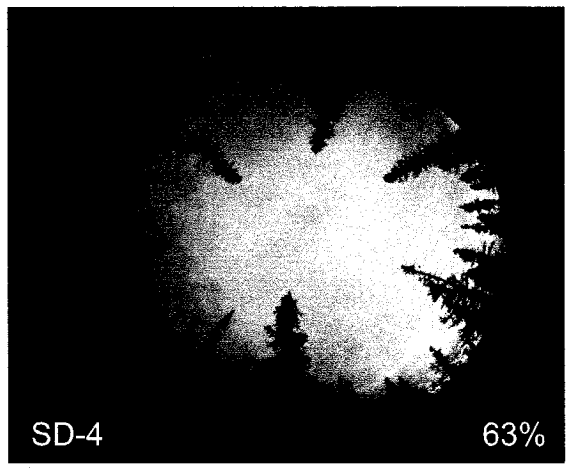

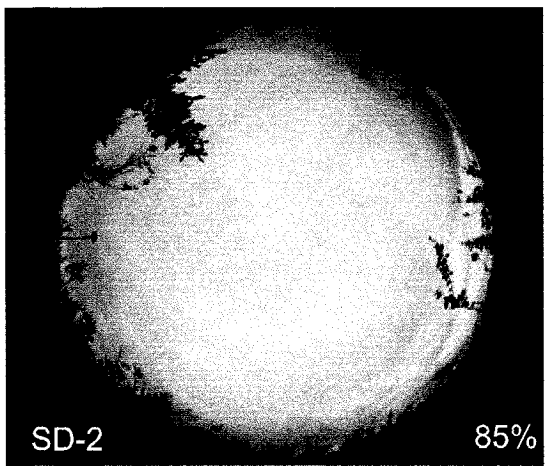

SD-5: No photo available

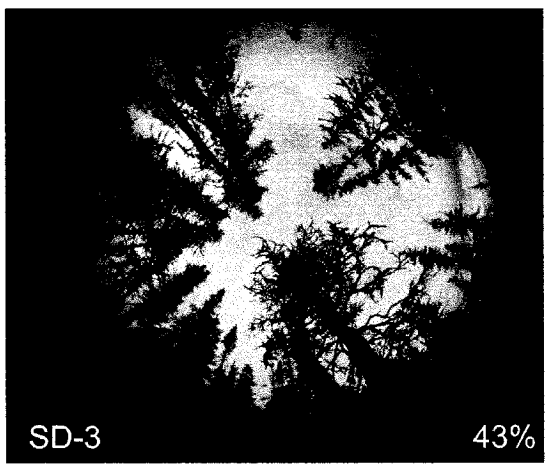

Figure 4.2b - Series of fisheye lens photos for the Sourdough Hill sites. Site number is identified in the bottom left-hand corner. Percent canopy openness as computed by GLA is indicated in the bottom right-hand corner.

Table 4.6. Estimates of canopy openness and ground shading provided by the vegetation canopy using hemispherical photography and GLA software. Estimate of annual solar shortwave radiation arriving at each site with topographic shading. Calculations made in ARCINFO with the "*shortwavc.aml*" function (Zimmerman 2000).

Site	Canopy Openness (%)	Annual shortwave radiation (kJ m^{-2})	Rank	Annual shortwave radiation to reach ground surface (kJ m^{-2})	Rank
KH-1	100	3698700	7	3698700	3
KH-2	98	4319800	4	4233404	1
KH-3	73	4678200	3	3415086	4
KH-4	46	5117400	1	2354004	6
KH-5	25	4782900	2	1195725	9
KH-6	24	4013900	5	963336	11
SD-1	99	3834600	6	3796254	2
SD-2	85	3517200	8	2989620	5
SD-3	43	2278000	11	979540	10
SD-4	63	2404400	10	1514772	8
SD-5	~60*	2776200	9	1665720	7

*estimate, no photo taken at this site

example, KH-4 receives the most solar radiation on an annual basis, but is ranked in the middle in terms of the amount of radiation that reaches the ground surface due to the dense canopy cover. It should be noted, however, that the amount solar radiation that reaches the ground surface at this site is an underestimate because the deciduous canopy is not present for the whole time when solar radiation is high and snowcover is absent, such as late-May and mid-September.

A solar compass was also used to estimate the total amount of solar energy received at the ground surface incorporating both topographic and vegetative shading (Fig. 4.3). The instrument was developed in Switzerland for forest applications and has been applied to permafrost studies in the Alps (Phillips 2000, 32). The device is composed of a solar chart for the desired latitude inside a transparent dome-shaped cover. A compass and a leveling instrument complete the design. The user places the solar compass perpendicular to the sky and oriented so the compass points to true north. The horizon, which includes vegetation and adjacent hills, is reflected on the domed cover and an outline is visible on the solar chart. The user then draws the shaded pattern on the solar chart onto a piece of paper displaying the same solar chart. In this study, the solar compass measurements were analyzed based on the percentage of the compass area that was shaded (Table 4.7). The rankings of radiation received at the ground surface produced by the two methods are similar. With the exception of KH-3 and SD-3, the sites are within one or two ranks of each other (Tables 4.6 and 4.7). When the site rankings for the two methods of solar radiation estimates were compared with a Spearman rank correlation test (Ebdon 1985, 97), the rankings were found to be similar at the 0.05 significance level with Spearman rank correlation coefficient (r_s) of 0.71.

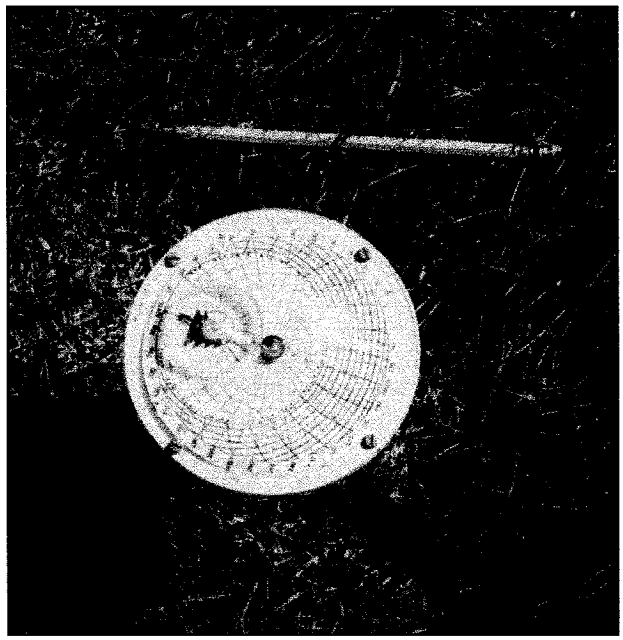

Figure 4.3 - Photo of solar compass used to estimate the total amount of solar radiation received at the ground surface.

Table 4.7. Shading due to vegetation and topographic influences as estimated by the solar compass. Sites were ranked from lowest (1) to highest (11) amount of vegetation shading.

Site	% Shading due to vegetation and topographic influences	Site rank
KH-1	15	2
KH-2	23	3
KH-3	91	9
KH-4	87	7
KH-5	90	8
KH-6	98	11
SD-1	12	1
SD-2	34	4
SD-3	69	5
SD-4	93	10
SD-5	73	6

4.3.6. Snow Cover

Snow depth was measured at graduated snow stakes installed at or near each site on Keno Hill. No stakes were installed on Sourdough Hill because of difficult winter access. Dr Marcia Phillips, a post-doctoral fellow at Carleton University, conducted field work in the Mayo-Keno area in December 2000 and March and April 2001. Dr Phillips measured the depth of the snow cover on four occasions (Table 4.8). Dr C.R. Burn measured the snow depth at the Keno Hill sites in February 2002.

4.4. Site Instrumentation

A schematic diagram of the ground and air temperature measurement apparatus is shown in Figure 4.4. A solar radiation shield was installed at the top of the apparatus to protect the air temperature sensor from incident sunlight, and to prevent snow from accumulating around the thermistor as well as moisture wetting the sensor. All air temperature measurements were made 1 to 1.5 m above the ground surface.

Air and ground temperatures were measured and logged by HOBO® four-channel data loggers (model # H08-006-04). Three ground temperature thermistors were fastened to a piece of wooden dowel at target standard depths of 20 cm, 50 cm, and 100 cm. In many cases, a depth of 100 cm was not obtainable with the available equipment (see section 5.4.2). The dowel was then placed in a PVC pipe in the ground and any void space was filled with dry sand to minimize air conduction around the thermistors. The PVC pipe was then capped with a silicon sealant to prevent moisture from entering the pipe and influencing the temperature.

Table 4.8. Summary of snow measurements taken at sites on Keno Hill, winter 2000-01 and 2001-02. Winter 2000-01 measurements were taken at snow stakes near the sites, whereas measurements on February 17, 2002 were taken at the sites.

Site	Elevation (m)	Dec. 11, 2001 (cm)	March 27, 2001 (cm)	April 15, 2001 (cm)	April 21, 2001 (cm)	Feb. 17, 2002 (cm)
KH-1	1845	43	56	No data	34	25
Sign post	1695	45	40	46	49	No data
KH-2	1515	No data	No data	18	No data	24
KH-3	1371	54	48	52	48	70
KH-4	1177	35	50	50	32	61
KH-5	1057		Unable to access			41
KH-6	1014		Unable to access			45

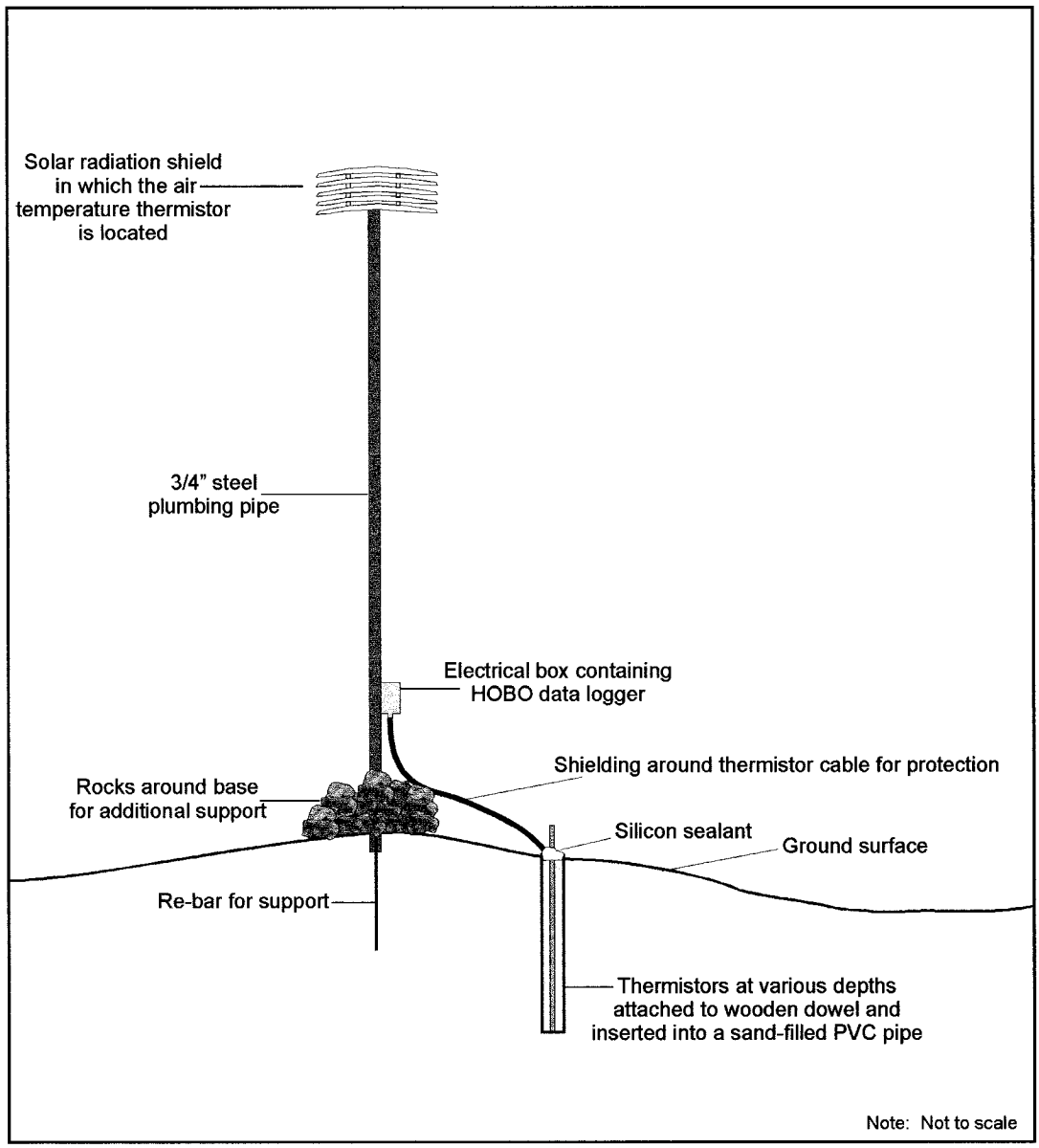

Figure 4.4 - Typical air and ground temperature monitoring station.

Prior to installation, the thermistors were calibrated in an ice bath. The data loggers were set to measure and record ground and air temperatures every 1.5 hrs throughout the year.

4.5. Site Descriptions

Keno Hill Site 1 (KH-1, Figure 4.5a)

KH-1 is situated at the summit of Keno Hill at an elevation of approximately 1845 m. This site is located in a typical alpine area, well above treeline with a low vegetation cover dominated by lichens and grass species. There are no obstructions to incoming solar radiation since there is no canopy and no topographic shading. The air temperature sensor at this site was destroyed in early September 2000, although the ground temperature sensors were left undisturbed.

Keno Hill Site 2 (KH-2, Figure 4.5b)

This south-facing site is in the upper boundary of the subalpine-alpine zone at 1515 m, and is best described by the vegetation class "shrub birch dwarf shrub" from the Ecosystem Classification for the Southeast Yukon (Zoladeski *et al.* 1996), the only comprehensive classification system for the Territory. The dominant vascular vegetation in this area is dwarf birch (*Betula glandulosa*), less than 50 cm in height and occurring in thickets. Mosses and lichens are abundant and rock patches occur. This site is above treeline, but stunted and wind-abraded alpine fir krummholz (*Abies lasiocarpa*) occur in isolation. The slope is moderate and the snow cover is variable due to wind redistribution. The data record is complete for this site.

Keno Hill Site 3 (KH-3, Figure 4.5c)

KH-3 at an elevation of 1371 m, is situated in the "shrub birch medium/tall shrub" class and is dominated by dwarf birch 1.5 m to 0.5 m in height, overtopped by occasional single short alpine fir trees. This vegetation type is characteristic of the upper subalpine zone. This area has a strong slope of 11° and a soil pit was easily excavated along the edge of an old track made by mining machinery. A thin moss/lichen layer covers approximately 70% of this area. A relatively thick snow cover was observed at this site. The data record is complete for this site.

Keno Hill Site 4 (KH-4, Figure 4.5d)

This "open trembling aspen forest" is situated on a very strong, well-drained south slope at 1177 m. The trunks of the trembling aspen (*Populus tremuloides*) are sinuous, which is evidence of moisture stress (C.A.S. Smith, personal communication). The understory is shrub-rich, although in addition to shrub species commonly associated with this forest type, there is an abundance of blueberry (*Vaccinium uliginosum*) due to the acidic soil. This site has the lowest percent cover of moss/lichen of all sites as well as a very thin organic layer. A low and variable snow cover was observed at this site. The data record is complete for this site.

Keno Hill Site 5 (KH-5, Figure 4.5e)

This strongly sloped south-facing site at 1057 m is mixture of black spruce (*Picea mariana*) and thin trembling aspen trees and can therefore be classed as an "Open black spruce aspen forest". This ground is covered by mixture of moss/lichen cover and bare

ground covered with a woody/leaf material, which contribute to an organic layer thickness of approximately 15 cm. A complete data set is available for this site.

Keno Hill Site 6 (KH-6, Figure 4.5f)

This valley bottom site at 1014 m, is dominated by hybrid spruce trees (*Picea mariana x Picea glauca*) and can be best classified as an "open black spruce forest" following the ecosystem classification guidelines (Zoladeski *et al.* 1996). The spruce trees at this site range in size from over 5 m to approximately 50 cm representing various stages of development. The ground surface is 80% covered by a 20-cm thick moss cover dominated by *Tomenthypnum nitens*, *Pleurozium schreberi*, and *Sphagnum angustifolium*. In addition to topographic shading, a moderately dense understory of shrubs shields the ground from incoming solar radiation. Lightening Creek is located approximately 10 m from the study site, although there was no evidence in the vegetation or soil pit of the site being periodically flooded. Ground water seepage was observed at 40 cm. The air and ground temperature records for this site are complete.

Sourdough Hill Site 1 (SD-1, Figure 4.5g)

This north-facing site at the summit of Sourdough Hill is in the upper boundary of the subalpine-alpine zone at 1446 m. The vegetation is similar to KH-2 and can be classified as "shrub birch dwarf shrub". The dominant vascular vegetation in this area is dwarf birch (*Betula glandulosa*), less than 50 cm in height and occurring in thickets and usually in depressions. Mosses and lichens are abundant and non-sorted circles are common. The active layer is 75 cm under the shrubs, but is difficult to determine in other

areas due to the cobbles and stones. The logger failed on August 16, 2000, therefore the data record is incomplete for this site.

Sourdough Hill Site 2 (SD-2, Figure 4.5h)

This north-facing site at 1374 m has similar vegetation as KH-3, and can also be classified as "shrub birch medium/tall shrub". The area is dominated by dwarf birch 1.5 m to 0.5 m in height and is overtopped by taller dwarf birch and the occasional single short alpine fir. The slope is variable, but generally moderately sloping (6°). A thin moss/lichen and leaf litter layer covers approximately 70% of this area. This site was dismantled, although undamaged, one day after it was winterized, therefore limited data are available for this site.

Sourdough Hill Site 3 (SD-3, Figure 4.5i)

This site at 1228 m is dominated by alpine fir trees of varying heights, representing a regenerating forest, and can be classed as an "open alpine fir forest". The shrub layer is also abundant and well developed. The ground is covered by a 30-cm thick moss layer and lichens are plentiful. The active layer is approximately 50 cm and ground water seepage above the permafrost was observed. This site is also north-facing and has a very strong slope (19°). The data logger failed at the end of August 2000, therefore the air and ground temperature data for this site are limited.

Sourdough Hill Site 4 (SD-4, Figure 4.5j)

The vegetation at this site can best be described as a shrub/grass mixture, although there is no such class in the ecosystem classification system. This site is located on a very strong (20°) north-facing slope at 1053 m and is dominated by various graminoid species and shrubs (e.g., *Alnus crispa, Betula glandulosa*) ranging in height from 2 to 0.5 m. The site is poorly drained and seepage occurs at the base of the active layer. A 25-cm organic layer overlies the mineral soil, which is strongly cryoturbated. This site has a complete air and ground temperature record.

Sourdough Hill Site 5 (SD-5, Figure 4.5k)

SD-5 is situated above Lightening Creek near the valley bottom (1002 m) with a strong (13°) north-facing slope. The area is dominated by black spruce trees (*Picea mariana*) and is classified as an "open black spruce forest". This site is similar to KH-6, although there are fewer spruce trees and their growth is more stunted. The shrub layer is also less developed. The ground surface is 75% covered by a 30-cm thick moss cover dominated by *Pleurozium schreberi*. This site is poorly drained with an active layer of approximately 60 cm. The air and ground temperature records for this site are also complete.

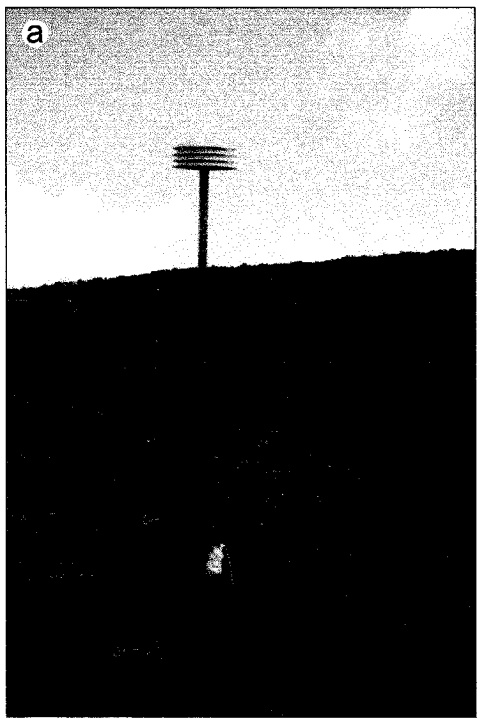

Keno Hill Site 1 (KH-1)

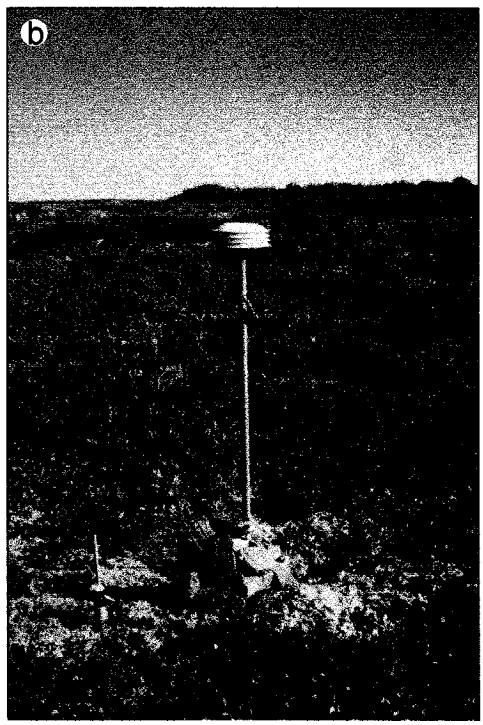

Keno Hill Site 2 (KH-2)

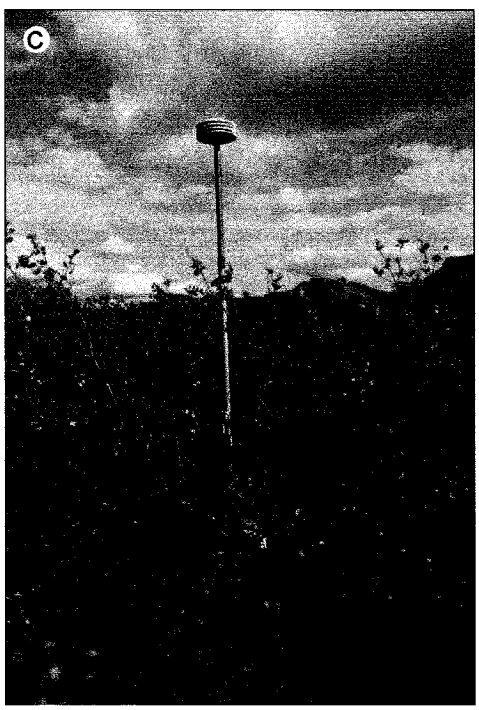

Keno Hill Site 3 (KH-3)

Keno Hill Site 4 (KH-4)

Figure 4.5a-d - Keno Hill and Sourdough Hill study sites.

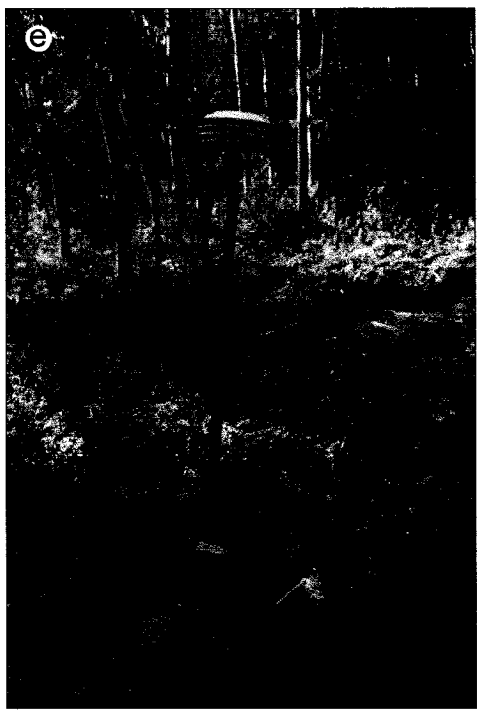

Keno Hill Site 5 (KH-5)

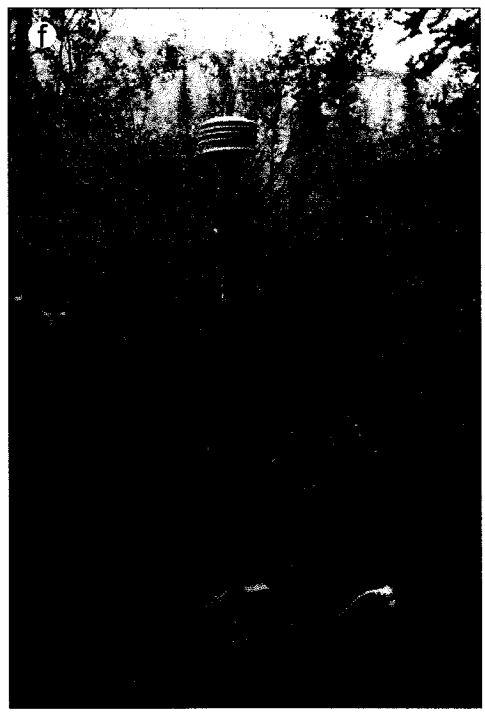

Keno Hill Site 6 (KH-6)

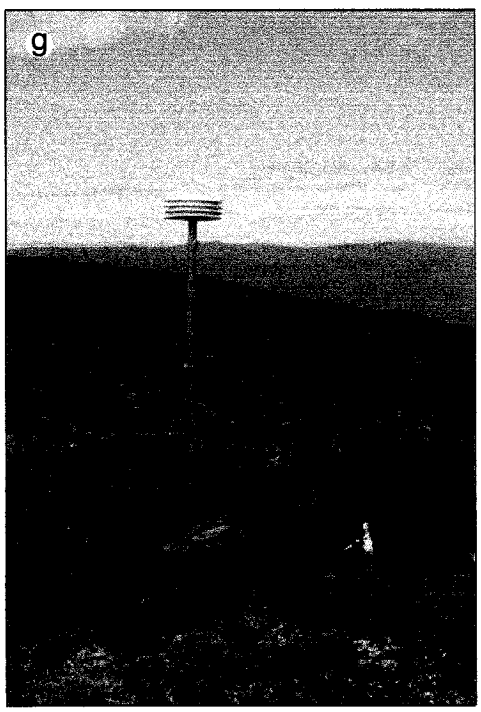

Sourdough Hill Site 1 (SD-1)

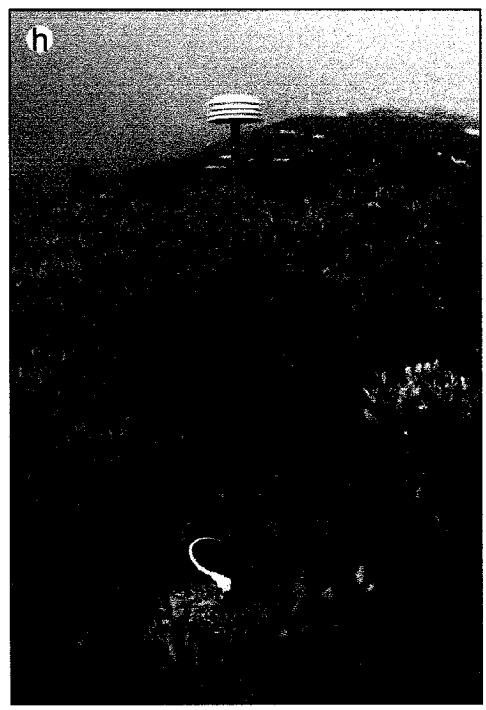

Sourdough Hill Site 2 (SD-2)

Figure 4.5e-h - Keno Hill and Sourdough Hill study sites.

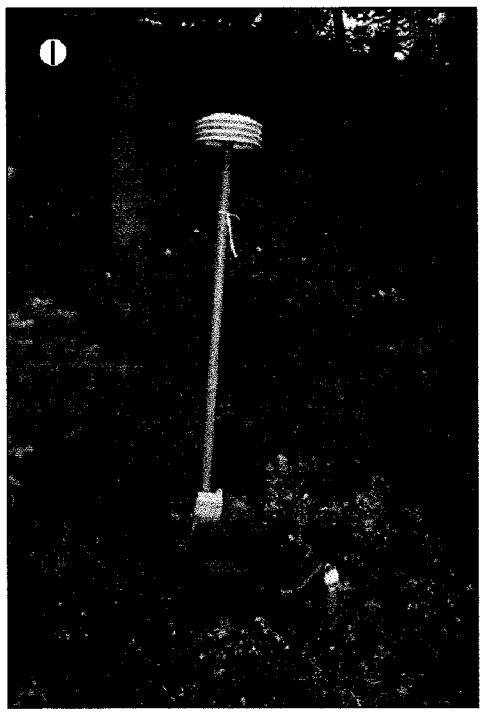

Sourdough Hill Site 3 (SD-3)

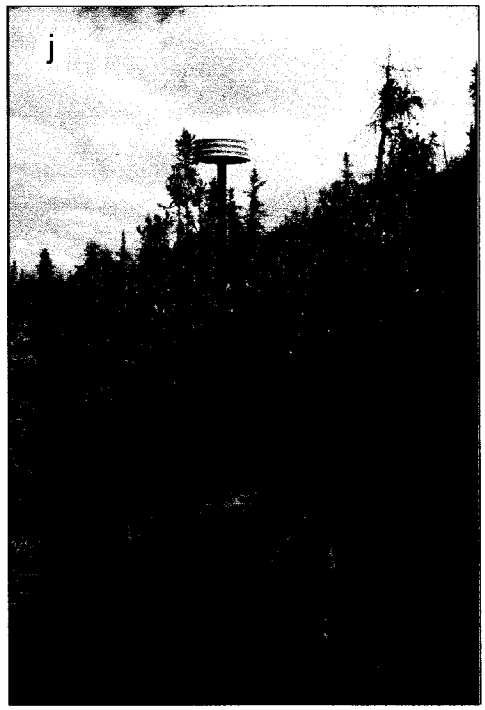

Sourdough Hill Site 4 (SD-4)

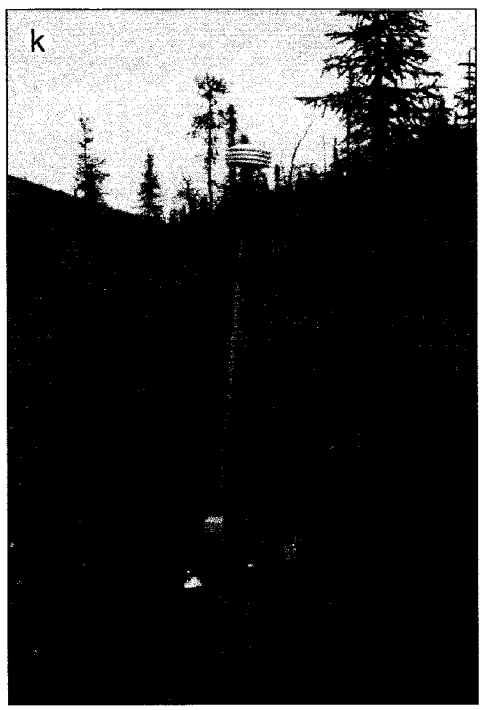

Sourdough Hill Site 5 (SD-5)

Figure 4.5i-k - Keno Hill and Sourdough Hill study sites.

CHAPTER 5
DETERMINATION OF EMPIRICAL RELATIONS BETWEEN SITE CHARACTERISTICS AND PERMAFROST OCCURRENCE

5.1. Introduction

The first part of this chapter describes the air and ground temperature regime at the study sites on Keno Hill and Sourdough Hill. Trends in air temperature due to elevation and aspect are examined and the frequency and strength of winter air temperature inversions are documented. The three methods used to determine the presence or absence of permafrost at a study site are discussed. The second part of this chapter describes the empirical model developed to summarize the associations between the physical characteristics and the occurrence of frozen ground at the study sites. The results of the testing of the empirical model are presented in the following chapter.

5.2. Elevational Trends in Air Temperature

The annual mean air temperature (AMAT) for 2000-01 was calculated for sites with complete annual air temperature records (Fig. 5.1). The warmest site is KH-4, the open trembling aspen forest, with an AMAT of –2.1°C. The valley bottom (KH-6) is the coldest site, with a slightly lower AMAT than KH-2 the shrub birch dwarf shrub class at 1515 m. The observed AMATs represent a departure of up to 3.2°C from predicted temperatures under a normal environmental lapse rate of –6°C km^{-1} (Fig. 5.1). In all cases the AMATs are warmer than expected under normal environmental lapse conditions demonstrating the warming effect of temperature inversions at upper elevations and cooling at lower elevations (Fig. 5.1).

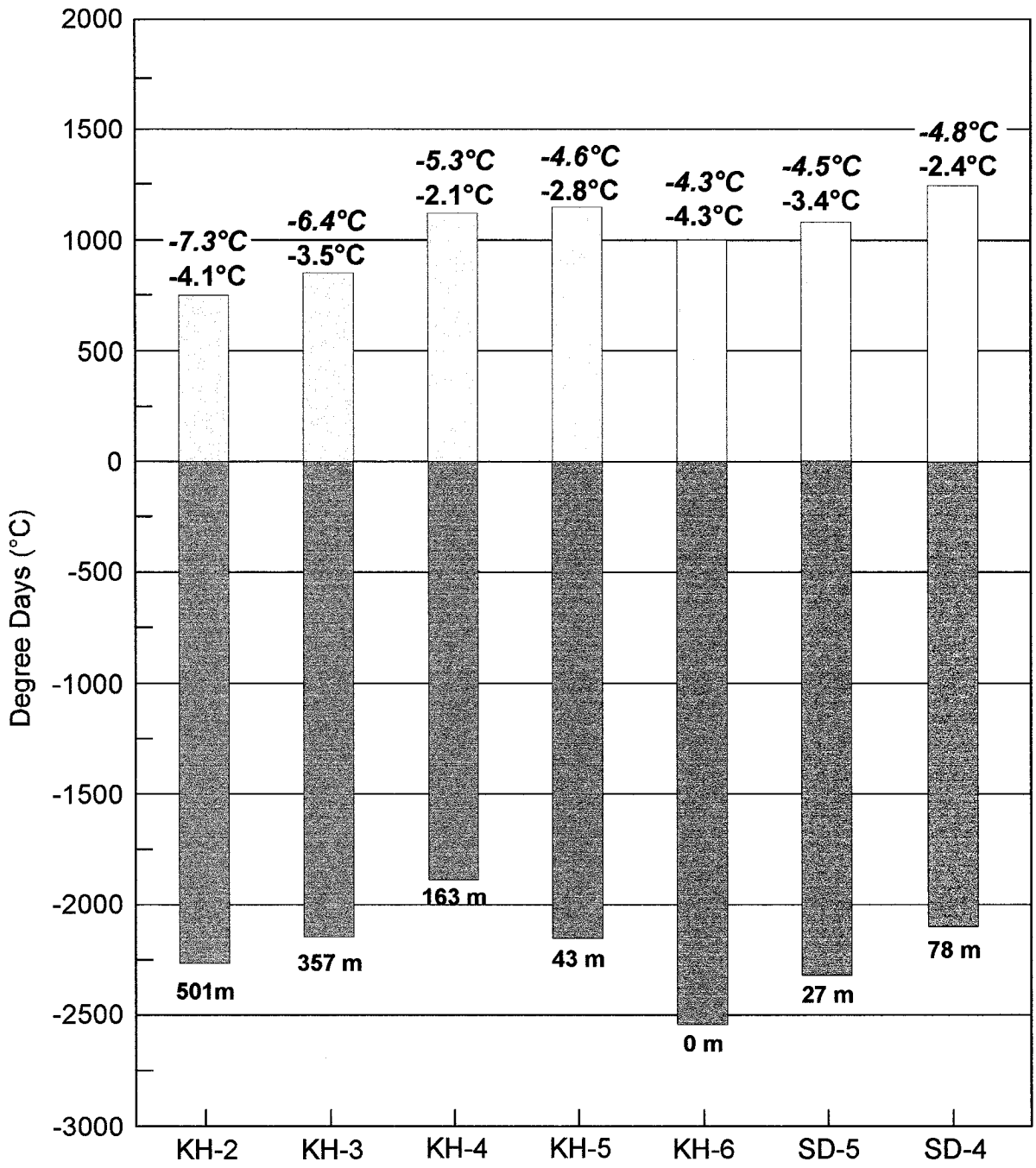

Figure 5.1 - Annual mean air temperature (in bold) and thawing and freezing degree-days (bars) for all sites with a complete annual air temperature record. The expected annual mean temperature under a normal environmental lapse rate of 6.0°C km^{-1} is presented in blue italics. Height above the valley floor of each site is also indicated.

Freezing and thawing degree-days were calculated for each site as the sum of temperature deviations above and below 0°C (Fig. 5.1). Degree-day comparisons allow for an understanding of the seasonal components that make up the mean annual temperature. The degree-day plots (Fig. 5.1) show that the variability in the AMAT at the various sites is associated primarily with differences in freezing degree-days and that the thawing degree-days are similar between the coldest (KH-6) and warmest (KH-4) sites. This indicates that the major temperature differences between these sites occur during the winter.

Table 5.1 presents the frequency with which each site on the south-facing slope is the warmest on a monthly basis. KH-6 was rarely the warmest site on the slope, indicating that temperature inversions occur nearly all the time (Table 5.1). In summer, vegetative and topographic shading result in cold valley bottom temperatures, whereas in the winter KH-6 had the lowest temperatures because of cold-air drainage and pooling. The site with the warmest temperature also indicates the approximate location of the top of the inversion and provides an estimate of the depth of the inversion. For approximately 85% of the year the inverted layer was situated in the lower valley between KH-4 and KH-5 or between 163 m and 43 m above the valley floor (Table 5.1). However, KH-2 is the warmest site in December over 50% of the time, which demonstrates the deepening of the inversion layer to at least 500 m in winter when cold-air pooling occurs. A deep inversion layer also occurred in February, since the frequency of KH-2 and KH-4 as the warmest sites was equal. This trend was not present in January 2001, possibly because the month was warmer than usual (see section 5.4).

Table 5.1. Percent frequency by month of site with the warmest daily mean air temperature on the south-facing slope of Keno Hill. Elevation above the valley floor for each site is also presented.

	Frequency (%)				
	KH-2 (501 m)	KH-3 (357 m)	KH-4 (163 m)	KH-5 (43 m)	KH-6 (0 m)
January	0.0	6.5	80.6	12.9	0.0
February	39.3	3.5	39.3	17.9	0.0
March	3.2	0.0	35.5	61.3	0.0
April	6.6	0.0	46.7	46.7	0.0
May	0.0	0.0	9.7	87.1	3.2
June	0.0	0.0	63.3	36.7	0.0
July	16.1	0.0	48.4	32.3	3.2
August	0.0	0.0	35.5	64.5	0.0
September	3.3	0.0	23.4	70.0	3.3
October	0.0	3.2	58.1	38.7	0.0
November	20.0	6.7	46.7	23.3	3.3
December	51.6	3.2	35.5	6.5	3.2
Annual	11.4	1.9	44.6	41.5	1.4
Summer (June to Aug)	5.4	0.0	49.1	44.5	1.0
Fall (Sept to Nov)	7.8	3.3	42.7	44.0	2.2
Winter (Dec to Feb)	30.3	4.4	51.9	12.4	1.0
Spring (March to May)	3.3	0.0	30.6	65.0	1.0

A comparison of the inversion conditions between KH-2 and KH-6, and KH-4 and KH-6, show that when inversions are present the temperature differences between the sites and the valley bottom are similar, but that the inversion strength (°C km^{-1}) is much greater between KH-4 and KH-6 (Tables 5.2a and b). The mean winter inversion strength between KH-2 and KH-6 was 10.2±0.9°C km^{-1}, which is nearly the same as the calculated strength between Keno and Mayo of 10.2±1.6°C km^{-1} (Table 3.4). The mean duration of inversion events was shorter between KH-2 and KH-6 than between KH-4 and KH-6 (Table 5.2b) because of the warm conditions in January 2001.

To further investigate the mean daily temperature trends with varying elevation, the year-long record was divided into four seasons based on the calendar months. One study site was selected to represent higher elevation sites, KH-2, mid-elevation sites, KH-4, and the valley bottom KH-6 from the five sites on this slope with complete temperature records.

Autumn, September through November, trends show three distinct periods. The first period, the month of September (Fig. 5.2a), represents the normal condition where KH-2 is the coldest location because of altitude, followed by KH-6 because of topographic shading and KH-4 was the warmest. During this period a mean daily temperature difference of 4-5°C was consistently observed between the warmest and coldest sites. The second identifiable period in the autumn record was the month of October. As October progressed, the amount of incoming solar radiation rapidly decreased and on several occasions, the valley bottom (KH-6) became the coldest site. These inversion events were of relatively short duration (Table 5.2b). No clear pattern of warmest to coldest site was established, nor was a consistent temperature difference

Table 5.2a. Monthly and seasonal mean temperature difference and inversion strength and standard error on Keno Hill transect for KH-2 vs. KH-6 (elevation difference = 501 m) and KH-4 vs. KH-6 (elevation difference = 163 m), using daily mean temperatures July 31, 2000 to July 31, 2001.

		KH-2 vs. KH-6			KH-4 vs. KH-6		
	Number of observations	% days with inversion	Mean temperature difference (°C)	Mean inversion strength and standard error (°C km^{-1})	% days with inversion	Mean temperature difference (°C)	Mean inversion strength and standard error (°C km^{-1})
January	31	77	3.0	6.0±1.1	100	4.7	28.7±3.2
February	28	79	5.7	11.3±1.4	89	4.0	24.8±3.3
March	31	26	1.2	2.3±0.5	87	1.9	11.4±2.0
April	30	17	0.8	1.6±0.5	73	2.1	12.7±1.8
May	30	0	-	N/A	75	0.6	3.8±0.5
June	30	13	0.1	0.3±0.1	80	1.8	11.0±1.0
July	29	38	2.3	4.6±1.0	80	1.3	7.8±1.4
August	23	4	-	N/A	60	1.5	9.2±1.6
September	30	17	1.1	2.2±0.2	63	1.7	10.3±1.8
October	31	42	2.6	5.3±1.0	77	2.3	17.9±2.9
November	30	57	4.1	8.2±1.2	90	3.0	18.5±2.9
December	31	90	6.5	13.0±1.5	100	6.0	36.6±3.2
Summer (June to Aug)	84	19	1.6	3.3±0.8	73	1.5	9.3±1.3
Fall (Sept to Nov)	91	39	3.2	6.3±0.7	77	2.3	15.6±2.5
Winter (Dec to Feb)	90	82	5.1	10.2±0.9	96	4.9	30.0±3.2
Spring (March to May)	92	14	0.9	1.9±0.3	78	1.5	9.3±1.4
Frozen season (Oct to April)*	182	55	3.4	6.8±1.0	88	3.4	21.5±2.8

* For comparison with data from Taylor *et al.* 1998.

Table 5.2b. Monthly and seasonal inversion duration and standard error on Keno Hill transect for KH-2 vs. KH-6 (elevation difference = 501 m) and KH-4 vs. KH-6 (elevation difference = 163 m), using daily mean temperatures July 31, 2000 to July 31, 2001.

	KH-2 vs. KH-6 mean inversion duration and standard error (days)	KH-4 vs. KH-6 mean inversion duration and standard error (days)
January	4.0±1.3	31
February	5.5±3.0	6.3±3.3
March	1.6±0.4	5.4±1.2
April	1.7±0.3	3.7±0.9
May	-	3.3±1.0
June	1.3±0.3	8.0±3.5
July	2.8±1.4	4.2±2.0
August	-	3.5±0.5
September	1.3±0.3	3.8±1.5
October	3.3±0.9	4.8±1.6
November	2.8±0.7	9.0±3.5
December	9.3±4.8	30.0
Summer (June to Aug)	2.0±0.7	5.2±2.0
Fall (Sept to Nov)	2.5±0.4	5.9±2.2
Winter (Dec to Feb)	5.7±1.5	22.4±1.1
Spring (March to May)	1.6±0.3	4.1±1.0
Frozen season (Oct to April)*	4.0±1.6	12.8±1.5

* For comparison with data from Taylor *et al.* 1998.

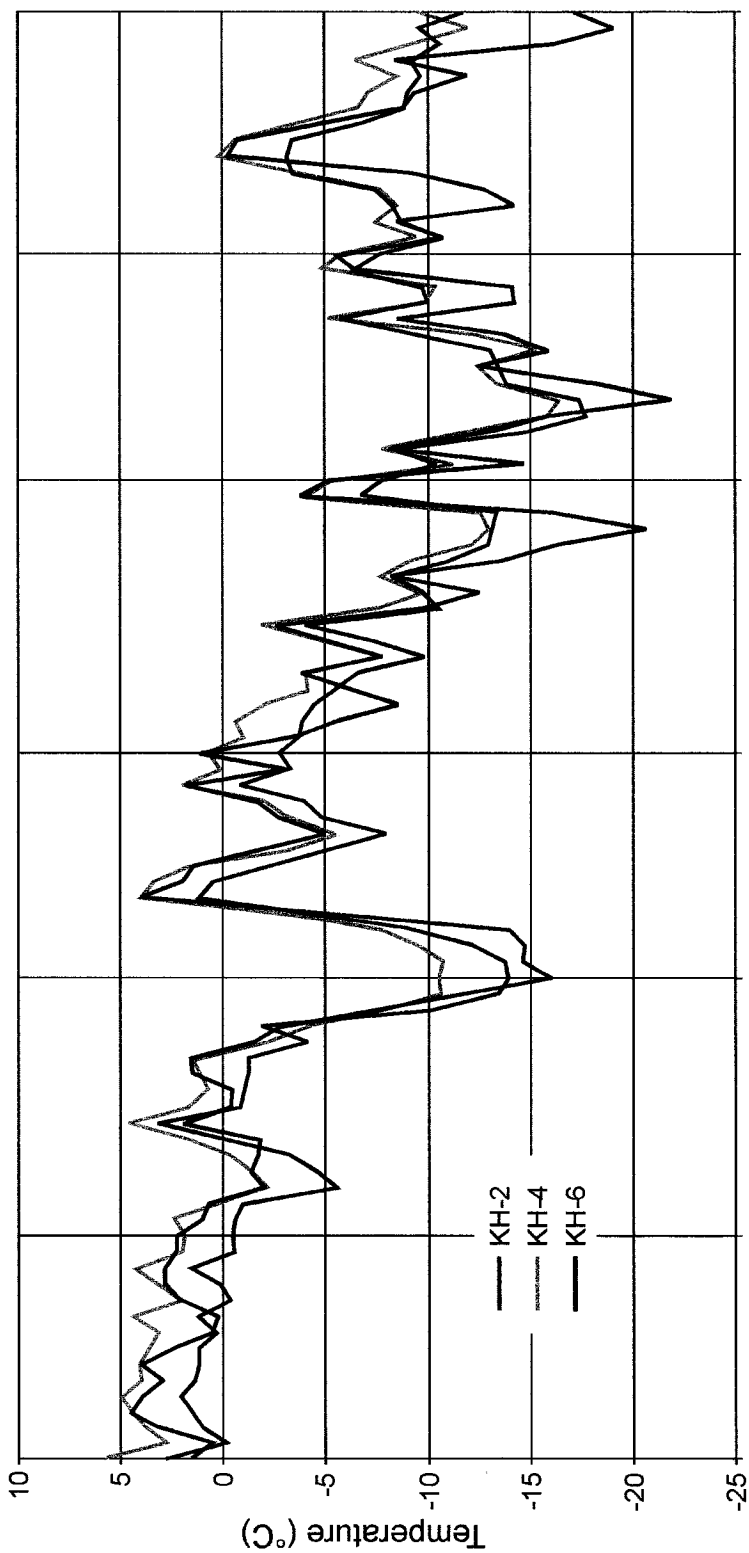

Figure 5.2a - Autumn (September, October and November) mean daily temperatures at three sites on the south-facing slope of Keno Hill.

observed as during September. The frequency of valley bottom inversions increased during November (Fig. 5.2a and Table 5.2b) and the inversion began to deepen. The duration of the inversions was still short (Table 5.2b).

During the winter months of December, January and February inversion conditions due to cold-air drainage dominated (Table 5.2a). In December, the month with the lowest amount of insolation, shallow inversions between KH-4 and KH-6 occurred 96% of the days, while deep inversions developed between KH-2 and KH-6 on 82% of the days (Table 5.2a). Inversion conditions decreased slightly in strength and duration in January and February. The largest mean daily temperature difference between the sites occurred in February (Fig. 5.2b, point 1) when a difference of nearly 15°C was observed between KH-2 and the bottom of the hill (~30°C km^{-1}).

The inversion frequency between KH-2 and KH-6 dropped dramatically from the beginning of March until mid-April at which point the top of the hill was always colder than the bottom. Meanwhile, the inversion conditions were frequent between KH-4 and KH-6 throughout this period due to radiative heating difference.

The summer months of June, July and August comprised the temperature records for two different years, August 2000 and June and July 2001. During the summer, KH-4 and KH-2 were nearly always the warmest and coldest sites respectively due to radiative warming and altitudinal cooling. Inversions between the top and bottom of the hill were infrequent and weak when they did occur, although the frequency of inversion between KH-4 and KH-6 remained high because of radiative heating at KH-4 and vegetative and topographic shading at KH-6 (Table 5.2a).

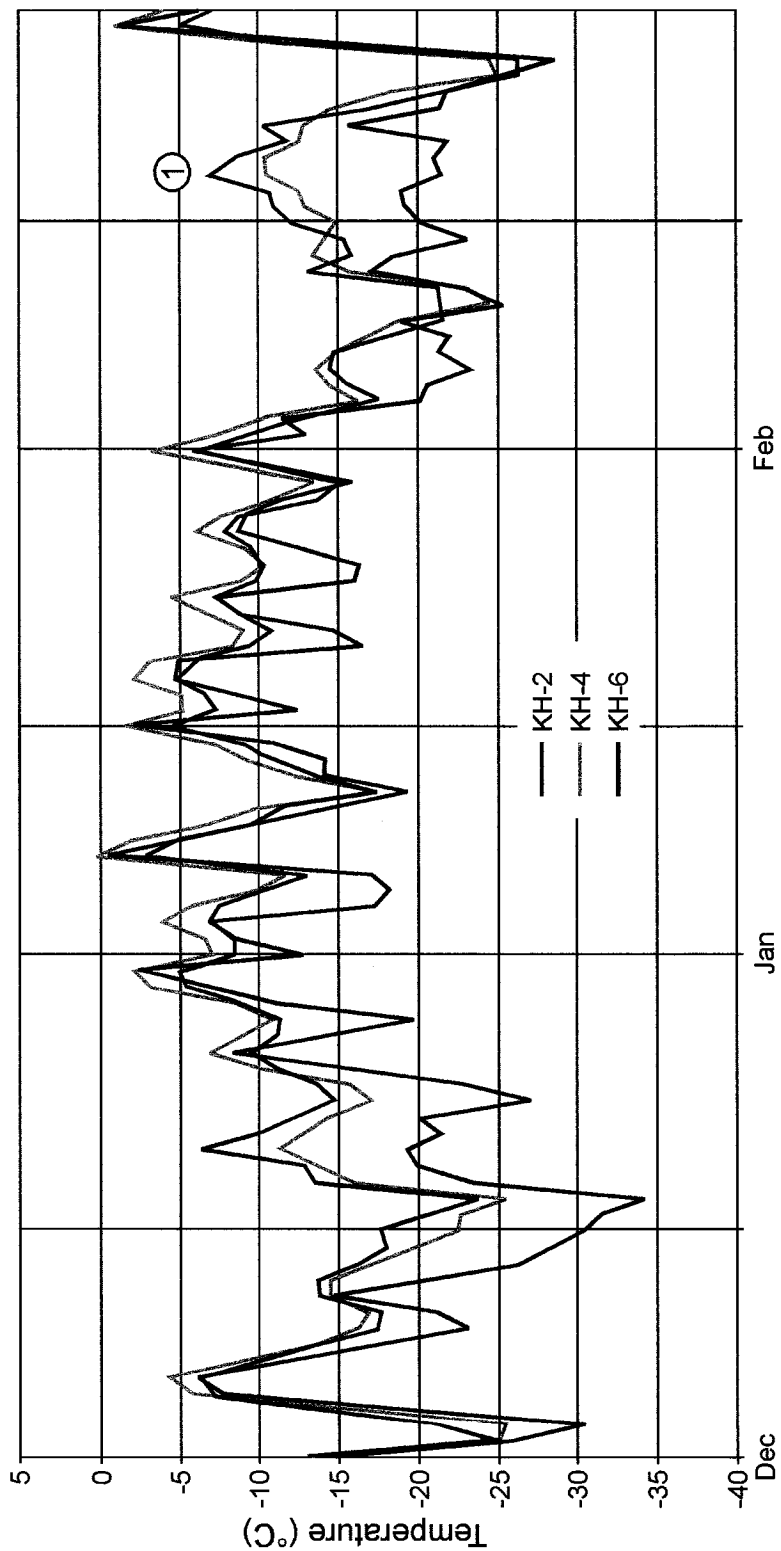

Figure 5.2b - Winter (December, January and February) mean daily temperatures at three sites on the south-facing slope of Keno Hill.

5.3. Aspect Trends in Air Temperature

The analysis of air temperature trends due to difference in aspect is limited to the lower elevations because only two sites on the north-facing slope had complete air and ground temperature records. The mean monthly temperature record for these two sites, SD-4 at 78 m above the valley floor (AVF) and SD-5 at 27 m AVF, were compared to KH-5, the south-facing site at 43 m AVF, as well as to KH-6. The mean monthly temperatures at these sites were similar throughout the year (Fig. 5.3). A Student's t-test, a parametric test of difference between two samples, was conducted to compare the mean monthly temperatures on the two slopes with each other and with the valley bottom mean monthly temperatures (Ebdon 1985, 61). It was hypothesized that the north-facing slope would be colder than the south-facing slope due to lower annual insolation. The one-tailed Student's t-test found that no significant difference could be distinguished in mean daily temperature, on a monthly basis, between KH-5, KH-6, SD-4 and SD-5, at the 0.05 level (Table 5.3).

The similarity of mean monthly temperatures at the various low-elevation sites may be explained with respect to solar radiation and canopy cover differences between the sites, as well as by cold-air drainage. When solar radiation is low from December to February, both slopes receive very little insolation and heating differences are minimal. In addition, pooling of cold air in the valley bottom by cold-air drainage occurs. The temperature observations indicate that the cold-air drainage produces a 50 m to 80 m band of cold air in the valley bottom, with the coldest air directly in the valley bottom (KH-6) (Fig. 5.3). During the other months of the year, cold-air drainage is not a prominent feature of the climate and a different explanation for the similarity of the mean

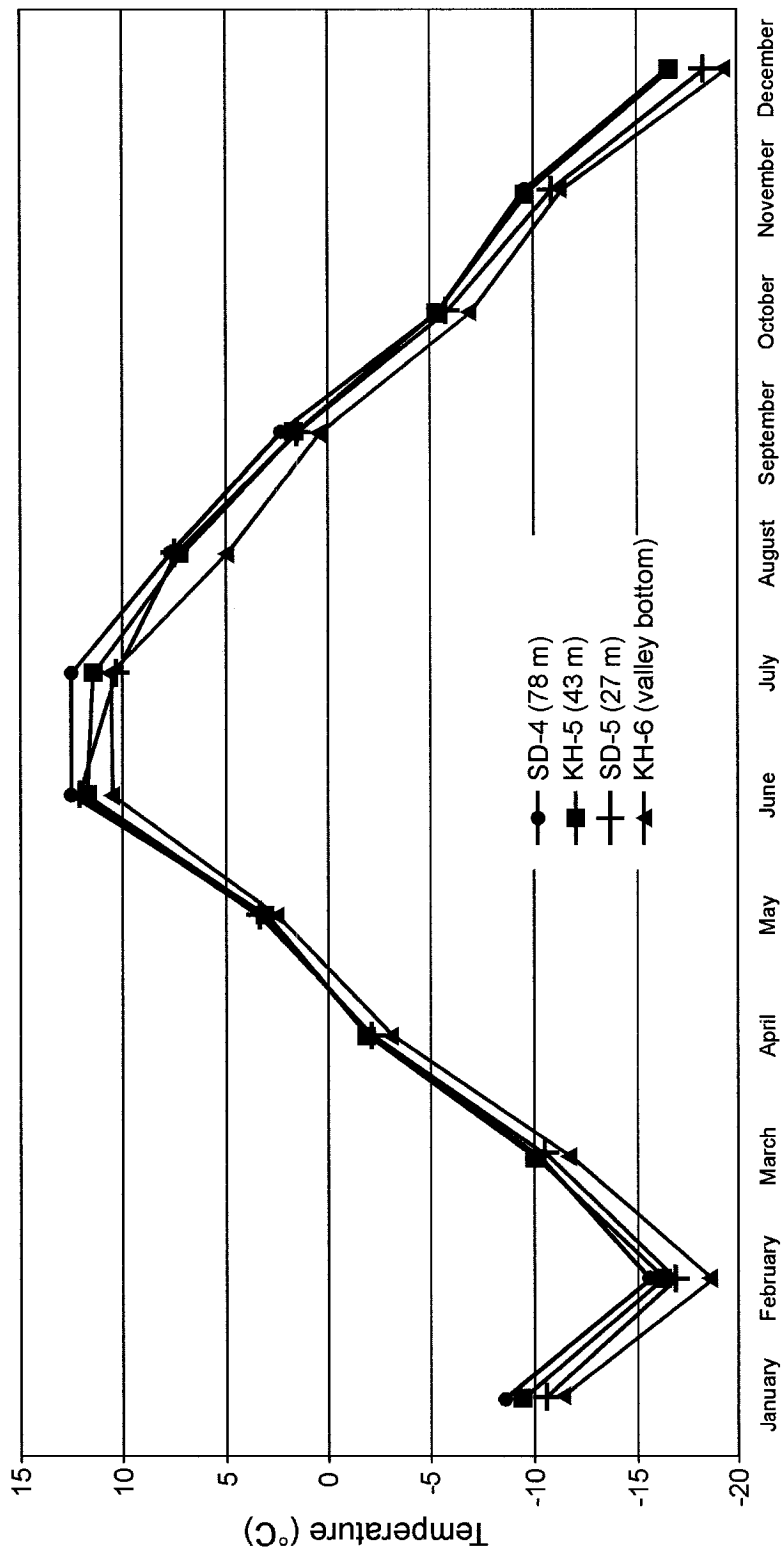

Figure 5.3 - Monthly mean air temperatures at four sites on adjacent north and south facing slopes, central Yukon.

Table 5.3. Mean daily air temperature differences (°C) and standard error of the differences at Keno Hill and Sourdough Hill sites for 2000-2001.

	KH-5 vs. KH-6	SD-5 vs. KH-6	SD-4 vs. KH-6	KH-5 vs. SD-4	KH-5 vs. SD-5
January	1.8±0.2	0.8±0.3	2.5±0.3	-0.6±0.2	1.1±0.2
February	2.3±0.3	1.7±0.3	3.1±0.4	-0.8±0.2	0.6±0.2
March	1.7±0.2	1.0±0.2	1.3±0.3	0.4±0.2	0.7±0.1
April	1.1±0.1	0.9±0.2	1.2±0.3	0.0±0.2	0.3±0.1
May	0.7±0.1	0.7±0.1	0.6±0.1	0.0±0.1	-0.1±0.1
June	1.1±0.1	1.5±0.1	2.0±0.2	-0.9±0.1	-0.4±0.1
July	0.8±0.1	1.0±0.2	1.8±0.2	-1.0±0.1	-0.6±0.2
August	1.0±0.2	1.1±0.1	1.2±0.2	-0.3±0.1	-0.2±0.1
September	1.1±0.1	1.0±0.1	1.3±0.2	-0.2±0.1	0.1±0.1
October	1.4±0.2	1.0±0.2	1.6±0.3	-0.2±0.1	0.5±0.1
November	1.5±0.2	0.4±0.2	1.5±0.3	-0.1±0.1	1.1±0.2
December	2.6±0.3	1.1±0.3	3.1±0.4	-0.5±0.2	1.5±0.2

monthly temperatures is required. Solar radiation is abundant in March through October, although the north-facing slope at these low elevations receives approximately 25 to 50% less solar radiation than low elevation sites on the south-facing slope (Table 4.6). This difference in solar radiation creates the potential for differential heating of the two slopes, although this is not observed (Fig. 5.3). This difference in solar radiation appears to be offset by the differences in vegetation canopy closure (Table 4.6). The vegetation canopies at KH-5 and KH-6 shade the ground by approximately 75% and therefore block a large proportion of the direct incoming solar radiation. In contrast, vegetation shading estimates at SD-4 and SD-5 are much lower at 37% and 40% respectively, which may account for the similarity in the air temperatures at the north- and south-facing low elevation sites (Table 4.6). Turbulent mixing of the air due to anabatic and katabatic winds may also contribute to these comparable temperatures (Barry 1992, 158).

5.4. Representativeness of 2000-2001 Air Temperature Record

To assess whether the 2000-2001 temperature record was representative of the temperature regime in central Yukon, the Mayo Airport temperature record was compared with the 1970-2000 mean monthly temperatures and standard deviations (Meteorological Service of Canada 2002) (Table 5.4a). The mean monthly temperature at Mayo Airport for 1974-82, the period of record for which temperature data at Keno 700 mine were available, was compared with the 1970-2000 monthly normals (Table 5.4a). No significant difference in temperature at Mayo was observed; therefore it is suitable to use the 1974-82 Keno temperature data to determine whether air temperature conditions during 2000-2001 were representative of the climate in the area.

Table 5.4a. Analysis of representativeness of the 2000-2001 air temperature record at Mayo Airport based on the 1970-2000 and 1974-1982 mean monthly temperatures and standard deviations. The number of asterisks indicates the number of standard deviations above or below the temperature mean the value is within.

	Mean temperature (°C)	Mean temperature (°C) and standard deviation	
	2000-2001	1970-2000	1974-82
January	-11.8**	-25.7±8.0	-26.1±10.1
February	-18.7	-18.8±6.5	-20.2±8.8
March	-7.6	-9.4±3.7	-9.9±3.6
April	0.8	-1.1±2.4	0.6±1.8
May	6.9**	8.5±1.5	8.4±1.6
June	15.0	14.0±1.1	13.3±0.9
July	15.3	16.0±0.9	15.7±0.8
August	11.1**	13.0±1.5	13.4±1.3
September	3.2**	6.3±1.8	7.3±1.4
October	-3.2	-2.8±2.7	-1.3±2.8
November	-10.0	-15.6±5.9	-13.3±6.3
December	-20.9	-22.2±6.7	-24.6±7.5
Mean Annual	-1.7	-3.9±3.5	-3.0±1.7

The mean monthly temperatures at KH-2 and KH-3 were compared with the monthly temperature statistics from Keno 700 mine, located on the south-facing slope of Keno Hill at 1472 m ASL, between KH-2 and KH-3 (Table 5.4b). December 2000 and January 2001 were unusually warm with mean monthly temperatures 7-8°C above the expected mean. August 2000, September 2000, and May 2001 all had mean monthly temperatures below one standard deviation from the mean. The warmer than expected months offset the cooler than expected months to produce a mean annual temperature of –4.2°C at KH-2 and –3.6°C at KH-3 for 2000-2001. These means are very similar to the 1974-1982 mean annual temperature at Keno 700 of –3.9°C (Table 5.4b). It can be concluded that the 2000-2001 air temperatures in the Keno area are within the expected range of climate variability, except for September 2000, and are thus reasonably representative of the climate conditions in this area.

5.5. Locating Permafrost at the Study Sites

Permafrost presence or absence at the eleven study sites was determined using both physical and thermal evidence collected in the field.

5.5.1. Physical Evidence

Observation of frozen ground and/or ground ice is regarded as direct physical evidence for the occurrence of permafrost. Frozen ground was encountered at KH-6, SD-1, SD-3, SD-4, and SD-5 during manual excavation in late summer 2001. Additional confirmation of the presence of permafrost in the valley bottom was provided by gold mining operations on Lightning Creek during summer 2000 and 2001. The creek bed

Table 5.4b – Analysis of representativeness of the 2000-2001 air temperature record based on the 1974-1982 mean monthly temperature values recorded at Keno 700 mine (aspect=S, elevation=1472 m). The number of asterisks indicates the number of standard deviations above or below the temperature mean the value is within.

	Observed 2000-2001		1974-82 Mean and Standard Deviation
	Mean temperature at KH-2 (°C)	Mean temperature at KH-3 (°C)	Mean temperature (°C) and standard deviation at Keno 700
Elevation	1515 m	1371 m	1472 m
January	-9.2**	-8.6**	-16.8±5.3
February	-14.3*	-14.4*	-13.9±2.5
March	-13.1**	-12.2*	-11.3±1.3
April	-5.1*	-4.0*	-4.7±1.3
May	-1.0**	0.3**	1.9±1.4
June	8.9**	9.8**	7.8±0.9
July	10.5*	10.2*	10.5±0.9
August	4.4***	5.1***	8.9±1.8
September	-1.1****	-0.4****	3.3±1.2
October	-6.9*	-6.3*	-5.6±1.4
November	-9.6*	-9.3*	-11.0±3.9
December	-13.4**	-13.7**	-16.2±2.3
Mean Annual	-4.2	-3.6	-3.9

was excavated to bedrock, a depth of ~ 40 m and the soil profile revealed that ground ice was present in the upper 5 m along the ~ 300 m cut. All other sites were too rocky to dig deep enough to encounter frozen ground, if indeed it occurred. According to Williams and Burn (1996) a diagnostic factor for permafrost presence in central Yukon is high soil moisture content (>24%) in conjunction with a thick organic horizon (>11 cm). Based on this criterion, permafrost should be present at KH-6, SD-4, and SD-5 (Tables 4.3 and 4.4). Therefore, physical evidence indicates that permafrost occurs at SD-1, SD-3, SD-4, SD-5, and KH-6.

5.5.2. Ground Thermal Evidence

Annual mean ground temperature profiles at sites with complete records are presented in Figure 5.4. Sites with a mean annual ground temperature of less than 0°C are considered to have permafrost. The ground temperature records indicate that permafrost is present at the bottom two sites on Sourdough Hill (SD-4 and SD-5) and at the top (KH-1 and KH-2) and at the bottom (KH-6) of Keno Hill. The occurrence of permafrost based on the mean annual ground temperature at KH-5 is inconclusive because the ground temperatures at 50 cm and 75 cm are very close to 0°C. Permafrost is not present at KH-3 and KH-4 as ground temperatures are well above 0°C at all instrumented depths.

A "thermal offset" of increasing mean annual temperature with proximity to the ground surface is observed at SD-4, SD-5, KH-5 and KH-6. The offset between 5 cm and 20 cm varies from 0.2 to 1.5 °C, and is thought to result from the higher thermal

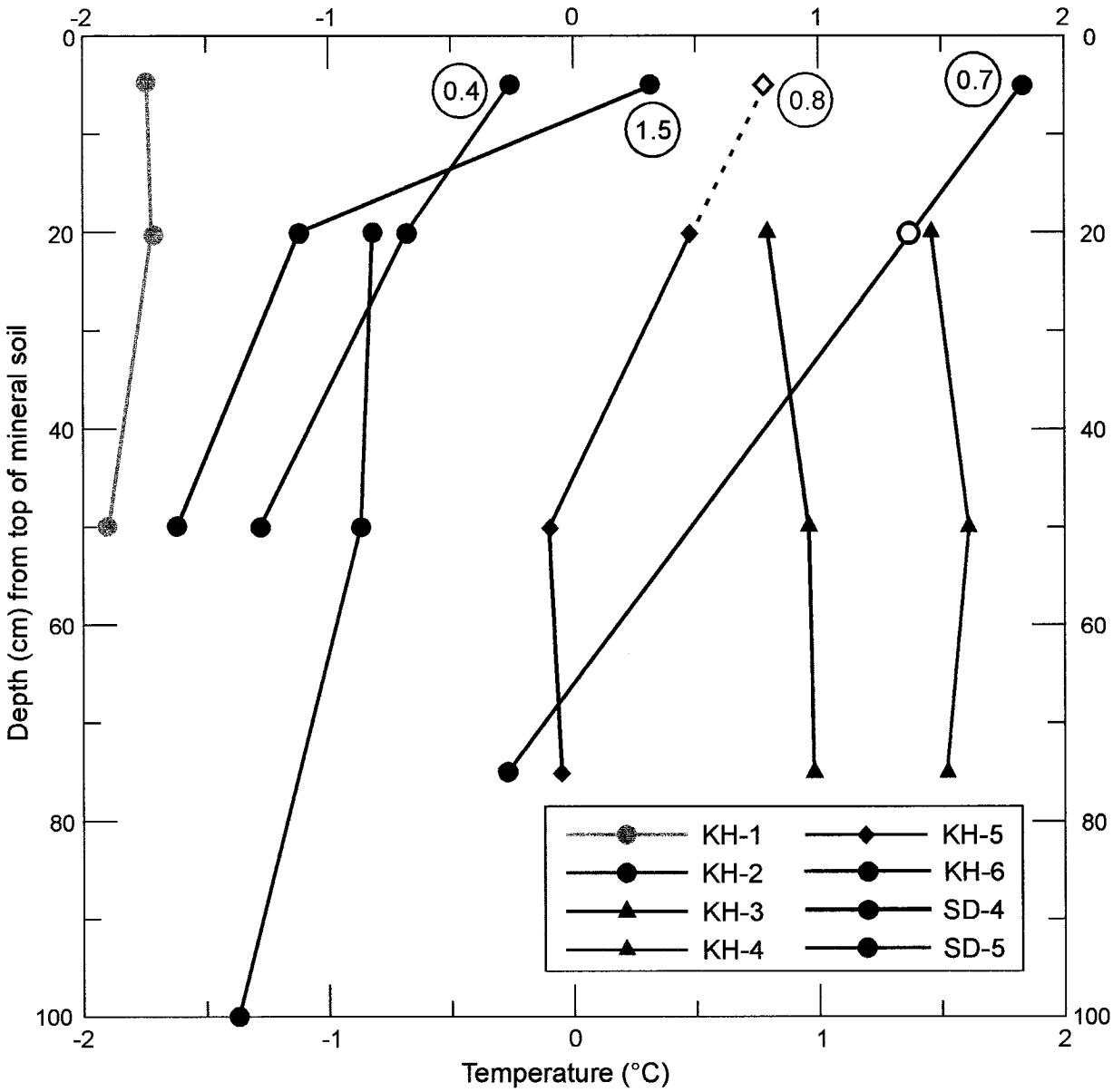

Figure 5.4 - Mean annual ground temperatures at instrumented depths for study sites with complete records on Keno and Sourdough Hills, central Yukon. Filled circles indicate sites where permafrost occurs or is likely to occur, filled triangles represent locations where permafrost is not likely to occur, whereas filled diamonds indicate uncertain permafrost conditions. The calculated or projected thermal offset (°C) between 5 cm and 20 cm is also presented.

conductivity of moist soils when frozen than thawed, similar to the effect of peat (Goodrich 1978, 1982; Burn and Smith 1988). The late season moisture values (Table 4.4) support this hypothesis as the sites with higher moisture content had a higher thermal offset. No thermal offset was observed at between 5 cm and 20 cm at KH-1 and KH-2.

A third method to determine whether permafrost is present or absent at a site based on a ground temperature record is to examine the progression of the ground temperature series during the freezing period. If no permafrost occurs at a site, the ground temperature will remain relatively warm after the ground initially cools because of the addition of latent heat as the unfrozen ground below continues to freeze throughout the winter. When permafrost is present at a site, the ground will cool after freeze-back of the active layer is complete. The ground temperature will continue to decrease throughout the winter because the underlying material is frozen and there is relatively little further supply of latent heat. The mean daily ground temperature plots for the eight sites with complete data records indicate that permafrost is present at KH-1, KH-2, KH-6, SD-5 and SD-4 and is absent at KH-3, KH-4 and KH-5 (e.g. Figs 5.5a and 5.5b).

In an attempt to clarify whether permafrost was present or absent at SD-2, the surface characteristics of SD-2 were compared to those of KH-3, the site it most closely resembles and for which a complete thermal record is available (Table 5.5). All site characteristics, except aspect and insolation are very similar. In particular the vegetation layer, which affects the surface offset between the air and ground temperature, is nearly identical. The percent cover of shrubs is the same at the two sites, and the organic-layer thickness at both sites is thin. Soil properties, such as soil moisture, drainage conditions,

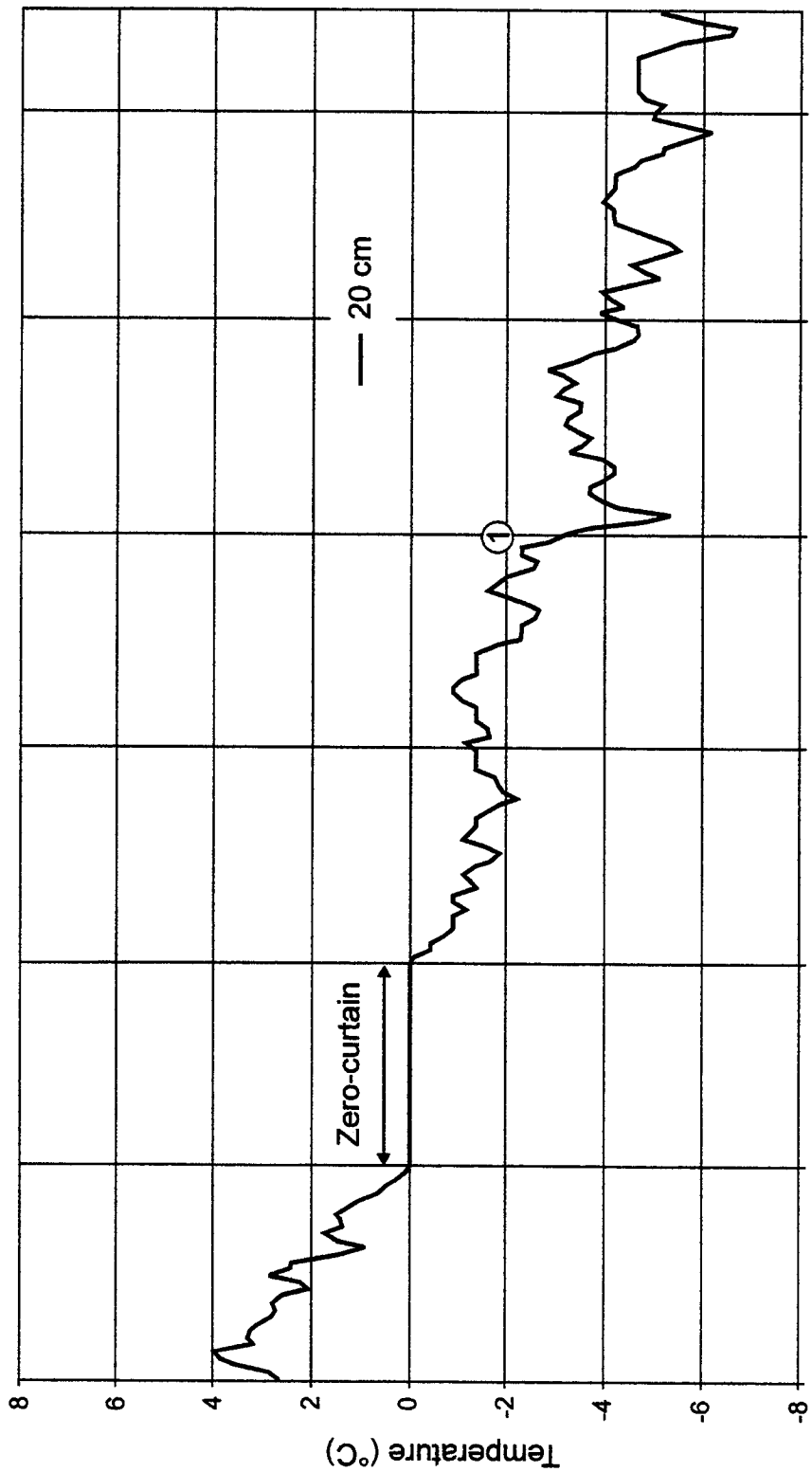

Figure 5.5a - Daily mean ground temperatures during freeze-back at KH-2. Freeze-back complete at point 1, after which the ground temperature continues to decrease indicating that permafrost is present at this site.

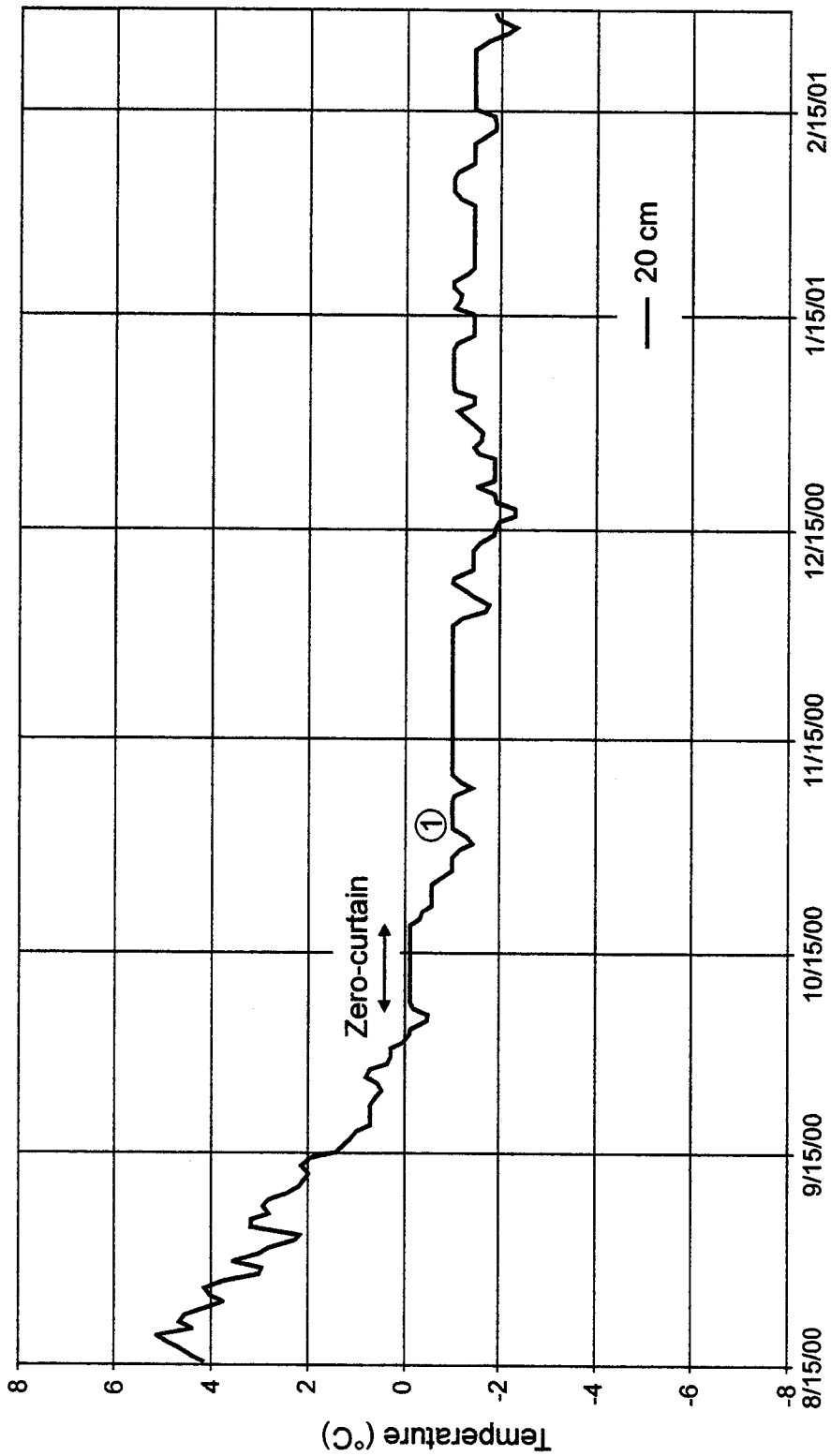

Figure 5.5b -Daily ground temperatures at KH-3. Freeze-back complete at point 1, after which the ground temperature stabilizes, and responds only to changes in air temperature, indicating that permafrost is absent at this site

Table 5.5 – Comparison of physical characteristics and temperature data of KH-3 and SD-2.

Physical Characteristics	KH-3	SD-2
Elevation (AVF) (m)	357	399
Elevation (m)	1371	1374
Organic layer thickness (cm)	10	10
Drainage	Moderately well	Moderately well
End of season soil moisture (%)	21	24
Slope (°)	11	6
Vegetation cover (%)	27	15
Annual isolation (% of KH4)	91	69
Aspect	175 (S)	350 (N)
Coarse materials (%)	49	51
Fine materials (%)	59	41
Textural class	Silty loam	Silty loam
Trees cover (%)	5	1
Shrub cover (%)	60	60
Herb cover (%)	25	50
Moss/lichen cover (%)	70	70
Other cover (%)	10	10
Position of site relative to treeline	Edge of treeline	Edge of treeline
Thermal Characteristics	**KH-3**	**SD-2**
Mean 20 cm ground temperature at end of thaw season (Aug 1-12, 2001) (°C)	7.9	4.0
Mean 50 cm ground temperature at end of thaw season (Aug 1-12, 2001) (°C)	6.0	2.6
Mean 80 cm ground temperature at end of thaw season (Aug 1-12, 2001) (°C)	5.0	1.2
Mean air temperature Aug 1-12, 2001 (°C)	10.5	11.2

and textural class are all similar suggesting that the thermal properties of the soil should be similar at the two sites.

However, comparison of ground temperatures at SD-2 and KH-3 near the end of the thaw season (August 1-12, 2001) shows that temperatures at SD-2 were colder at all measured depths (Table 5.5). Two factors could explain these temperature differences. Snow could persist longer in the spring at the north-facing site (SD-2), resulting in a shorter time that the ground is exposed to thawing conditions resulting in colder ground temperatures. Colder ground temperatures could also occur because SD-2 receives approximately 22% less solar radiation on an annual basis than the south-facing site, although this did not translate into an apparent difference in the mean daily temperatures for August 1-12, 2001 (Table 5.5). The thermal plots for the August 1-12, 2001 data (Fig. 5.6) confirm that permafrost is absent at KH-3 as the line curves away from 0°C. The SD-2 thermal line is linear for this portion of the data and suggests that permafrost would be present at a depth of approximately 110 cm, deeper than the depth of the soil pit excavated at this site.

From the above analyses, summarized in Table 5.6, it can be concluded that permafrost is absent at KH-3, KH-4 and KH-5, and present at KH-1, KH-2, KH-6, SD-1, SD-2, SD-3, SD-4 and SD-5.

5.6. Determination of the Physical Factors Influencing the Distribution of Alpine Permafrost in the Study Area

An expert system is a model that is created based on specialized knowledge and experience in a particular field. In this study, the physical and thermal characteristics of

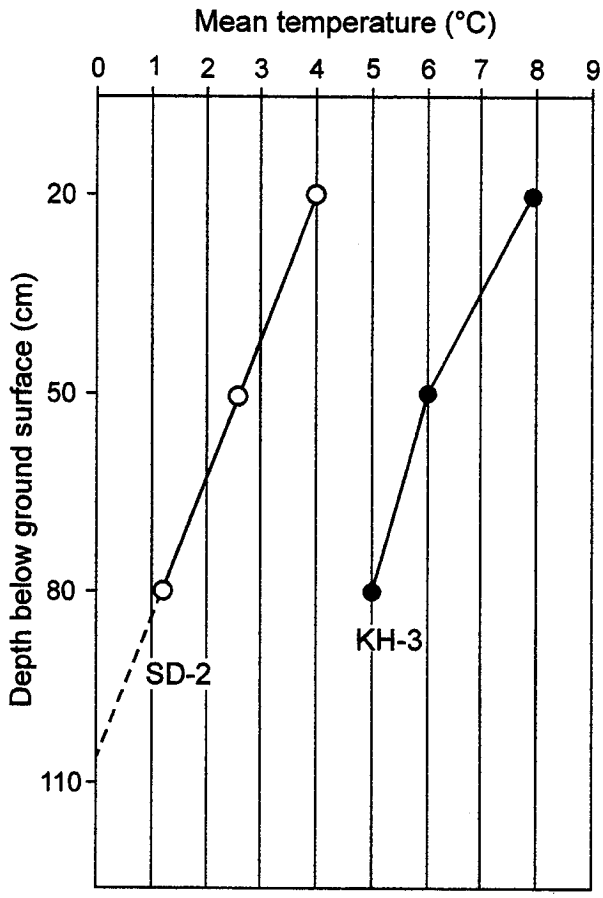

Figure 5.6 - Plot of mean ground temperature for August 1-12, 2001, at three depths at SD-2 and KH-3.

Table 5.6. Summary of the physical and thermal evidence for the occurrence of permafrost at the eleven study sites on Keno and Sourdough hills, central Yukon.

	Physical Evidence	Thermal Evidence			Conclusion
	Soil Pit	Mean Annual Ground Temperature Below 0°C	Progression of ground temperature series during freezing period	End of season ground temperature at 50 cm	Permafrost Present?
KH-1	0	1	1	-	Yes
KH-2	0	1	1	-	Yes
KH-3	0	0	0	-	No
KH-4	0	0	0	-	No
KH-5	0	Inconclusive	0	-	No
KH-6	1	1	1	-	Yes
SD-1	1	-	-	-	Yes
SD-2	0	-	-	1	Yes
SD-3	1	-	-	-	Yes
SD-4	1	1	1	-	Yes
SD-5	1	1	1	-	Yes

Where, "1" represents evidence for permafrost presence
"0" represents no evidence for permafrost presence
"-" represents data not analysed

the eleven test sites form the knowledge base from which a set of rules determining the presence or absent of permafrost in mountainous terrain has been developed.

Figure 5.7 presents an expert system that could be used to determine whether permafrost was present or absent in a biogeoclimatic zone. The expert system consists of a short series of decisions, determined by vegetation characteristics of an area as interpreted from a remote source such as aerial photographs. A DEM of the area is also useful because it provides aspect, slope and elevation information which may assist interpretation of aerial photographs and decision-making on the occurrence of permafrost. For example, the position of treeline is influenced not only by elevation, but also by aspect with treeline typically being lower on north-facing slopes than on south-facing ones. Differences in topographic shading may also be manifest in the position of the treeline.

The following two sections justify each decision in the empirical model based on the knowledge acquired from the test sites on Keno Hill and Sourdough Hill.

5.6.1. Empirical Model

Decision 1 (Fig. 5.7) ⇒ Above treeline, permafrost is likely to occur.

The first criterion the expert system considers is location relative to treeline. Treeline is defined as the uppermost elevation that upright trees grow. Trees may exist above this limit, but are in krummholz form. At lower elevations, where more favourable conditions exist, the same species grow upright (Wardle 1974, 371). Study sites that are above treeline are KH-1 and SD-1, where no trees exist, and KH-2 where krummholz of alpine fir are present.

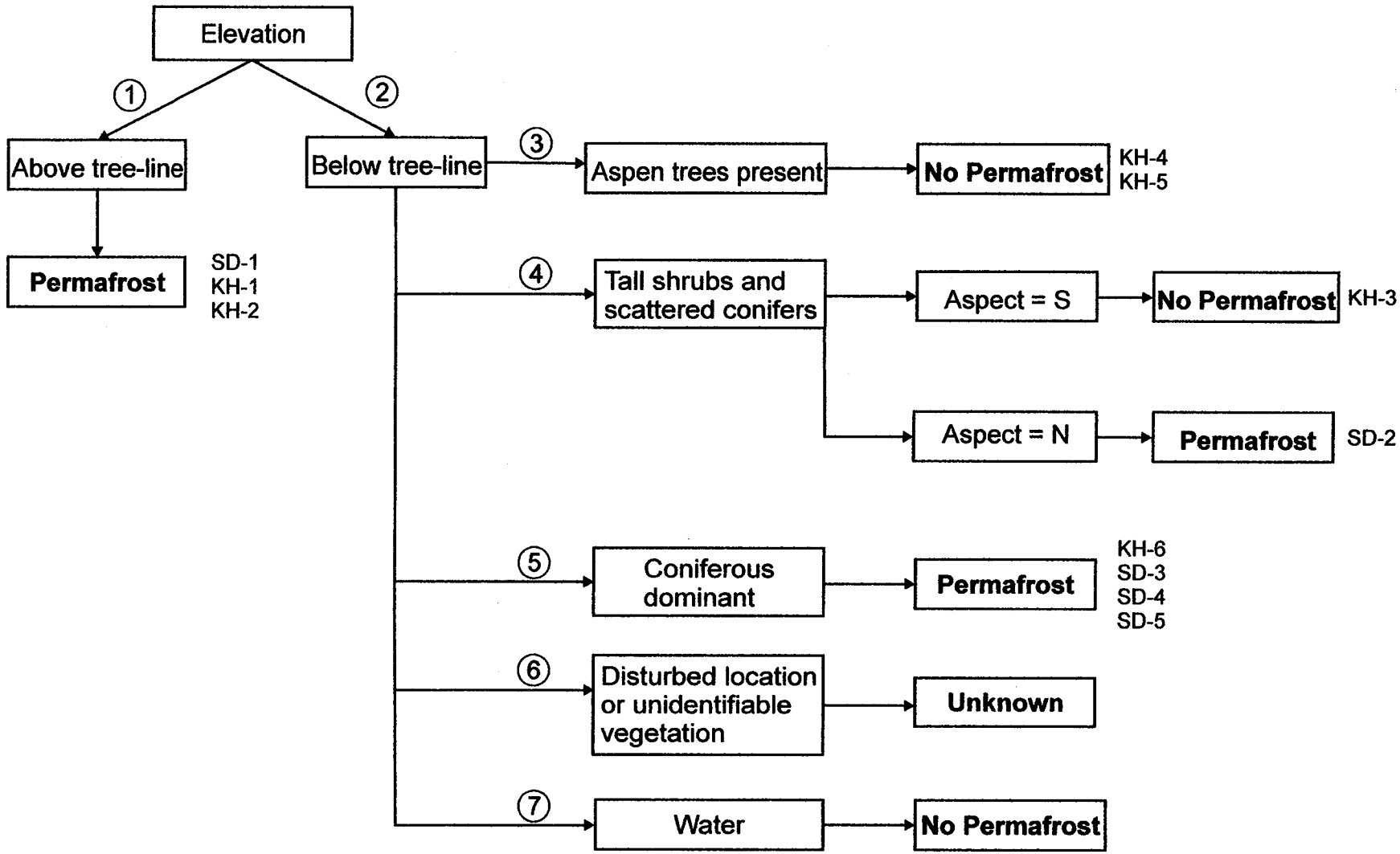

Figure 5.7 - Expert system describing a set of rules to determine whether permafrost is present or absent in mountainous terrain in central Yukon based on vegetation characteristics derived from aerial photographs and a DEM. The numbers in the circles identify the various decisions as discussed in the text.

Permafrost is likely present at locations above treeline because of the climate, vegetation and snow cover characteristics of these areas. The climate is cool throughout the year (Fig. 5.1). In the winter, these sites are situated above the inversion layer at least 60% of the time, thus the winters are relatively cold. In summer, these sites are also relatively cold because of high altitude. Although abundant, the vegetation cover at these sites is low to the ground and is dominated by mosses, lichens, and forbes/grasses. Low shrubs are also numerous where krummholz exist. Organic layer thicknesses above treeline also tend to be low because of low primary productivity.

This low vegetation cover influences the thermal regime of the ground, particularly in winter. The snow cover is redistributed by wind, leaving thin snow packs in areas of low vegetation. In the short thaw season, relatively thick active layers (at least 75 cm) develop despite the cool air temperatures. The active layer is able to thaw rapidly in summer because little ground shading occurs and the vegetation/organic buffer layer is thin, resulting in a small surface offset between the air and ground temperatures (Fig. 5.4).

Decision 2 (Fig. 5.7) ⇒ Below tree-line, additional decisions must be made

Sites below treeline must be classed into one of four categories based on vegetation characteristics.

Decision 3 (Fig. 5.7) ⇒ Aspen trees present, permafrost is not likely to occur:

Aspen trees require specific growing conditions, namely relatively warm air temperatures and well-drained, loamy soils (MacKinnon *et al.* 1999). They will not

tolerate permanently saturated soil conditions. Aspen forests are confined to areas with favourably warm microclimates and, in the study area, occur primarily on well-drained south-facing slopes at relatively low elevations. These growing requirements are similar to conditions that promote seasonal ground freezing only, as at KH-4 and KH-5. Therefore, the presence of aspen trees in pure stands or in conjunction with coniferous trees may be considered diagnostic of permafrost-free sites.

Aspen trees are easily identified on aerial photographs as they appear as bright patches. Paper birch (*Betula papyrifera*) is the only other deciduous species that grows to be tree-sized in alpine areas of central Yukon and it grows under similar conditions as aspen. Other deciduous species, *Populus* spp. and *Salix* spp., are commonly found only as shrubs in this region. Elevation, aspect and slope information from the DEM are also useful in classifying areas of aspen forest and distinguishing them from willow stands, the dominant deciduous small tree/shrub in the study area. Willows are found in a variety of environments, some of which are not commonly associated with the site characteristics that support aspen growth.

Decision 4 (Fig. 5.7) ⇒ Tall shrubs and scattered conifers, permafrost likely to be present on north-facing slopes, and absent of south-facing slopes:

The band of vegetation near the elevational limit of treeline comprises tall shrub cover and scattered conifers. The two test sites for this tall shrub and scatter conifer class, SD-2 and KH-3, had very similar physical characteristics except for ground thermal conditions and annual insolation (Table 5.5). Snow cover is thick in tall shrub vegetation because *in situ* and blowing snow are trapped within the branches during winter (Table

4.8). Snowmelt occurs later in spring on north-facing than on south-facing slopes due to lower amounts of solar radiation. The ground is therefore exposed to thawing conditions for less time, resulting in perennially frozen ground beneath tall shrubs on north-facing slopes, while permafrost is absent beneath this vegetation type on south-facing slopes (Price 1971). This vegetation type can be distinguished from areas of low shrubs on aerial photographs by the presence of trees. Elevational information is also helpful in defining these areas.

Decision 5 (Fig. 5.7) ⇒ Coniferous dominant, permafrost likely to occur:

The final vegetation class considered is coniferous forest. The presence of numerous coniferous trees, alone or in conjunction with tree/shrub types other than aspen, may be considered diagnostic of locations where permafrost exists. Thick (15-30 cm) moss layers are commonly associated with this forest type, which inhibit ground warming when the surface layer is dry, usually in summer, and assist ground cooling when moist or frozen. Areas dominated by coniferous vegetation are easily defined on aerial photographs. Species differentiation is more difficult, but is not required.

Decision 6 (Fig. 5.7) ⇒ Disturbed site or indiscernible vegetation cover, unknown permafrost conditions:

Locations that are disturbed, such as old mining areas, and areas where vegetation cover is not identifiable on the aerial photographs are excluded from the model, as permafrost conditions are unknown at these locations.

Decision 7 (Fig. 5.7) ⇒ Water body, no permafrost:

Permafrost is unlikely to occur beneath the water bodies in the study area, because the mean annual air temperatures are not cold enough for the lakes to freeze to the bottom in winter (e.g. Burn and Smith 1990). This results in an annual lake bottom temperature above 0°C, and a talik beneath the lake.

5.7. Chapter Summary

This chapter presented the air temperature records for August 2000-2001 at the various study sites on the south-facing slope of Keno Hill and the north-facing slope of Sourdough Hill. Shallow temperature inversions between KH-4 and KH-6 occurred on 96% of the days in December, January and February, with an average strength of 30.0±3.2°C km^{-1}. Deep winter temperature inversions of 500 m occurred on 82% of days with an average strength of 30.0±3.2°C $km^{-1}$and an average duration of 5.7±1.5 days, similar to the averages at Norman Wells (Taylor *et al.* 1998).

The ground temperature records at each site were coupled with physical evidence from soil pits to determine at which site permafrost occurred. On Keno Hill permafrost is present at KH-1 and KH-2, due to low vegetation cover and low mean annual temperature. It is present at KH-6 because of cold-air drainage in winter resulting in very cold winter temperatures coupled with a thick 30 cm moss cover, which insulates the ground from warm summer temperatures. Permafrost is absent at KH-4 and KH-5, sites in which aspen trees are present, because of the high solar radiation receipt and good drainage. Mean annual air temperature is highest at KH-4 because it is frequently positioned above the top of the inversion layer in winter. The thick snow cover at KH-3

insulates the ground from cold winter temperatures and preserves summer ground heat, resulting in permafrost-free conditions at the site.

Permafrost occurs at all sites on Sourdough Hill. The ground at SD-1 is perennially frozen for the same reasons that permafrost is present at KH-1 and KH-2, while permafrost is likely at SD-2 possibly because of late-lying snow cover. Permafrost occurs at SD-3, SD-4, and SD-5 primarily because of thick insulating moss cover. Air temperature data from SD-4 and SD-5 show that the sites are affected by cold-air drainage in winter.

Analysis of the air and ground temperature records and site characteristics at the study sites allowed development of an expert system to predict the occurrence of permafrost in mountainous terrain in central Yukon. The following chapter presents verification of the expert system at 12 test sites situated at various elevations and aspects in the hills around Keno.

CHAPTER 6
RESULTS AND DISCUSSION OF TESTING OF THE EMPIRICAL MODEL

6.1. Introduction

This chapter presents test results for the empirical model developed from the study of the thermal and physical characteristics of eleven sites in different biogeoclimatic zones in mountainous terrain in central Yukon.

The purpose of the exercise was to determine whether permafrost could be mapped in mountainous areas based on vegetation characteristics discernible from aerial photographs. The resolution of this mapping is dependent on the scale of the aerial photographs used.

6.2. Predicting Occurrence of Permafrost from Vegetation and DEM

A vegetation map for the Keno area was constructed using black and white aerial photographs at a scale of 1:20,000 (NAPL 1984) and a Kargl projector. The map was digitized in ArcView GIS, a proprietary GIS software, and a vegetation class was assigned to each polygon through interpretation of the aerial photographs, and elevation, slope and aspect information from the DEM (Fig. 6.1). The tall shrub vegetation class was divided into two separate classes based on aspect. North-facing slopes were defined as areas in the aspect map, derived from the DEM, with values ranging from 0-45° (N to NE) and 315-360° (NW to N). All other slopes were considered "south-facing". In ArcView GIS, the aspect map and the vegetation map were queried to extract areas where

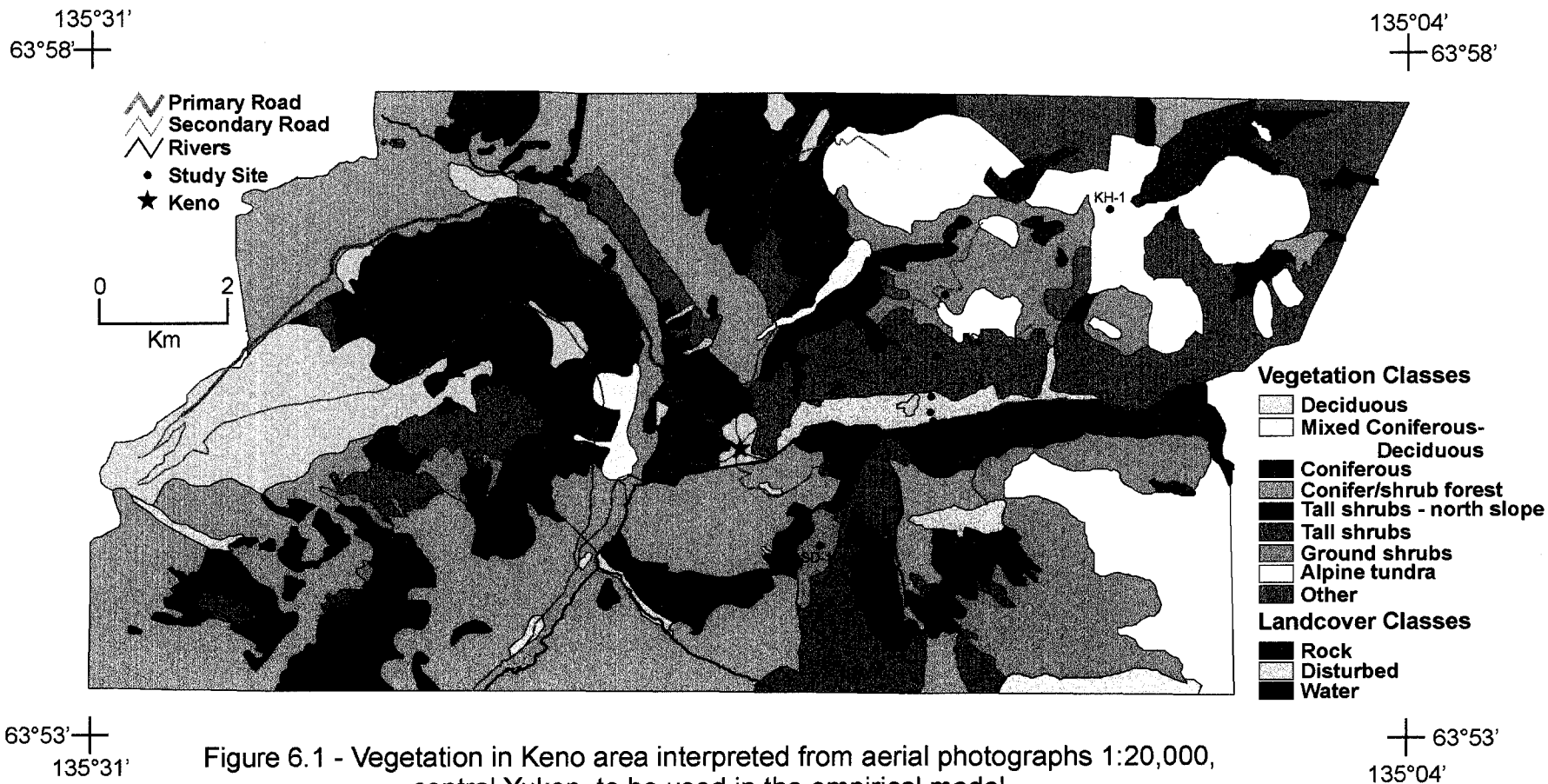

Figure 6.1 - Vegetation in Keno area interpreted from aerial photographs 1:20,000, central Yukon, to be used in the empirical model.

tall shrubs occurred on north-facing slopes. Areas with this new vegetation class had to be greater than 20,000 m^2 to be considered resolvable on the aerial photos and to be retained in the map.

The landscape in the study area is dominated by coniferous vegetation with over 50% of the area covered by mixed coniferous/shrub forest or coniferous forest (Table 6.1). The alpine tundra and very low shrubs vegetation classes, and the rock landcover class, occupy the area above tree-line and comprise 21% of the area. Vegetation that was not identifiable as belonging to one of the vegetation classes was classified as "other". The majority of this vegetation class was found in the valley and was unclassifiable because it is influenced by an adjacent creek. Numerous areas, totalling 6% of the study region, have been disturbed by mining activity. The Keno town site is also classified as disturbed.

Following the criteria outlined in the expert system (Fig. 5.7), the vegetation map was used to determine where permafrost was likely to occur or likely to be absent (Fig. 6.2). The empirical model predicted that 75% of the study area is likely to be underlain by permafrost (Table 6.2).

6.3. Testing the Permafrost Maps

6.3.1. Sampling Methods

To assess the accuracy of the map of predicted permafrost occurrence (Fig. 6.2), twelve accessible test zones were selected (Fig. 6.3), which were independent of the study sites. Within each test zone, 1-16 sampling sites were selected. The first sampling point was located at an accessible location within the zone and subsequent points were

Table 6.1. Summary of the percent area for vegetation and landcover class in the study region.

Vegetation Class	Area in Study Region (%)
Mixed forest - conifer and shrub	30
Coniferous	24
Tall shrubs	15
Alpine tundra	11
Very low shrubs and moss	9
Deciduous	2
Other	1
Mixed forest – conifer and deciduous	1
Landcover Class	
Disturbed	6
Rock	1
Water	>1

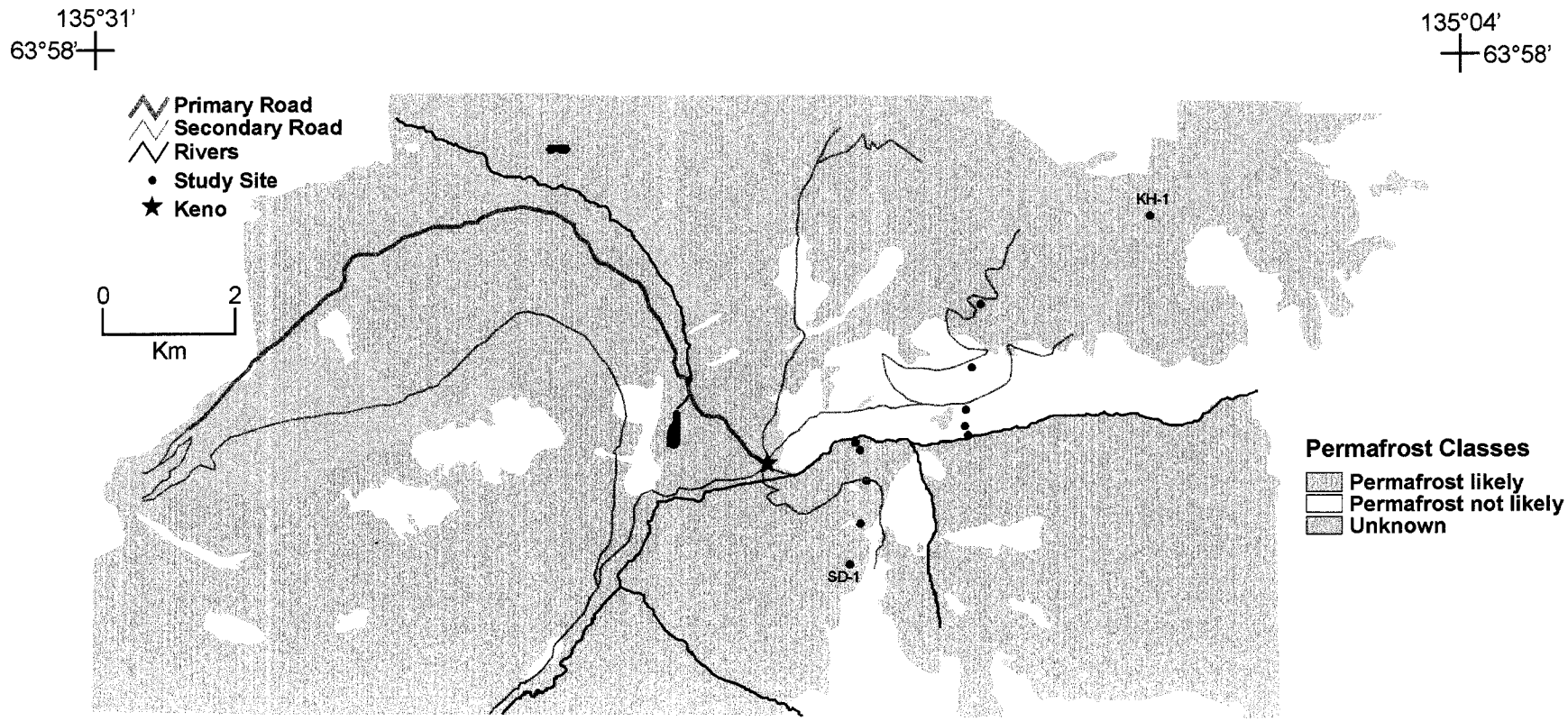

Figure 6.2 - Map of predicted permafrost occurrence in Keno area, central Yukon, constructed using the criteria outlined in the empirical model.

Table 6.2. Predicted percent area with and without permafrost in the Keno region based vegetation cover map derived from aerial photographs and the expert system created from the eleven study sites on Keno Hill and Sourdough Hill.

	Model
Permafrost Unlikely	17 %
Permafrost Likely	75 %
Unknown	8 %

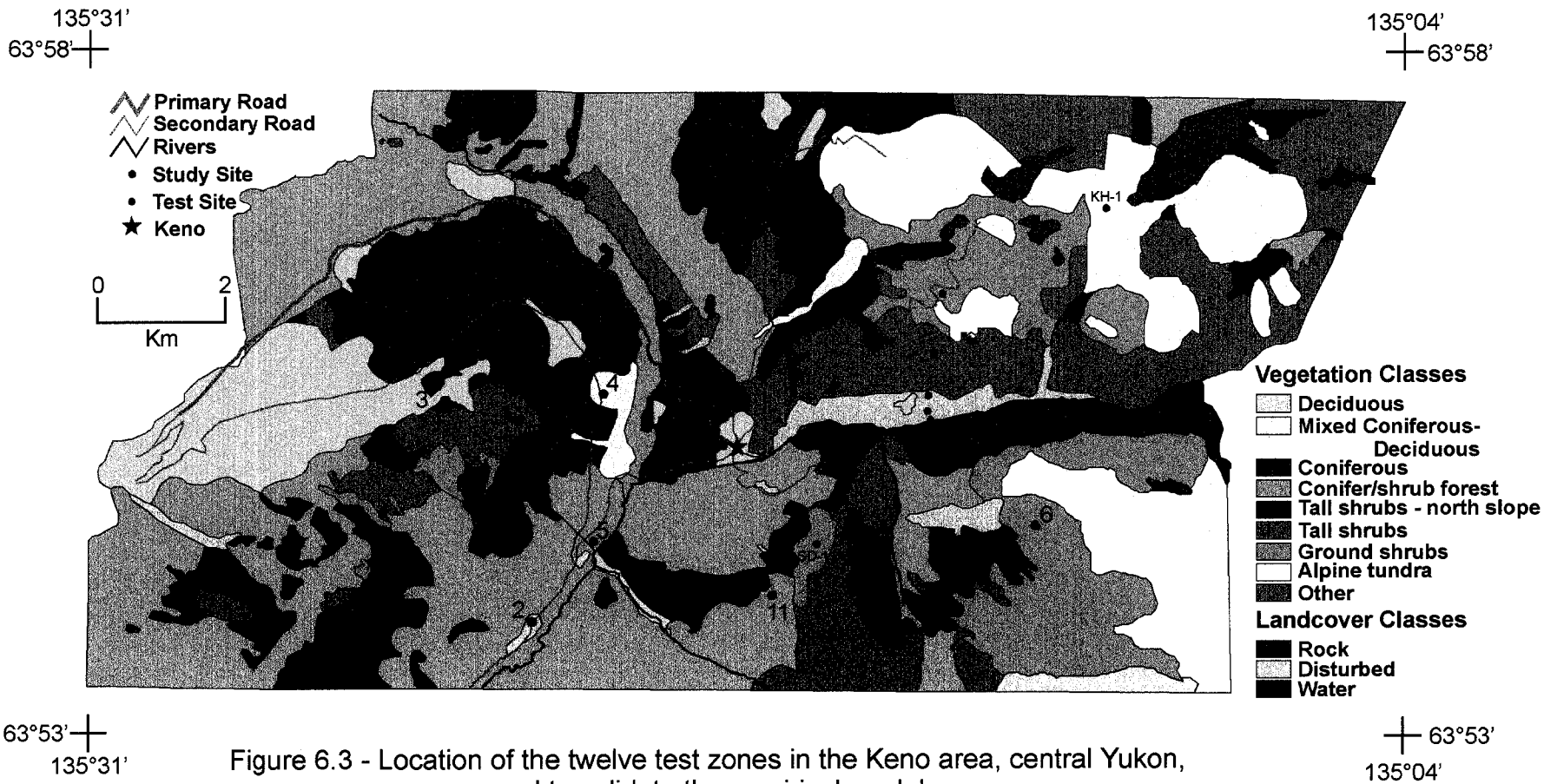

Figure 6.3 - Location of the twelve test zones in the Keno area, central Yukon, used to validate the empirical model.

spaced approximately 50-75 m apart. Testing was conducted from August 3-14, 2001, near the end of the thaw season, when ground temperatures were likely warmest and the active layer relatively thick.

Within each test polygon a summary of the physical characteristics of the area was recorded using methods similar to those at the study sites on Keno and Sourdough hills. A simplified vegetation study was conducted at one representative sampling site in each zone, to note percent cover for each stratum, as well as the dominant species in each stratum. Average slope and aspect were measured using an Abney level and a compass. One soil pit was dug to characterize the soil, with particular interest in the thickness of the organic layer. Ground temperatures were recorded with a steel ground probe with a thermistor near its tip at depths of 20 cm and 50 cm at each sampling point. If soil conditions permitted, i.e. frozen ground was not encountered or soil conditions were not too rocky, temperature was measured at a third depth greater than 50 cm.

A total of 138 points were sampled, with ground temperatures measured at a total of 320 depths, within the 12 test zones. At least one test zone was visited for each of the vegetation units: coniferous forest, deciduous forest, mixed coniferous/shrub forest, tall shrubs and ground shrubs. The coniferous forest vegetation was tested most often because it was the most accessible class that occurred over a range of elevations and aspects. A summary of the characteristics for each test zone is presented in Table 6.3.

Table 6.3. Summary of the sampling points used to verify empirical map of permafrost occurrence in Keno area, central Yukon.

Test Site	Number of Sampling Points	Total number of test depths	Elevation from DEM (m)	Vegetation Unit	Organic Layer Thickness (cm)	Aspect	Slope (°)
1	7	27	1345-1370	Tall shrubs	15	E	4
2	15	33	890-945	Deciduous forest	10	NE	22
3	16	41	1305-1345	Coniferous forest	30	N-NW	9 to 20
4	15	30	1060-1175	Mixed forest	15	SE	14
5	15	36	865-890	Conifer-shrub forest	30	SE	4
6	15	35	1250-1325	Low shrubs	15	S	18
7	15	35	1180-1220	Coniferous forest	25	NW	15
8	15	32	865-945	Coniferous forest	20	N	6 to 28
9	10	23	1310-1390	Coniferous forest	18	E	14 to 24
10	5	13	1110-1220	Coniferous forest	25	W	14
11	6	14	1160-1270	Conifer-shrub forest	15	W	14
12	1	1	1465	Tall shrubs	15	N	1

6.3.2. Determination of Permafrost Presence or Absence at Sampling Sites

Direct observations, either visual or thermal, of the occurrence of ground ice were obtained at only 15% of the sampling points due to relatively thick active layers and generally stony soil conditions. Therefore, to determine whether permafrost was present or absent at each sampling site, a thermal threshold was defined from the temperature data collected at the study sites on Keno and Sourdough hills. The near-end of thaw season (August 3-13, 2001) mean ground temperature at a depth of 50 cm was calculated for each study site (Table 6.4). Study sites with permafrost all had an end of thaw season temperature below 4.6°C at 50 cm, whereas at sites without permafrost the corresponding temperature was above 6.0°C. These two temperatures were classified as the threshold values for the presence or absence of permafrost respectively at the sampling sites. Permafrost occurrence at sampling sites with temperatures between 4.6°C and 6.0°C at 50 cm were classified as "uncertain" as the study sites did not provide enough information in this range.

6.3.3. Testing Methods and Results for the Expert System

To determine the accuracy of the model in predicting the occurrence of permafrost, the observed and/or inferred presence or absence of permafrost at each site was compared to conditions predicted in the permafrost map created from the vegetation classification. Of the 138 sampling points, 2 points fell within areas that were classified as disturbed where no permafrost information was available. An additional 14 sampling points had ground temperatures at 50 cm between 4.7°C and 6.0°C, the temperature range

Table 6.4. August 1-13, 2001 mean ground temperature at 50 cm. Occurrence of permafrost is also noted.

Site	Mean Temperature at 50 cm August 1-12, 2002 (°C)	Permafrost Present
KH-1	2.5	Yes
KH-2	4.7	Yes
KH-3	6.0	No
KH-4	8.4	No
KH-5	6.3	No
KH-6	-0.0*	Yes
SD-1	3.5	Yes
SD-2	2.6	Yes
SD-3	0.9	Yes
SD-4	0.3	Yes
SD-5	-0.1	Yes

* depth of 75 cm

where permafrost conditions are uncertain. These 17 sampling points were excluded from further analysis. The empirical model correctly predicted the presence and absence of permafrost in 75% of the cases (Table 6.5).

Table 6.6 summarises the accuracy of the model based on vegetation type. The two vegetation classes that predicted the presence of permafrost most accurately were the coniferous forest class and the conifer/shrub forest class, where 100% and 95% percent of the sampling points coincided with the prediction. These two classes occur over 53% of the study area and are easily discriminated on the aerial photographs. Based on the classes of permafrost defined by Heginbottom *et al.* (1995), these two vegetation classes can be considered to represent terrain in the continuous permafrost zone as 90 to 100% of the ground tested beneath these vegetation types was perennially frozen.

The success of prediction for the mixed forest, deciduous forest and tall shrub classes was not as high as for the first two vegetation classes. The errors in these vegetation classes may be discriminant errors produced by local conditions, not resolvable at the 1:20,000 scale of this model.

The mixed forest and deciduous forest classes were predicted to be permafrost-free in the model and both had success rates of 45% and 54% during testing (Table 6.6). In the field, the vegetation at the mixed forest test zone was found to be variable in terms of both species composition and percent coniferous and deciduous. Deciduous tall tree species included paper birch and trembling aspen, with willows as the primary understory tree, while white spruce, hybrid white-black spruce and alpine fir were all found in the test area. The thickness of the moss cover was also variable, although generally less than

Table 6.5. Summary of results of testing of the empirical model.

	Modified Model
Correct (Model/Test Site)	92 (75%)
Yes/Yes	78
No/No	14
Incorrect (Model/Test Site)	30 (25%)
Yes/No	15
No/Yes	15
Total Complete Sites	122
Uncertain (Model/Test Site)	16
Uncertain/Yes	2
Yes/Uncertain	7
No/Uncertain	7

Table 6.6. Summary of results of testing of the modified empirical model on a vegetation unit basis.

	Coniferous	Conifer/shrub	Mixed Coniferous & Deciduous	Deciduous	Tall shrub	Tall shrub - north	Low shrubs
Correct (Model/Test Site)	59 (100%)	18 (95%)	5 (45%)	7 (54%)	2 (40%)	1 (100%)	0 (0%)
Yes/Yes	59	18	0	0	0	1	0
No/No	0	0	5	7	2	0	0
Incorrect (Model/Test Site)	0 (0%)	1 (5%)	6 (55%)	6 (46%)	3 (60%)	0 (0%)	14 (100%)
Yes/No	0	1	0	0	0	0	14
No/Yes	0	0	6	6	3	0	0
Total Complete Sites	59	19	11	13	5	1	14
Uncertain (Model/Test Site)	2	2	4	2	5	0	1
Uncertain/Yes	1	1	0	0	0	0	0
Yes/Uncertain	1	1	4	0	0	0	1
No/Uncertain	0	0	0	2	5	0	0

10 cm, throughout the test zone. The variability of the sampling site characteristics and the ground temperatures at 50 cm within this test zone illustrate the importance of microscale characteristics in the determination of the occurrence of permafrost. The empirical model and the 1:20,000 scale of the aerial photographs were not detailed enough to identify sub-areas of mixed forest for classification. At the deciduous forest sampling sites, similar microscale differences most likely resulted in permafrost being absent in some areas and present in others. Although these two vegetation classes are rare in the Keno area and cover only 3% of the study area, additional sampling sites are required to confirm the vegetation-permafrost relation. At the scale of this model, the mixed forest area can tentatively be associated with the occurrence of extensive discontinuous permafrost, as 50 to 90% of the terrain appears to be underlain by permafrost, and the ground beneath deciduous forest can be classified as sporadic discontinuous permafrost, with 10 to 50% of the area containing permafrost.

The model was accurate for 40% of sampling cases for the tall shrubs vegetation class at the test zone on the east-facing slope of Galena Hill, and was correct for the one sampling point on the north-facing slope of Keno Hill (Table 6.6). Approximately half the sampling points for this vegetation type yielded inconclusive results because the temperature at 50 cm classified as uncertain (4.7°C to 6.0°C) based on the thermal thresholds. More sampling sites are required to thoroughly analyse the relation between tall shrubs, aspect and permafrost occurrence. Based on this study, the tall shrub class on north-facing slopes falls within the continuous permafrost class with 90 to 100% of the ground underlain by permafrost, whereas sites with tall shrubs on other slopes may be classified as in extensive discontinuous permafrost.

From the KH-2 and SD-1 test sites, it was determined that low shrub vegetation would be associated with the occurrence of permafrost. One low shrub test zone was visited during the model verification and 15 sampling points were sampled. From thermal evidence at 50 cm, fourteen of the sampling points were classified as permafrost-free and one was uncertain, resulting in the model being incorrect 100% of the time. Two explanations are possible to account for this error. Permafrost may be present at this test location, but the active layer may be very thick resulting in ground temperature at 50 cm above the 6.0°C threshold specified in the model. Site characteristics conducive to thick active-layer development included a very strong slope (18°) and rocky texture for the material, producing conditions for good soil drainage, and high amounts of solar radiation associated with the south-facing aspect of this slope.

The second possible explanation for the error associated with this low shrub vegetation class is a logic problem within the model. Slope angle, and hence drainage, may be a discriminating factor for permafrost presence at a low shrub site. The slopes at the two study sites were more moderate at 6° and 2°, than the 18° measured at the test zone (Tables 4.2 and 6.3). Further sampling at various slope values within this vegetation unit is required to determine the relation between low shrubs and permafrost.

6.3.4. Permafrost Evidence from Mining Records

The locations of the mines where ground ice conditions were reported in mining records were plotted on Figure 6.4 (also see section 3.5). These observations of permafrost presence and absence support the distribution of permafrost in the Keno area generated by the expert system.

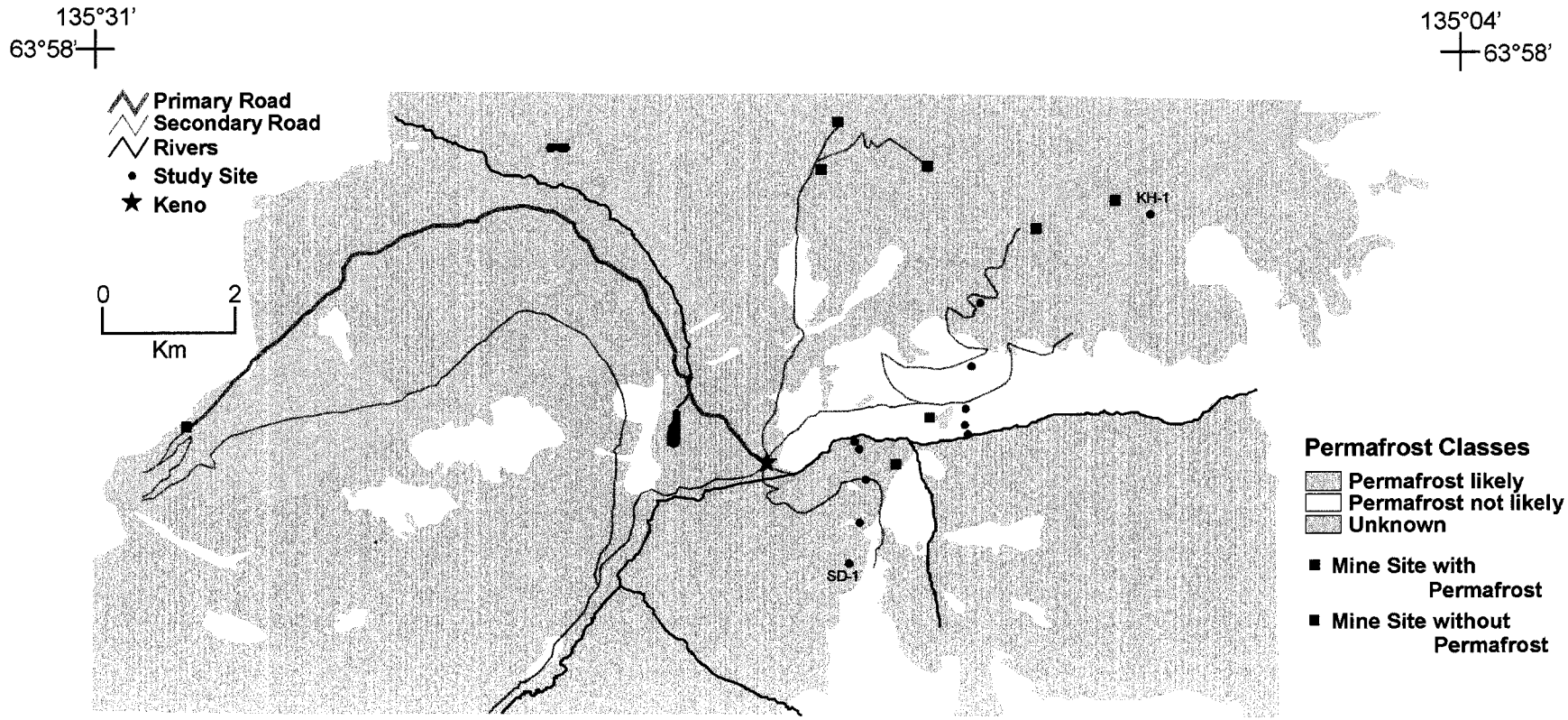

Figure 6.4 - Locations of mines in Keno area where observations of permafrost and permafrost-free soils have been made (also see section 3.5).

6.3.5. A Revised Map of Permafrost Distribution

Based on the results of the testing of the empirical model, a revised map of permafrost occurrence in the study area was produced (Fig. 6.5) using the permafrost classes on the permafrost map of Canada (Heginbottom *et al.* 1995). From this revised map, continuous permafrost was found beneath 66% of the study area, extensive discontinuous permafrost underlay <1% of the region, and sporadic discontinuous permafrost occurred in 24% of the study area (Table 6.7). The deciduous and mixed forest where the aspen trees were present on the south-facing slope of Keno Hill and the ground beneath lakes were classified as permafrost free, and occupied ~1% of the area. This revised map provides a more detailed estimate of the distribution of permafrost in the Keno area that is appropriate at the 1:100,000 spatial scale of the map. Previously, the distribution of permafrost in the whole area was described as extensive discontinuous based on national scale maps (Heginbottom *et al.* 1995; Marshall and Schut 1999). A weighted average for the permafrost classes in Figure 6.5 supports this observation.

6.4. Influence of Temperature Inversions on Permafrost Distribution

The influence of the winter temperature inversions and solar radiation on the distribution of permafrost is apparent on the south-facing slope of Keno Hill with continuous permafrost occurring in the valley bottoms and the mountain tops, while a band of sporadic discontinuous permafrost occurs in between (Fig. 6.5). This banding does not appear to occur on slopes at other aspects in the study area most likely due to differences in slope, moisture content, radiation receipt and organic-layer thickness at the various sites.

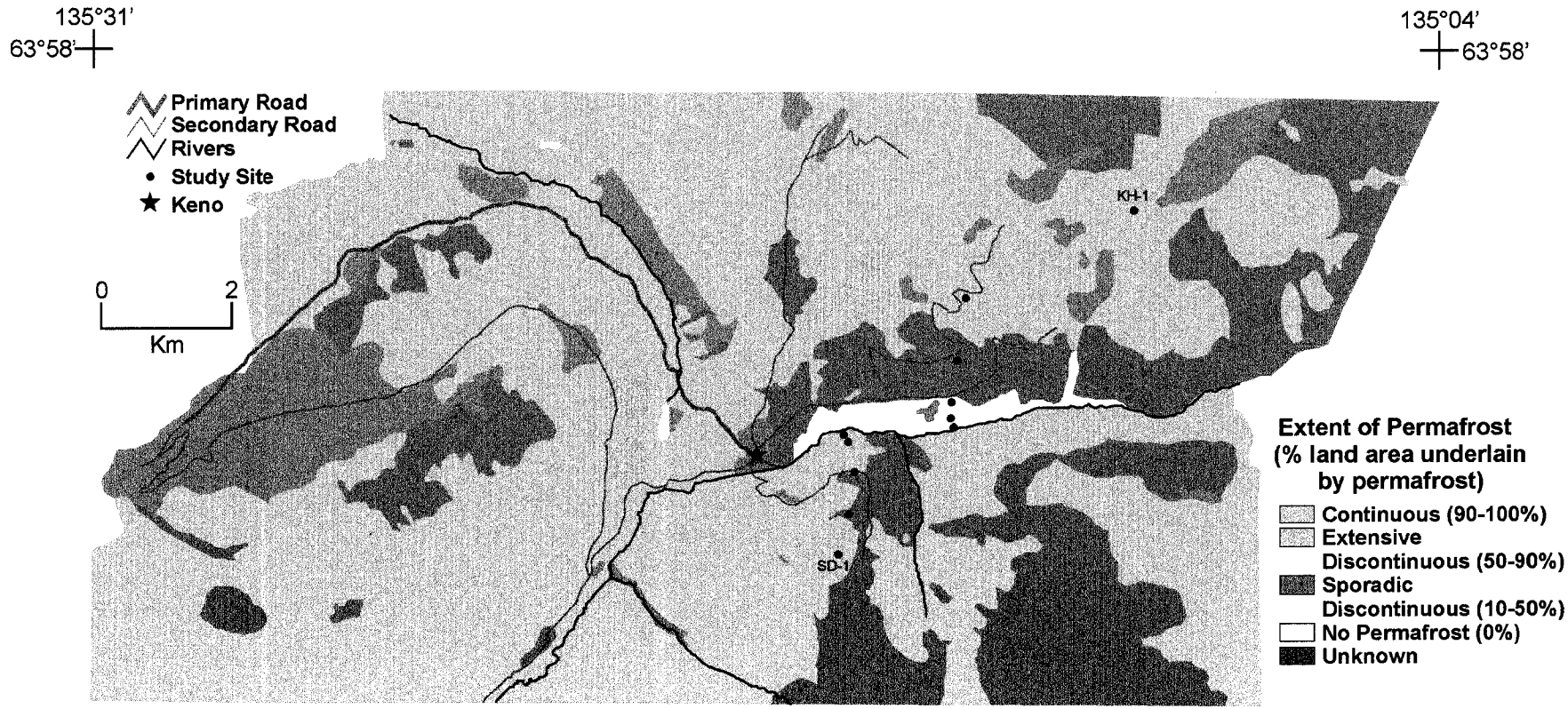

Figure 6.5 - Revised map of permafrost occurrence in the Keno study area based on the testing results of the empirical model and using the permafrost classes from the permafrost map of Canada.

Table 6.7. Percent area with various permafrost classes in the Keno area derived from testing of the empirical model.

	Percent area (%)
Continuous Permafrost Likely (90-100%)	66
Extensive Discontinuous Permafrost Likely (50-90%)	1
Sporadic Discontinuous Permafrost Likely (10-50%)	24
No Permafrost Likely (0%)	1
Unknown Permafrost Conditions	8

6.5. Discussion of Modelling Results

This work presents the first attempt to quantify empirical associations of surficial characteristics with the occurrence of discontinuous permafrost in mountain environments in Canada. The research complements the investigation on surficial characteristics associated with the occurrence of permafrost near Mayo conducted by Williams and Burn (1996), which focused on low elevation sites, primarily below 608 m ASL. The effect of the cooler climate at higher elevation is observed through a comparison of the associations between vegetation and permafrost in the Mayo area (Williams and Burn 1996) with those in the Keno area.

In this present study, the presence of coniferous forest or conifer/shrub forest was diagnostic of permafrost occurrence, and land beneath these vegetation types was classified as continuous permafrost. Williams and Burn (1996) found permafrost at 73% of coniferous forest study sites, resulting in low elevation coniferous forests being associated with extensive discontinuous permafrost. While the mixed forest class was related to extensive discontinuous permafrost in the Keno area, only 18% of the mixed forest sites in the Mayo area were in permafrost terrain. Finally, the deciduous class was diagnostic of permafrost-free soil near Mayo, whereas this vegetation class appears to be permafrost-free only on south-facing slopes in the Keno area. These observations indicate that the cooler climate near Keno produces differences in the nature of permafrost distribution and its association with surficial characteristics.

The ability to identify areas that are likely underlain by permafrost based on vegetation characteristics from 1:20,000 aerial photographs has many practical applications. Land-use planners interested in developing land in the Keno area and who

want to avoid to the costs of constructing on permafrost terrain, could use aerial photographs and a DEM for the area and immediately select the south-facing deciduous forest as a likely area for permafrost absence. The model developed would also recognize 65% of the area as unsuitable for building by identifying areas likely underlain by continuous permafrost such as coniferous forest, conifer/shrub forest and alpine regions. Standard techniques of permafrost or ground-ice delineation, such as geophysical surveys (Sinha and Stevens 1983) or drilling and ditching (Nixon *et al.* 1991) could then be conducted at specific sites in discontinuous permafrost.

6.6. **Chapter Summary**

This chapter presented the results of the testing of the empirical model developed in Chapter 5. The model predicted the presence or absence of permafrost with an accuracy of approximately 75%. The coniferous forest and conifer/shrub forest correctly predicted the occurrence of permafrost in these areas at 100% and 95% respectively. It was concluded that these vegetation units represent zones of continuous permafrost. The tall-shrubs on north-facing slopes also appear to be associated with continuous permafrost, although additional sampling points are required to confirm this relation. The model performed less successfully for mixed coniferous/deciduous forest, deciduous forest and the tall shrub vegetation class, but the results indicated that these vegetation units are in areas of discontinuous permafrost. Following verification of the model, a revised map of permafrost distribution was produced which identified ~66% of the area as likely being underlain by continuous permafrost, ~24% by sporadic discontinuous permafrost, and ~1% each for extensive discontinuous permafrost and no permafrost.

CHAPTER 7
CONCLUSIONS

Four conclusions can be drawn from this thesis:

1) Both shallow and deep winter temperature inversions occur in the Keno area on 82% and 96% of December to February days respectively, due to cold air pooling in the valley bottom. Shallow inversions are very strong with a mean strength of $30.0 \pm 3.2°C\ km^{-1}$, while deep inversions are weaker at $10.2 \pm 0.9°C\ km^{-1}$. Shallow inversions occurred at the study sites for 75% of the remainder of the year, dominantly due to topographic shading.

2) Data from the elevational transect on the south-facing slope of Keno Hill demonstrate the effect of temperature inversions on the thawing degree-days (DDT), freezing degree-days (DDF) and the annual mean air temperature (AMAT). KH-4, 163 m AVF, had the warmest AMAT temperature at –2.1°C, due to relatively high DDF. KH-6, in the valley bottom, and KH-2, located 500 m AVF, had similar AMATs, of –4.3°C and -4.1° respectively. Cold-air drainage as well as topographic shading produced cold AMATs at KH-6, while altitudinal cooling during spring, summer and fall produced cold AMATs at KH-2. A comparison of four low elevation sites with northerly, southerly and no aspect produced no significant difference in mean monthly temperatures. In winter this trend is attributed to the depth of the cold air in

the valley; during the remainder of the year, differences in vegetative shading may compensate for insolation differences on the two slopes.

3) As hypothesized, a band of unfrozen ground was present on the south-facing slope at ~10 to 170 m AVF of Keno Hill. This unfrozen zone was not observed on the north-facing slope of Sourdough Hill due to difference in slope, moisture content and organic-layer thickness between the two hills. The upper elevations of both hills were underlain with discontinuous and continuous permafrost.

4) Ground thermal and physical evidence from the study sites were used to develop an empirical model that predicts the presence or absence of frozen ground based on vegetation characteristics visible in aerial photograph and aspect and elevation information generated by a DEM. This site-specific model was then extrapolated to the Keno area, and at 122 test points had a map accuracy ~75%. It was possible to produce a map of permafrost distribution at a scale of approximately 1:100,000 based on the percent of ground underlain by permafrost through interpretation of vegetation from aerial photographs at a scale of 1:20,000.

REFERENCES

ACGR. 1988. Glossary of Permafrost and Related Ground-Ice Terms. Permafrost Subcommittee, Associate Committee on Geotechnical Research. National Research Council of Canada, Ottawa. Technical memorandum #142.

Adaptation and Impacts Research Group. 1999. Canada country study: Climate impacts and adaptation, volume I: Responding to global climate change in the British Columbia and Yukon region. *Edited by* E. Taylor and B. Taylor. Atmospheric and Environmental Services, Environment Canada.

Barry, R.G. 1992. Mountain weather and climate, 2nd edition. Routledge, London.

Barry, R.G., and Chorley, R.J. 1998. Atmosphere, weather and climate, 7th edition. Routledge, London.

Becker, P., Erhart, D.W., and Smith, A.P. 1989. Analysis of forest light environments, Part 1: Computerized estimation of solar radiation from hemispherical canopy photographs. Agricultural and Forest Meteorology, **44:** 217-232.

Bilello, M.A. 1966. Survey of Arctic and Subarctic Temperature Inversions. Cold Regions Research and Engineering Laboratory, Hanover, New Hampshire. Report 84-32.

Bond, J.D. 1998. Surficial geology of Keno Hill, central Yukon, NTS 105 M/14. Exploration and Geological Services Division, Indian and Northern Affairs Canada, Geoscience Map 1998-4, 1:50,000.

Bradley, R.S., Keimig, F.T., and Diaz, H.F. 1992. Climatology of surface-based inversions in the North American Arctic. Journal of Geophysical Research, **97:** 15,699-15,712.

Briggs, D., Smithson, P., Ball, T., Johnson, P., Kershaw, P., and Lewkowicz, A. 1993. Fundamentals of physical geography, 2nd Canadian edition. Copp Clark Pitman Ltd., Toronto.

Brown, R.J.E. 1963. Influence of vegetation on permafrost. *In* Proceedings, Permafrost International Conference. National Academy of Science, National Research Council, Publication 1287, Washington, D.C., pp. 20-25.

Brown, R.J.E. 1966. The relation between mean annual air and ground temperatures in the permafrost regions of Canada. *In* Proceedings, 1st International Conference on Permafrost, November 11-15, 1963, Lafayette, Indiana,. National Academy of Science, National Research Council, Publication 1287, Ottawa, pp. 241-246.

Brown, R.J.E. 1970. Permafrost in Canada: its influence on northern development. University of Toronto Press, Toronto.

Brown, R.J.E. 1975. Permafrost investigations in Quebec and Newfoundland (Labrador). National Research Council, Division of Building Research, Technical Paper 449.

Brown, R.J.E., and Péwé, T.L. 1973. Distribution of permafrost in North America and its relationship to the environment: a review, 1963-1973. *In* Proceedings, 2nd International Conference on Permafrost, North American Contribution, July 13-28, 1973, Yakutsk, U.S.S.R. National Academy Press, Washington, D.C., pp. 71-100.

Bryson, R.A. 1966. Air masses, streamlines and the boreal forest. Geographical Bulletin, **8**: 228-269.

Burgess, M.M., and Smith, S.L. 2000. Shallow ground temperatures. *In* The Physical Environment of the Mackenzie Valley, Northwest Territories: a Base Line for the Assessment of Environmental Change. *Edited by* L.D. Dyke and G.R. Brooks. Geological Survey of Canada Bulletin 547, pp. 89-103.

Burn, C.R. 1991. Permafrost and ground ice conditions reported during recent geotechnical investigations in the Mayo District, Yukon Territory. Permafrost and Periglacial Processes, **2**: 259-268.

Burn, C.R. 1993. Comments on "Detection of climatic change in the western North American arctic using a Synoptic climatological approach". Journal of Climate, **6**: 1473-1475.

Burn, C.R. 1998a. Field investigations of permafrost and climatic change in northwest North America. *In* Proceedings, 7th International Conference on Permafrost, June 23-26, 1998, Yellowknife, N.W.T. *Edited by* A.G. Lewkowicz and M. Allard. Nordicana, Québec, pp. 107-120.

Burn, C.R. 1998b. The response (1958 to 1997) of permafrost and near-surface ground temperatures to forest fire, Takhini River valley, southern Yukon Territory. Canadian Journal of Earth Sciences, **35**: 184-199.

Burn, C.R. 2000. The thermal regime of a retrogressive thaw slump near Mayo, Yukon Territory. Canadian Journal of Earth Sciences, **37**: 967-981.

Burn, C.R., and Smith, C.A.S. 1988. Observations of the "Thermal Offset" in near-surface mean annual ground temperatures at several sites near Mayo, Yukon Territory, Canada. Arctic, **41**: 99-104.

Burn, C.R., and Smith, M.W. 1990. Development of thermokarst lakes during the Holocene at sites near Mayo, Yukon Territory. Permafrost and Periglacial Processes, **1:** 161-175.

Canadian Society of Soil Science. 1993. Soil sampling and methods of analysis. *Edited by* M.R. Carter. Lewis Publishers, Boca Raton.

Desrochers, D.T., and Granberg, H.B. 1988. Schefferville snow-ground interface temperatures. *In* Proceedings, 5th International Conference on Permafrost, August 2-5, 1988, Trondheim, Norway. Tapir Publishing, Trondheim, **1:** 67-73.

Dingman, S.L., and Koutz, F.R. 1974. Relations among vegetation, permafrost, and potential insolation in central Alaska. Arctic and Alpine Research, **6**: 37-42.

Ebdon, D. 1985. Statistics in Geography, 2nd edition. Basil Blackwell Ltd., New York.

Environment Canada. 1982. Canadian climate normals, 1951-1980, Temperature and Precipitation, The North - Y.T. and N.W.T. Atmospheric Environment Service.

Environment Canada. 1993. Canadian climate normals, 1961-90, Yukon and Northwest Territories. Environment Canada, Canadian Climate Program.

Environment Canada. 1994. Canadian Monthly Climate Data and 1961–1990 Normals. CD-ROM data and access software.

Etzelmüller, E., Berthling, I., and Sollid, J.L. 1998. The distribution of permafrost in southern Norway – a GIS approach. *In* Proceedings, 7th International Conference on Permafrost, June 23-26, 1998, Yellowknife, N.W.T. *Edited by* A.G. Lewkowicz and M. Allard. Nordicana, Québec, pp. 251-257.

Farouki, O. 1981. Thermal properties of soils. CRREL Monograph 81-1, United States Army Corps of Engineers, Hanover, New Hampshire.

Frazer, G.W., Canham, C.D., and Lertzman, K.P. 1999. Gap Light Analyzer (GLA), Version 2.0: Imaging software to extract canopy structure and gap light transmission indices from true-colour fisheye photographs, users manual and program documentation. Simon Fraser University, Burnaby, British Columbia, and the Institute of Ecosystem Studies, Millbrook, New York.

French, H.M. 1970. Soil temperatures in the active layer, Beaufort Plain. Arctic, **23**: 229-239.

French, H.M. 1996. The Periglacial Environment, second edition. Essex, England, Longman, Inc.

Funk, M., and Hoelzle, M. 1992. A model of potential direct solar radiation for investigating occurrences of mountain permafrost. Permafrost and Periglacial Processes, **3**: 139-142.

Gold, L.W., and Lachenbruch, A.H. 1973. Thermal conditions in permafrost: a review of North American literature. *In* Permafrost, 2nd International Conference, North American Contribution, July 13-28, 1973, Yakutsk, Russia. National Academy of Sciences, Washington, D.C., pp. 3–23.

Goodrich, L.E. 1978. Some results of a numerical study of ground thermal regimes. *In* Proceedings, 3rd International Conference on Permafrost, July 10-13, 1978, Edmonton, Alberta. National Research Council of Canada, Ottawa, **1:** 29-34.

Goodrich, L.E. 1982. The influence of snow cover on the ground thermal regime. Canadian Geotechnical Journal, **19**: 421-432.

Gorbunov, A.P. 1978. Permafrost investigations in high-mountain regions. Arctic and Alpine Research, **2**: 283-294.

Gray, J.T., and Brown, R.J.E. 1979. Permafrost existence and distribution in the Chic-Chocs Mountains, Gaspesie, Quebec. Géographie physique et Quaternaire, **33:** 299-316

Haeberli, W. 1978. Special aspects of high mountain permafrost methodology and zonation in the Alps. *In* Proceedings, 3rd International Conference on Permafrost, July 10-13, 1978, Edmonton, Alberta. National Research Council of Canada, Ottawa, **1:** 379-384.

Harris, S.A. 1982. Cold air drainage west of Fort Nelson, British Columbia. Arctic, **35:** 537-541.

Harris, S.A. 1983. Comparison of the climatic and geomorphic methods of predicting permafrost distribution in Western Yukon Territory. *In* Proceedings, 4th International Conference on Permafrost, July 17-22, 1983, Fairbanks, Alaska. National Academy Press, Washington, D.C., pp. 450-455.

Harris, S.A. 1987. Altitude trends in permafrost active layer thickness, Kluane Lake, Yukon Territory. Arctic, **40:** 179-183.

Harris, S.A. 1988. The alpine periglacial zone. *In* Advances in Periglacial Geomorphology. *Edited by* M.J. Clark. John Wiley & Sons Ltd., New York., pp. 369-412.

Harris, S.A. 2001. Twenty years of data on climate-permafrost-active layer variations at the lower limit of alpine permafrost, Marmot Basin, Jasper National Park, Canada. Geografiska Annaler, **83A:** 1-14.

Harris, S.A., and Brown, R.J.E. 1982. Permafrost distribution along the Rocky Mountains in Alberta. *In* Proceedings, 4th Canadian Permafrost Conference, March 2-6, 1980, Calgary. National Research Council of Canada, Ottawa, pp. 59-67.

Hartmann, D.L. 1994. Global physical climatology. Academic Press, San Diego.

Heginbottom, A.J., Dubreuil, M.A., and Harker, P.A. 1995. Canada-Permafrost. *In* The National Atlas of Canada, 5th Edition. National Atlas Information Service, Natural Resources Canada, Ottawa. Plate 2.1. MCR 4177.

Hoelzle, M. 1992. Permafrost occurrences from BTS measurements and climatic parameters in the eastern Swiss Alps. Permafrost and Periglacial Processes, **3:** 143-147.

Ives, J.D. 1973. Permafrost and its relationship to other environmental parameters in a midlatitude, high-altitude setting, Front Range, Colorado Rocky Mountains. *In* Proceedings, 2nd International Conference on Permafrost, North American Contribution, July 13-28, 1973, Yakutsk, U.S.S.R. National Academy Press, Washington, D.C., pp. 121-125.

Ives, J.D. 1979. A proposed history of permafrost development in Laborador-Ungava. Géographie Physique et Quaternaire, **33:** 233-244.

Jorgenson, M.T., and Kreig, R.A. 1988. A model for mapping permafrost distribution based on landscape component maps and climatic variables. *In* Proceedings, 5th International Conference on Permafrost, August 2-5, 1988, Trondheim, Norway. Tapir Publishing, Trondheim, **1:** 176–182.

Kahl, J.D. 1990 Characteristics of the low-level temperature inversion along the Alaskan Arctic coast. International Journal of Climatology, **10:** 537-548.

Kahl, J.D, Serreze, M.C., and Schnell, R.C. 1992. Tropospheric low-level temperature inversions in the Canadian Arctic. Atmosphere-Ocean, **4:** 511-529.

Keller, F., Frauenfelder, R., Gardez, J.-M., Hoelzle, M., Kneisel, C., Lugon, R., Phillips, M., Reynard, E., and Wenker, L. 1998. Permafrost map of Switzerland. *In* Proceedings, 7th International Conference on Permafrost, June 23-28, 1998, Yellowknife, N.W.T. *Edited by* A.G. Lewkowicz and M. Allard. Nordicana, Québec, pp. 557-562.

King, L. 1986. Zonation and ecology of high mountain permafrost in Scandinavia. Geografiska Annaler, **68A**: 131-139.

King, L. 1990. Soil and rock temperature in discontinuous permafrost: Gornergrat and Unterrothorn, Wallis, Swiss Alps. Permafrost and Periglacial Processes, **1:** 177-188.

Klene, A.E., Nelson, F.E., Shiklomanov, N.I., and Hinkel, K.M. 2001. The N-factor in natural landscapes: Variability of air and soil-surface temperatures, Kuraruk River Basin, Alaska, USA. Arctic, Antarctic and Alpine Research, **33:** 140–148.

Kondratyev, K.Y., and Federova, M.P. 1977. Radiation regime of inclined slopes. World Meteorological Organization Technical Note 152. World Meteorological Organization, Geneva.

Kumar, L., Skidmore, A.K., and Knowles, E. 1997. Modelling topographic variation in solar radiation in a GIS environment. International Journal for Geographical Information Science, **11:** 475-497.

Lachenbruch, A.H., Cladouhos, T.T., and Saltus, R.W. 1988. Permafrost temperature and the changing climate. *In* Proceedings, 5th International Conference on Permafrost, August 2-5, 1988, Trondheim, Norway. Tapir Publishing, Trondheim, **3:** 9–17.

Lieb, G.K. 1998. High-mountain permafrost in the Austrian Alps (Europe). *In* Proceedings, 7th International Conference on Permafrost, June 23-28, 1998, Yellowknife, N.W.T. *Edited by* A.G. Lewkowicz and M. Allard. Nordicana, Québec, pp. 663-668.

Löve, D. 1970. Subarctic and subalpine: where and what? Arctic and Alpine Research, **2:** 63-73.

Lunardini, V.J. 1978. Theory of N-factors. *In* Proceedings, Third International Conference on Permafrost, July 10-13, 1978, Edmonton, Canada. National Research Council of Canada, Ottawa, **1:** 40–46.

Luthin, J.N., and Guymon, G.L. 1974. Soil moisture-vegetation-temperature relationships in central Alaska. Journal of Hydrology, **23:** 233-246.

Mackay, J.R., and MacKay, D.K. 1974. Snow cover and ground temperatures, Garry Island, N.W.T. Arctic, **27**: 287-296.

MacKinnon, A., Pojar, J., and Coupé, R. 1999. Plants of Northern British Columbia, 2nd edition. B.C. Ministry of Forests and Lone Pine Publishing, Vancouver.

Marshall, I.B., and Schut, P.H. 1999. A national ecological framework for Canada. Ecosystems Science Directorate, Environment Canada and Research Branch, Agriculture and Agri-Food Canada http://sis.agr.gc.ca/cansis/nsdb/ecostrat/intro.html (accessed on May 16, 2002).

Mathews, W.H. 1955. Permafrost and its occurrence in the south Coast Mountains of British Columbia. The Canadian Alpine Journal, **38**: 94-98.

McConnell, R.G. 1905. Report on the Klondike goldfields. *In* Annual report of the Geological Survey of Canada, Vol. 14, 1901. Part B. 1-71.

Meteorological Service of Canada. 2002. Historical Canadian Climate Database,Version 2. Monthly Rehabilitated Precipitation and Homogenized Temperature Data Sets provided by the Climate Monitoring and Data Interpretation Division of the Climate Research Branch. http://www.cccma.bc.ec.gc.ca/hccd/ (accessed on May 16, 2002).

Mueller-Dombois, D., and Ellenberg, H. 1974. Aims and Methods of Vegetation Ecology. Wiley, New York.

National Airphoto Library. 1984. Black and white aerial photographs A26587, 73-80 and A26587, 108-116. Scale 1:20,000.

Nelson, F.E., Hinkel, K.M., Shiklomanov, N.I., Mueller, G.R., Miller, L.L., and Walker, D.A. 1998. Active-layer thickness in north-central Alaska: systematic sampling, scale and spatial autocorrelation. Journal of Geophysical Research, **103**: 28 963–28 973.

Nicholson, F.H. 1976. Permafrost thermal amelioration tests near Schefferville, Québec. Canadian Journal of Earth Sciences, **13:** 1694-1705.

Nicholson, F.H. 1978. Permafrost modification by changing the natural energy budget. *In* Proceedings, 3rd International Conference on Permafrost, July 10-13, 1978, Edmonton, Alberta. National Research Council of Canada, Ottawa, **1:** 61-67.

Nixon, J.F., Saunders, R., and Smith, J. 1991. Permafrost and thermal interfaces from Norman Wells pipeline ditchwall logs. Canadian Geotechnical Journal, **28:** 738-745.

Oke, T.R. 1987. Boundary Layer Climates. Methuen & Co., New York.

Outcalt, S.I., Nelson, F.E., and Hinkel, K.M. 1990. The zero-curtain effect: heat and mass transfer across an isothermal region in freezing soil. Water Resources Research, **26:** 1509-1516.

Overpeck, J., Hughen, K., Hardy, D., Bradley, R., Case, R., Douglas, M., Finney, B., Gajewski, K., Jacoby, G., Jennings, A., Lamoureux, S., Lasca, A., MacDonald, G., Moore, J., Retelle, M., Smith, S., Wolfe, A., and Zielinski, G. 1997. Arctic environmental change of the last four centuries. Science, **278:** 1251-1256.

Pike, A.E. 1966. Mining in permafrost. *In* Proceedings, 1st International Conference on Permafrost, November 11-15, 1963, Lafayette, Indiana. National Academy of Science, National Research Council, Publication 1287, Ottawa, pp. 512-515.

Price, L.W. 1971. Vegetation, microtopography, and depth of active layer on different exposures in subarctic alpine tundra. Ecology, **52:** 638-647.

Rampton, V.N. 1982. Quaternary geology of the Yukon coastal plain. Geological Survey of Canada, Bulletin 317.

Rich, P.M. 1990. Characterizing plant canopies with hemispherical photographs. Remote Sensing Reviews, **5:** 13-29.

Riseborough, D.W. 2001. An analytical model of the ground surface temperature under snowcover with soil freezing. *In* Proceedings, 58th Annual Eastern Snow Conference May 17 -19, 2001, Ottawa, pp. 363-372.

Roots, E.F. 1989. Climate change: high latitude regions. Climatic Change, **15:** 223-253.

Rouse, W. 1984. Microclimate of arctic tree line. 2. Soil microclimate of tundra and forest. Water Resources Research, **20:** 67-73.

Rouse, W. 1993. Northern climates. *In* Canada's Cold Environments. *Edited by* H.M. French and O. Slaymaker. McGill-Queen's University Press, Montreal, pp. 65-92.

Sellman, P.V., and Hopkins, D.M. 1984. Subsea permafrost distribution on the Alaskan shelf. *In* Proceedings, 4th International Conference on Permafrost, July 17-22, 1983, Fairbanks, Alaska. National Academy Press, Washington, D.C., pp. 75-82.

Serreze, M.C., Kahl, J.D., and Schnell, R.C. 1992. Low-level temperature inversions of the Eurasian Arctic and comparisons with Soviet drifting stations. Journal of Climate, **5:** 615-630.

Serreze, M.C., Walsh, J.E., Chapin, F.S., Osterkamp, T., Dyurgerov, M., Romanovsky, V., Oechel, W.C., Morison, J., Zhang, T., and Barry, R.G. 2000. Observational evidence of recent change in the northern high-latitude environment. Climatic Change, **46:** 159-207.

Phillips, M. 2000. Influence of snow supporting structures on the thermal regime of the ground in alpine permafrost terrain. Eidgenössisches Institut für Schnee- und Lawinenforschung, Davos, Switzerland.

Sinha, A.K., and Stevens, L.E. 1983. Deep electromagnetic sounding over the permafrost terrain in the Mackenzie Delta, N.W.T., Canada. *In* Proceedings, 4th International Conference on Permafrost, July 17-22, 1983, Fairbanks, Alaska. National Academy Press, Washington, D.C., pp. 1166-1171.

Slaymaker, O. 1993. Cold mountains of western Canada. *In* Canada's Cold Environments. *Edited by* H.M. French and O. Slaymaker. McGill-Queen's University Press, Montreal, pp. 171-197.

Smith, M.W. 1975. Microclimatic influences on ground temperatures and permafrost distribution, Mackenzie Delta, Northwest Territories. Canadian Journal of Earth Sciences, **12**: 1421-1438.

Smith, M.W., and Riseborough, D.W. 1996. Ground temperature monitoring and detection of climate change. Permafrost and Periglacial Processes, **7:** 301–310.

Smith, M.W., and Riseborough, D.W. 2002. Climate and the limits of permafrost: a zonal analysis. Permafrost and Periglacial Processes, **13:** 1-15.

Soil and Plant Analysis Council, Inc. 2000. Soil Analysis: Handbook of Reference Methods. CRC Press, Boca Raton.

Soil Classification Working Group. 1998. The Canadian System of Soil Classification. Agriculture and Agri-Food Canada Publication 1646 (Revised).

Sturm, M., and Holmgren, J. 1994. Effects of microtopography on texture, temperature and heat flow in arctic and sub-arctic snow. Annals of Glaciology, **19:** 63-68.

Taylor, A., Nixon, M., Eley, J., Burgess, M., and Egginton, P. 1998. Effect of atmospheric temperature inversions on ground surface temperatures and discontinuous permafrost, Norman Wells, Mackenzie Valley, Canada. *In* Proceedings, 7th International Conference on Permafrost, June 23-28, 1998, Yellowknife, N.W.T. *Edited by* A.G. Lewkowicz and M. Allard. Nordicana, Québec, pp. 1043-1048.

Trichon, V., Walter, J.N., and Laumonier, Y. 1998. Identifying spatial patterns in the tropical rain forest structure using hemispherical photographs. Plant Ecology, **137:** 227-244.

Wahl, H.E., Fraser, D.B., Harvey, R.C., and Maxwell, J.B. 1987. Climate of Yukon. Atmospheric Environment Service, Environment Canada, Climatological Studies No.40.

Wang, B., and French, H.M. 1995. Permafrost on the Tibet Plateau, China. Quaternary Science Reviews, **14:** 255-274.

Wardle, P. 1974. Alpine timberlines. *In* Arctic and Alpine Environments. *Edited by* J.D. Ives and R.G. Barry. William Clowes and Sons Ltd., London, pp. 371-402.

Wernecke, L. 1932. Glaciation, depth of frost, and ice veins of Keno Hill and vicinity, Yukon Territory. Engineering and Mining Journal, **133:** 38-43.

White, M.P., Smith, C.A.S., Kroetsch, D., and McKenna, K. 1994. Soil landscapes of Canada, Yukon Territory. Contribution No. 89-05, *In* Agriculture Canada Publication 5281/B.

Wiken, E.B., Gauthier, D., Marshall, I., Lawton, K., and Hirvonen, H. 1996. A perspective on Canada's ecosystems: An overview of the terrestrial and marine ecozones. Canadian Council on Ecological Areas Occasional Paper #14.

Williams, D.J., and Burn, C.R. 1996. Surficial characteristics associated with the occurrence of permafrost near Mayo, central Yukon Territory, Canada. Permafrost and Periglacial Processes, **7:** 193-206.

Williams, P.J., and Smith, M.W. 1989. The Frozen Earth: Fundamentals of Geocryology. Cambridge University Press, Cambridge.

Veireck, L.A. 1965. Relationship of white spruce to lenses of perennially frozen ground, Mount McKinley National Park. Arctic, **18:** 262-267.

Vonder Mühll, D.V., Stucki, T., and Haeberli, W. 1998. Borehole temperatures in alpine permafrost: a ten year series. *In* Proceedings, 7th International Conference on Permafrost, June23-28, 1998, Yellowknife, N.W.T. *Edited by* A.G. Lewkowicz and M. Allard. Nordicana, Québec, pp. 1089-1095.

Zhang, T., Barry, R.G., Knowles, K., Heginbottom, J.A., and Brown, J. 1999. Statistics and characteristics of permafrost and ground-ice distribution in the northern hemisphere. Polar Geography, **23:** 132-154.

Zhou, Y., Qui, G., and Guo, D. 1991. Quaternary permafrost in China. Quaternary Science Reviews, **10:** 511-517.

Zimmermann, N.E. 2000. Shortwavc.aml: Calculation of direct solar radiation with northern-latitude corrected. AML downloaded from http://www.wsl.ch/staff/niklaus.zimmermann/programs/aml.html#1 (accessed on May 16, 2002).

Zoladeski, C.A., Dowell, D.W., and Ecosystem Classification Advisory Committee. 1996. Ecosystem classification for the southeast Yukon: field guide, first approximation. Yukon Renewable Resources and Canadian Forestry Service, Department of Indian Affairs and Northern Development, Whitehorse.